

**PERFORMANCE STUDY OF A WDM
OPTICAL NETWORK WITH FIBER
NONLINEAR EFFECTS**



A Thesis submitted to the Electrical and Electronic
engineering department of BUET , Dhaka,
in partial fulfillment of the degree of
Master of Science in Engineering
(Electrical and Electronic)

by

Md. Nuruzzaman Khan



Bangladesh University of Engineering and Technology, Dhaka.

March 1996

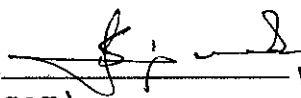
DEDICATED TO
MY SON SHADNAN SAZZAD KHAN.

APPROVAL

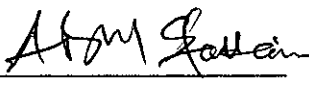
The thesis titled Performance Study of a WDM Optical network with fiber nonlinear effects, submitted by Md. Nuruzzaman Khan, Roll no. 901310F, session 1988-89 to the Department of Electrical and Electronic Engineering, Bangladesh University of Engineering and technology (B.U.E.T.) has been accepted as satisfactory for partial fulfillment of the requirements for the degree of Master of Science in Engineering (Electrical and Electronic).

Board of Examiners

1. Dr. Satya Prasad Majumder
Associate Professor
Department of EEE
B.U.E.T., Dhaka 1000

Chairman  11/10/96
(Supervisor)


2. Dr. A.B.M. Siddique Hossain
Professor and Head,
Department of EEE,
B.U.E.T., Dhaka 1000.

Member  01/10/96
(Ex-officio)

3. Dr. Md. Saifur Rahman
Assistant Professor,
Department of EEE,
B.U.E.T., Dhaka 1000.

Member  01/10/96

4. Engr. Ashraful Alim.
Div.Engineer, BTTB,
Telephone Bhaban,
Eskaton, Dhaka.


Member  1/10/96
(External)

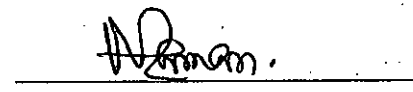
DECLARATION

This work has been done by me and it has not been submitted elsewhere for the award of any degree or diploma.

Countersigned

Signature of the student


1/10/96
(Dr. Satya Prasad Majumder)


(Md. Nuruzzaman Khan.)

CONTENTS

DEDICATION	(i)
APPROVAL	(ii)
DECLARATION	(iii)
CONTENTS	(iv)
ACKNOWLEDGEMENT	(vi)
ABSTRACT	(vii)
LIST OF ABBREVIATIONS	(viii)
LIST OF PRINCIPAL SYMBOLS	(xi)
LIST OF FIGURES	(xiv)

Chapter 1:

1.0 Introduction:	1
1.1 Advantages of Optical Fiber Communication	3
1.2 Elements of Optical Fiber Communication Link	4
1.3 Modulation, Multiplexing and Detection Schemes	6
1.4 Limitations of Optical Fiber Communication Systems	10
1.5 The Objective of this Thesis	16
1.6 Brief Introduction of this Thesis	16

Chapter 2:

Performance analysis of Multiwavelength Optical Transport Network with Direct Detection FSK Receiver.

2.1	Introduction	18
2.2	Four-wave mixing and its mechanism	20
2.3	System Architecture	21
2.4	The Optical Transport network Model	25
2.4.1	The Mach-Zehnder Interferometer	27
2.5	Theoretical Analysis of Multiwavelength Optical Transmission System	29
2.5.1	The Optical Signal	29
2.5.2	The FWM Signal	30
2.5.3	The Combined Optical Field	32
2.5.4	The Bit Error Rate Calculation	38
Chapter 3: Results and Discussions		42
Chapter 4: Conclusions and Suggestions		
4.1	Conclusions	79
4.2	Suggestions	80
REFERENCES		81
APPENDIX A		86
APPENDIX B		88
APPENDIX C		95

ACKNOWLEDGEMENTS

The author is pleased to acknowledge his indebtedness and profound respect to his supervisor Dr. Satya Prasad Majumder, Associate Professor of the department of Electrical and Electronic Engineering of Bangladesh University of Engineering and Technology (BUET), who cordially guided, supervised and helped. His most gracious encouragement and very valued constructive suggestions during the whole phase of this work are most sincerely appreciated. In addition the author would like to thank Dr. Mohammad Ali Choudhury, Professor of the department of Electrical and Electronic Engineering of Bangladesh University of Engineering and Technology (BUET) for his friendly help and cooperation.

The author is grateful to his beloved wife Shahnaz Zaman and also wishes to express his thanks to her, who helped him in many ways with special encouragement. Without her help it would be impossible for him to finish this thesis work.

The author also would like to thank Mamunur Rahman (Manik) and other relatives for their help, inspiration and encouragement to do this work.

ABSTRACT

A theoretical analysis is carried out to evaluate the performance of an optical multi-wavelength transport network (MWTN). An optical mesh network is considered and frequency shift - Keying (FSK) modulation of laser diode in the transmitter for each of the wavelength division multiplexed channels is used. A Mach-Zehnder Interferometer (MZI) is used as an optical frequency discriminator in the receiver. A single building block of the optical core network is considered to include optical in-line amplifiers, wavelength multi-demultiplexers (MUX, DMUX), splitters, fiber protection switch etc. . The analysis is carried out to evaluate the combined effect of fiber nonlinearities viz. four-wave mixing (FWM) and accumulated optical amplifier's spontaneous emission (ASE), on the overall system performance.

The bit error rate (BER) performance of the optical transmission system is evaluated at a bit rate of 2.5 Gb/s. For particular values of fiber parameters and optimum system parameters viz. optimum channel separation, maximum number of nodes, maximum allowable transmitter power per channel etc. are determined at an specific bit error rate.

LIST OF ABBREVIATIONS

APD	= Avalanche Photodiode
ASE	= Amplifier's Spontaneous Emission
ASK	= Amplitude Shift Keying
BER	= Bit Error Rate
BFSK	= Binary Frequency Shift Keying
BPPM	= Binary Pulse Position Modulation
BPSK	= Binary Phase Shift Keying
BW	= Bandwidth
CPFSK	= Continuous Phase FSK
dBm	= Decible relative to 1 mw
DD	= Direct detection.
DFA	= Doped fiber amplifier
DFB	= Distributed feedback
DFWM	= Degenerate Four-Wave Mixing
DMUX	= Demultiplexer
DPFSK	= Discontinuous phase FSK
DPSK	= Differential Phase Shift Keying
EDFA	= Erbium doped fiber amplifier
erfc	= Complementary error function
FCD	= Fiber Chromatic Dispersion
FDM	= Frequency Division Multiplexing

FM/AM = FM to AM conversion in photodetector

FM = Frequency modulation

FPI = Fabry Perot Interferometer

FSK = Frequency Shift Keying

FSK/DD= FSK with direct detection

FWM = Four-Wave Mixing

FWM-sp= FWM Spontaneous Emission

IM/DD = Intensity modulation and direct detection

ISI = Inter-symbol interference

Km = Kilometer

LASER = Light Amplification by Stimulated Emission of
Radiation.

LD = Laser Diode

LED = Light Emitting Diode

LW = Linewidth

MSK = Minimum Shift Keying.

MUX = Multiplexer.

MW = Micro wave

MWTN = Multiwavelength Transport Network.

MZI = Mach-Zehnder interferometer

NEB = Noise equivalent bandwidth

NRZ = Non-return to zero

OCDMA = Optical Code Division Multiplexing Access

OFD = Optical frequency discriminator

OFDM = Optical frequency division multiplexing
OOK = On-off keying
OTDM = Optical Time Division Multiplexing
pdf = Probability density function
PIN = Positive Intrinsic Negative
PN = Phase noise
PPM = Pulse Position Modulation
PSD = Power spectral density
PZT = Piezo-electric Transducer
RF = Radio Frequency
s-FWM = Signal FWM
SBS = Stimulated Brillouin Scattering
shot = shot
SLA = Semiconductor laser amplifier
SNR = Signal to noise ratio
sp-sp = Spontaneous-Spontaneous
SPM = Signal Phase Modulation
SRS = Stimulated Raman Scattering
ssp = Signal Spontaneous Emission
th = Thermal
W = Fiber Core Diameter
WDM = Wavelength Division Multiplexing

LIST OF PRINCIPAL SYMBOLS

*	Convolution.
α	Attenuation of fiber.
$\Delta\Psi_{S=FWM}$	Accumulated phase over the demodulation interval.
Δf	Frequency deviation.
ΔF	Frequency separation between two channels.
λ	Optical wavelength of the desired channel.
μm	Micro meter.
ν	Frequency of optical carrier.
σ^2	Variance of total noise power.
σ_m^2	Variance of noise power if 'mark' is transmitted.
σ_s^2	Variance of noise power if 'space' is transmitted.
τ	Delay time.
$\phi_s(t)$	Angle modulation (FSK).
χ	Nonlinear susceptibility.
$\Psi(t)$	Output phase.
A_{eff}	Effective core area.
B_e	Bandwidth of Receiver filter.
B_0	Bandwidth of optical amplifier.
B_r	Bit rate.
c	Velocity of light.
dB	Decibel.

D_c	Fiber chromatic dispersion factor.
$e_{ASE}(t)$	Optical amplifier's spontaneous emission.
$e_{FWM}(t)$	FWM output signal.
$e_o(t)$	Optical amplifier output signal.
$e_s(t)$	Output of the laser transmitter signal.
$f_i(i=p,q,r)$	Optical frequency of the i-th channel.
F_0	Noise figure of receiver.
f_p	Carrier frequency of the p-th channel.
f_{pqr}	FWM frequency.
f_q	Carrier frequency of the q-th channel.
f_r	Carrier frequency of the r-th channel.
G_1	Gain of optical amplifier no. 1.
G_2	Gain of optical amplifier no. 2.
G_T	Total Gain.
h	Modulation index.
I_s	Signal current due to P_{in} .
I_{sp}	Spontaneous emission current.
K_B	Boltzman's constant.
L/l	Fiber length / span.
L_{eff}	Effective fiber length.
L_f	Loss in the Fiber
L_D	Loss in the Multiplexer
L_{ps}	Loss in the Protection Switch
L_{sp}	Loss in the Splitter

L_{SW}	Loss in the optical space Switch
M	Number of Node(section) of the network.
$N(t)$	Total noise.
nm	Nano meter.
$p(\Delta\psi_{S-FWM})$	The pdf of $\Delta\psi_{S-FWM}$.
$p(e/\Delta\psi)$	Probability of error conditioned on $\Delta\psi$.
pdf	Probability density function.
P_f	Optical power launched into fiber.
P_{in}	Optical signal power from transmitter laser.
P_{pqr}	FWM power generated within the fiber.
P_s	Optical signal power received.
P_{s-FWM}	Signal FWM beat noise power.
P_{shot}	Shot noise power.
P_{sp}	Optical amplifiers spontaneous emission power.
P_{sp-sp}	ASE-ASE beat noise power.
P_{th}	Thermal noise power.
r	Modified radius.
R_d	Responsivity of photodetector (A/W).
R_l	Receiver load resistance.
β	Linewidth of laser.
T	Bit period.
$T_I(f), T_{II}(f)$	Transmittance of arm I and II of MZI.
W	Modified diameter of the fiber.
ω_s	Angular frequency of the optical carrier.

LIST OF FIGURES

- Fig.1.1 Block diagram of a basic optical fiber link.
- Fig.2.1 An schematic architecture of an optical mesh network.
- Fig.2.2 A single network module (building block)
- Fig.2.3(a) Block diagram of an optical transmitter.
- Fig.2.3(b) A typical model of MZI based optical CPFSK DD receiver.
- Fig.2.4 Transmittance of a Mach-Zehnder Interferometer (MZI).
- Fig.3.1 Bit error rate performance of optical multiwavelength transport network at a bit rate of 2.5 Gb/s as a function of the number of nodes M when number of channels $N=11$, fiber span $L=20$ Km, optical bandwidth $B_0=15$ GHz, $\Delta F=10$ GHz for different values of the optical transmitter power P_{in} (dBm).
- Fig.3.2 Bit error rate performance of optical MWTN at a bit rate of 2.5 Gb/s as a function of the number of nodes M when number of channels $N=51$, fiber span $L=20$ Km, optical bandwidth $B_0=15$ GHz, $\Delta F=10$ GHz for different values of the optical transmitter power P_{in} (dBm).
- Fig.3.3 Bit error rate performance of optical MWTN at a bit rate of 2.5 Gb/s as a function of the number of nodes M when number of channels $N=101$, fiber span $L=20$ Km, optical bandwidth $B_0=15$ GHz, $\Delta F=10$ GHz for different values of the optical transmitter power P_{in} (dBm).
- Fig.3.4 Bit error rate performance of optical MWTN at a bit rate of 2.5 Gb/s as a function of the number of nodes M when number of channels $N=51$, fiber span $L=50$ Km, $B_0=15$ GHz, $\Delta F=10$ GHz for different values of the optical transmitter power P_{in} (dBm).

- Fig.3.5 Bit error rate performance of optical MWTN at a bit rate of 2.5 Gb/s as a function of the number of nodes M when number of channels $N=51$, fiber span $L=100$ Km, $B_0=15$ GHz, $\Delta F=10$ GHz for different values of the optical transmitter power P_{in} (dBm).
- Fig.3.6 Bit error rate performance of optical MWTN versus number of nodes M , at a bit rate of 2.5 Gb/s for transmitter power $P_{in} = -4$ dBm and number of channels $N=11, 51, 101$ with $L=20$ Km and $B_0=15$ GHz, $\Delta F=25$ GHz.
- Fig.3.7 Bit error rate performance of optical MWTN versus number of nodes M , at a bit rate of 2.5 Gb/s for transmitter power $P_{in} = -4$ dBm and number of channels $N=11, 51, 101$ with $L=50$ Km and $B_0=15$ GHz, $\Delta F=25$ GHz.
- Fig.3.8 Bit error rate performance of optical MWTN versus number of nodes M , at a bit rate of 2.5 Gb/s for transmitter power $P_{in} = -4$ dBm and number of channels $N=11, 51, 101$ with $L=100$ Km and $B_0=15$ GHz, $\Delta F=25$ GHz.
- Fig.3.9 Bit error rate performance of optical MWTN versus number of nodes M , at a bit rate of 2.5 Gb/s for transmitter power $P_{in} = -4$ dBm and number of channels $N=11, 51, 101$ with $L=20$ Km and $B_0=25$ GHz, $\Delta F=25$ GHz.
- Fig.3.10 Bit error rate performance of optical MWTN versus number of nodes M , at a bit rate of 2.5 Gb/s for transmitter power $P_{in} = -4$ dBm and number of channels $N=11, 51, 101$ with $L=50$ Km and $B_0=25$ GHz, $\Delta F=25$ GHz.
- Fig.3.11 Bit error rate performance of optical MWTN versus number of nodes M , at a bit rate of 2.5 Gb/s for transmitter power $P_{in} = -4$ dBm and number of channels $N=11, 51, 101$ with $L=100$ Km and $B_0=25$ GHz, $\Delta F=25$ GHz.
- Fig.3.12 Variation of the allowable number of nodes M at $BER=10^{-9}$ versus the transmitter power P_{in} (dBm) in the presence of FWM effect when the number of channels $N=11, 51$ and 101 and channel separation $\Delta F=10$ GHz, $B_0=15$ GHz and fiber span, $L=20$ Km.
- Fig.3.13 Variation of the allowable number of nodes M at $BER = 10^{-9}$ versus the transmitter power P_{in} (dBm) in the presence of FWM effect when the number of channels $N=11, 51$ and 101 and channel separation $\Delta F=10$ GHz, $B_0=15$ GHz and fiber span, $L=50$ Km.

- Fig.3.14 Variation of the allowable number of nodes M at $BER=10^{-9}$ versus the transmitter power P_{in} (dBm) in the presence of FWM effect when the number of channels $N=11, 51$ and 101 and channel separation $\Delta F=10$ GHz, $B_0=15$ GHz and fiber span, $L=100$ Km.
- Fig.3.15 Variation of the allowable number of nodes M at $BER=10^{-9}$ versus the transmitter power P_{in} (dBm) in the presence of FWM effect when the number of channels $N=11, 51$ and 101 and channel separation $\Delta F=25$ GHz, $B_0=15$ GHz and fiber span, $L=20$ Km.
- Fig.3.16 Variation of the allowable number of nodes M at $BER=10^{-9}$ versus the transmitter power P_{in} (dBm) in the presence of FWM effect when the number of channels $N=11, 51$ and 101 and channel separation $\Delta F=50$ GHz, $B_0=15$ GHz and fiber span, $L=20$ Km.
- Fig.3.17 Variation of the allowable number of nodes M at $BER=10^{-9}$ versus the transmitter power P_{in} (dBm) in the presence of FWM effect when the number of channels $N=11, 51$ and 101 and channel separation $\Delta F=25$ GHz, $B_0=15$ GHz and fiber span, $L=50$ Km.
- Fig.3.18 Variation of the allowable number of nodes M at $BER=10^{-9}$ versus the transmitter power P_{in} (dBm) in the presence of FWM effect when the number of channels $N=11, 51$ and 101 and channel separation $\Delta F=50$ GHz, $B_0=15$ GHz and fiber span, $L=50$ Km.
- Fig.3.19 Plots of allowable number of nodes M in presence of FWM effect at a bit error rate of 10^{-9} as a function of the number of WDM channels N , when channel separation $\Delta F=10$ GHz, $B_0=15$ GHz and $L=20$ Km for different values of transmitter power P_{in} (dBm).
- Fig.3.20 Plots of allowable number of nodes M in presence of FWM effect at a bit error rate of 10^{-9} as a function of the number of WDM channels N , when channel separation $\Delta F=10$ GHz, $B_0=15$ GHz and $L=50$ Km for different values of transmitter power P_{in} (dBm).
- Fig.3.21 Plots of allowable number of nodes M in presence of FWM effect at a bit error rate of 10^{-9} as a function of the number of WDM channels N , when channel separation $\Delta F=10$ GHz, $B_0=15$ GHz and $L=100$ Km for different values of transmitter power P_{in} (dBm).

- Fig.3.22 Plots of allowable maximum number of nodes M in presence of FWM effect at a bit error rate of 10^{-9} as a function of the number of WDM channels N , when channel separation $\Delta F=10$ GHz, $B_0=15$ GHz and for $L=20,50,100$ Km.
- Fig.3.23 Plots of allowable maximum number of nodes M in presence of FWM effect at a bit error rate of 10^{-9} as a function of the number of WDM channels N , when channel separation $\Delta F=25$ GHz, $B_0=15$ GHz and for $L=20,50,100$ Km.
- Fig.3.24 Plots of allowable maximum number of nodes M in presence of FWM effect at a bit error rate of 10^{-9} as a function of the number of WDM channels N , when channel separation $\Delta F=50$ GHz, $B_0=15$ GHz and for $L=20,50,100$ Km.
- Fig.3.25 Plots of maximum allowable laser transmitter power $P_{in(max)}$ (dBm) at $BER=10^{-9}$ versus optical bandwidth B_0 (GHz) in the presence of FWM effect when fiber span $L=50$ Km and channel separation $\Delta F=25$ GHz for number of channels $N=11,51,101$
- Fig.3.26 Plots of maximum allowable laser transmitter power $P_{in(max)}$ (dBm) at $BER=10^{-9}$ versus number of WDM channel N , in the presence of FWM effect when fiber span $L=50$ Km and channel separation $\Delta F=25$ GHz for optical bandwidth $B_0=15,25,50$ GHz
- Fig.3.27 Plots of the allowable number of nodes M at $BER=10^{-9}$ as a function of channel separation ΔF (GHz) in the presence of FWM effect when the number of WDM channels $N=11$ and fiber span $L=50$ Km for different input power (dBm).
- Fig.3.28 Plots of the allowable number of nodes M at $BER=10^{-9}$ as a function of channel separation ΔF (GHz) in the presence of FWM effect when the number of WDM channels $N=51$ and fiber span $L=50$ Km for different input power (dBm).
- Fig.3.29 Plots of the allowable number of nodes M at $BER=10^{-9}$ as a function of channel separation ΔF (GHz) in the presence of FWM effect when the number of WDM channels $N=101$ and fiber span $L=50$ Km for different input power (dBm).



CHAPTER 1

1.0 Introduction:

A great interest in communication at the optical frequencies was created with the advent of the LASER in 1960 which made available a coherent optical source. Since optical frequencies are of the order of 5×10^{14} Hz, the laser communication system has a theoretical information capacity exceeding that of microwave system by a factor of 10^5 , which is approximately equal to the bandwidth of 10 million TV channels. With the potential of such wideband transmission capabilities, the optical communication system was conceived by Bell Laboratories in the late 1960's [1,2]. However, those systems were assumed to use lens waveguides and gas lasers and look far from practical at present.

In 1966 Kao et.al discovered that optical fibers can be used as ideal supports for the transmission of lightwaves. Yet it was not until 1970 that attenuation in fibers decreased from more than 100 dB/Km to over 20 dB/Km thereby making optical fibers a practical proportion for a wide range of uses [2].

Since 1966, optical fibers have been seriously considered as a wide range and long distance communication medium. Several fabrication techniques and specialized optical sources and detectors have been developed. It is now recognized that compared

to metal conductors or waveguides, optical fibers offer greater information capacity arising from a higher carrier frequency and lower material costs. Because of these reasons, during the last two decades there have been considerable advancements in the field of optical communications both in theory and practice [3]. Within the period upto 1975, optical transmission system using graded index fibers were developed operating at bit rates in the range of 8-140 Mbit/s and at wavelengths of 850-900 nm. However, the shortcomings of graded index fibers were soon apparent and by 1978 research had commenced on single mode fiber technology. This rapidly led to the establishment of 1300 nm single mode fiber design and system specifications for 140 Mbit/s operation [3,4]. By 1980, development of optical fibers were produced with attenuation levels of only 0.2 dB/Km at 1550 nm wavelength. Recently it is reported that fiber having 0.01 dB/Km attenuation loss has fabricated [3].

Optical fiber communication technology today has emerged from a mere theoretical concept to a commercial viability. Now a days, most of the communication fields adopted fiber optics technology. The need for and means of communication have always existed in human society. What we are observing today is a kind of communication revolution where information is created, managed, processed and distributed. This revolution is leading the human society to an integrated global network that will carry the information in the form of video, data and voice channels across national boundaries, transferring the globe into a local network, overcoming time and distance and changing the overall

concept of communication, business and ways of life. Beyond the technologies on the immediate horizon and the systems proposed or envisioned, several other opportunities can be deemed seen and still more expected. Some researchers predict that optical fiber technology may outstrip the capacity of the electronic devices to supply and receive data at rates that the optical fiber can handle; however, there may be an "electronic barrier" to higher data rates.

Bangladesh, the poorest member of the global telecommunication network is trying her best to adopt the latest technology like optical fiber with her telenetwork and also installed optical fiber as junction cable in several places. The details are shown in appendix c.

1.1 Advantages of Optical Fiber Communication:

Optical fiber communication systems have the advantages of having wide bandwidth and very high data rates with the higher energy and efficiency compared to Radio frequency (RF) and Micro wave (MW) communication systems. Yet, several other advantages may be mentioned as follows [3,4].

- (i) The fiber has low weight and small in size.
- (ii) It has lower cost of cables per unit length compared to that of metallic cables .
- (iii) It has very nominal shipping, handling and installation costs.
- (iv) It has the immunity to ambient electrical noise and electromagnetic interference.

- (v) There is no possibility of occurring of short circuits as in metal wires.
- (vi) It can be used in explosive environments.
- (vii) It is immune to any adverse temperature and moisture conditions.
- (viii) No additional equipments are required to protect the fiber against grounding and voltage problems.

Because of these advantages fiber optic communication is being currently utilized in telephone line loops, trunks, terminals, computers, cable television, space vehicles, avionics, ships, submarine cable and security and dark systems, electronic instrumentation systems, medical systems, satellite ground stations and industrial automation and process controls. The coming development of "integrated optic" technology is hoped to play an important role in influencing further departures from existing concepts of electronic systems for communication, control and instrumentation.

1.2 Elements of Optical Fiber Communication

Link.

The principal parts of the optical fiber communication system are the optical transmitter, the fiber and the optical receiver. Additionally optical amplifier, coupler, etc. are associated with it. Each of the parts has limited capabilities with respect to both the intensity and band width of the signals it can handle without distortion.

The block diagram of a basic optical communication link is as follows. The key sections are a transmitter consisting of a light source (LED) and its associated drive circuitry, a cable offering mechanical and environmental protection to the optical fibers contained inside and a receiver consisting of a photodetector plus amplifier and signal restoring circuitry.

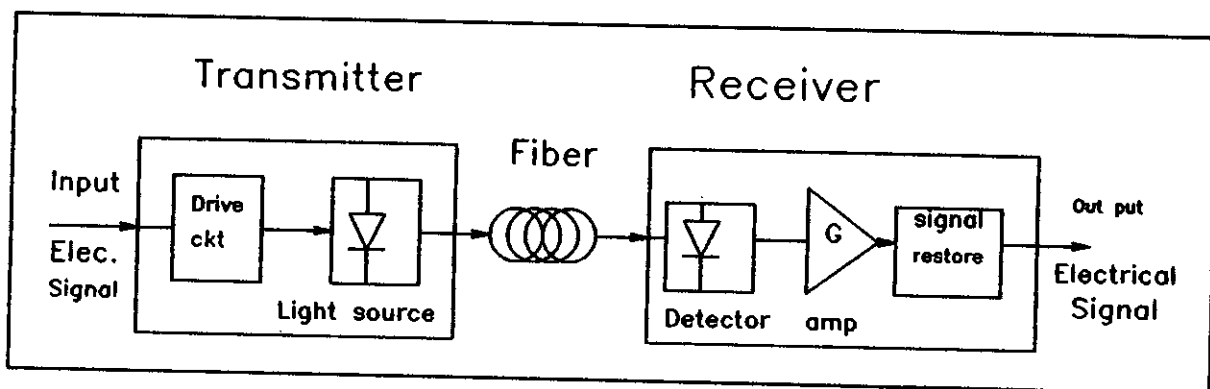


Fig. 1.1 Block diagram of a basic optical fiber link.

Once the cable is installed, a light source which is dimensionally compatible with the fiber core is used to launch optical power into the fiber. Semiconductor light emitting diodes (LEDs) and LASER diodes are suitable transmitter sources for this purpose since their light output can be modulated rapidly by simply varying the bias current. The electronic input signal, either analog or digital, is converted to an optical signal by varying the current flow through the light source. An optical source is a square law device, which means that a variation in device current results in a corresponding change in the optical output power. At 1100 to 1600 nm wave length InGaAsP alloy is the principal material for optical sources.

After an optical signal has been launched into the fiber, it will become progressively attenuated and distorted with increasing distance because of scattering, absorption and dispersions. At the receiver the attenuated, distorted and modulated optical power emerging from the fiber end will be detected by a photodetector diode. The photodiode converts the received optical power directly into an electrical signal (photo-current) output. Semiconductor PIN ("P" intrinsic "N") and Avalanche photodiode (APD) are the two types of photodetectors used in fiber optic links. For very low power optical signal APD is normally used since it provides higher receiver sensitivity owing to an inherent internal gain mechanism (avalanche effect). The principal figure of merit for a receiver is the minimum optical power necessary at the desired data rate to attain either a given error probability for digital systems or a specified signal to noise ratio for an analog system. The ability of a receiver to achieve a certain performance level depends on the photodetector type, the effects of noise in the system and the characteristics of the successive amplification stages in the receiver components of optical communication.

1.3 Modulations, Multiplexing and detection

Schemes:

The modulation schemes normally employed for optical transmission are intensity modulation, position modulation and frequency/Phase modulation as is used in conventional

communication system viz. OOK, PPM, ASK, PSK, FSK, QPSK, DPSK, MSK etc. [3-6]. Each of the modulation schemes has its own merits and demerits on the basis of information capacity and energy efficiency. In the optical fiber communication further the information viz. data, telephone signals, TV signals etc. from multiple user's may be transmitted over this system by using optical time division multiplexing (OTDM) and optical frequency or wavelength division multiplexing (OFDM/WDM) and optical code division multiple access (OCDMA) techniques [4]. The OTDM technique is generally preferred to OFDM technique because of the ease of transmission of error free data and voice information. However OFDM is still a more popular technique than OTDM due to the technological problems arising from building very high speed Laser transmitters required for OTDM. OFDM is efficient as long as each user requires the use of the network a large percentage of the time. If such is not the case, available bandwidth is being wasted since other users could have transmitted on these bandwidth. Having examined point to point link's, WDM is more sophisticated system to fully utilize the transmission capacity (B.W) of an optical fiber. Since optical sources have relatively narrow spectral widths, this type of transmission makes use of only a very narrow portion of the transmission bandwidth of a fiber [2,4,5].

Ideally, a dramatic increase in the information capacity of a fiber can thus be achieved by the simultaneously transmission of optical signals over the same fiber from many different light sources having properly spaced peak emission wavelengths. By operating each source at a different peak wavelength, the

integrity of the independent messages from each source is maintained for subsequent conversion to electrical signals at the receiving end. This is the basis of WDM. Conceptually it is the same as FDM. Our topic is to consider such multichannel dense wavelength division multiplexing (WDM) system when channel separation is of the order of a nanometer or less.

In light wave communication system, two important types of detection of received optical signals in the receiver are used viz. direct detection and heterodyne/coherent detection [5,6]. In direct detection receiver, the intensity of the received optical signal (field) is directly converted to an electrical signal (current) by a photodetector (photodiode). It is hence called intensity modulation direct detection (IM/DD) scheme. The term IM stems from two facts as the light intensity (not the amplitude) is modulated linearly with respect to the input signal voltage and that basically no attention is paid to the phase of the carrier. The original spectral spread of the optical carrier is usually much wider than the spread due to modulation. The term DD stems from that the signal is detected directly at the optical stage of the receiver; neither the frequency conversion nor sophisticated signal processing is required. On the other hand, the heterodyne (coherent) scheme became common since 1930. Even now a days sophisticated coherent modulations such as FM, PM, FSK and PSK are also widely used in RF/MW broadcasting and communications. In the late 1970's the IM/DD optical fiber communication became predominant. The heterodyne (coherent) scheme have been studied for last two decades and are more sensitive to learn phase noise compared to direct detection (DD) [5,7].

The IM/DD system has great advantages due to simplicity and low cost. On the other hand, some applications of the optical fiber communications exist in which long repeater separation is our primary concern, an example is the optical fiber communication between islands. In such a case, the improvement of the receiver sensitivity by a heterodyne type receiving technique or coherent modulation/demodulation scheme such as PCM-FSK or PCM-PSK may become advantageous, even at the sacrifice of simplicity and low cost. The expectation on the receiver sensitivity improvement is the principal motivation underlying the present effort toward the heterodyne coherent optical fiber communications. On the other hand, it is accepted by all the specialists that the IM/DD system will never retire because heterodyne/coherent systems are and will continue to be rather expensive. The relative receiver sensitivity of different modulation/detection schemes are summarized as follows [5,7],

IM/DD.

↓ 10-25 db improvement.

ASK(OOK) Heterodyne → 3 dB Improvement → ASK (Homodyne).

↓ 3 db improvement.

FSK/CPFSK heterodyne.

↓ 3 db improvement.

PSK heterodyne.

↓ 3 db improvement.

PSK homodyne.

Depending on the specific application various modulation /demodulation formats are employed such as ASK (OOK), BPSK, BFSK (CPFSK), DPFSK, MSK, BPPM etc. Each of the techniques with heterodyne/coherent, noncoherent (envelope detection), IM/DD, or diversity or delay demodulation has its merits and demerits and none has emerged as absolutely preferable [7].

1.4 Limitations of Optical Fiber Communication Systems:

Though optical communication system is more advantageous, there are some practical limitations due to non-ideal characteristics of lasers, photodetectors and optical fibers.

The important limitation in optical communication is that the sensitivity of an optical receiver is dictated by quantum effects. Other factors such as background light, dark current, post detection amplifier noise and transmitter imperfections also affect considerably the receiver sensitivity.

Other limitations of optical transmission systems are due to the fiber chromatic dispersion (FCD) [8-11] four-wave mixing (FWM) [12-22], Stimulated Brillouin Scattering (SBS) and Stimulated Raman Scattering (SRS), phase noise of laser, Relative intensity noise (RIN), Signal phase modulation (SPM) [8,12,15,17], Optical Amplifier's Spontaneous Emission (ASE), etc., [13,20-23].

Dispersion plays an increasing role on the overall system performance in future high-speed systems. Dispersion is an important characterization factor of optical fiber as it determines the distortion of the output signals launched into the fiber. This effect modifies the actual information carrying capacity or bit rate of the optical fiber transmission system. The dispersion in optical fiber may arise due to various reasons and in practice three main factors have been analyzed, namely [9,10],

- (i) material dispersion,
- (ii) waveguide dispersion and
- (iii) differential group delay or intermodal (or simply modal) dispersion.

The effect of chromatic dispersion can be overcome to some extent by dispersion compensation device which is based on differential time delay for the upper and the lower side band of the modulated signal [11].

Four-wave mixing (FWM) phenomenon is one of the important limiting factors in multichannel transmission systems. Four-wave mixing (FWM) refers to the process in which three input optical waves interact in a medium and generate a fourth wave, [12,13]. The combined interference and diffraction effects therefore correspond to four wave mixing (FWM) in the literature of non-linear optics. The process is called degenerate if the frequencies of the three incident waves and the generated wave are equal. Degenerate four-wave mixing (DFWM) is a simple method to achieve

phase conjugation i.e., to generate a wave with a phase which is the complex conjugate of one of the incident waves. In optical fiber transmission lines the generated FWM light accumulates and seriously influences optical FDM systems performance. Several studies have been reported on the influence of fiber four-wave mixing effect on multichannel systems [9,10,12-18]. FWM process, as well as Stimulated Brillouin Scattering (SBS) has the potential to influence significantly the operation of optical transmission systems in terms of data rate, transmission length, number of channels etc. while using low dispersion fibers with narrow-linewidth laser source. The theoretical and experimental results of the effects of FWM in OFDM system were reported in Ref. [13,14]. The theoretical expression for FWM power was presented to demonstrate the dependence of FWM power on various system parameters and the experimental results were provided and the system performance degradation due to FWM crosstalk in a 16-channel coherent system were described.

Litchman [17] has reported the bit-rate distance product limitations due to fiber non-linearities viz. SBS, FWM and dispersion limits in multichannel coherent optical communication system.

The theoretical performance limitations due to fiber chromatic dispersion on coherent ASK and DPSK system was reported in Ref. [9]. The experimental results of chromatic dispersion limitations on direct detection FSK and DPSK system was also reported [10].

The effect of FWM on direct detection FSK and FDM system is reported in Ref. [16] with some experimental demonstrations. The amount of crosstalk due to FWM is evaluated both theoretically and experimentally.

In the coherent transmission systems employing optical frequency division multiplexing (OFDM), it is necessary to determine the optimum channel frequency separation, optimum number of channels, optimum fiber span etc. at the operating wavelengths of the system as FWM process depends on the channel frequency separation, fiber chromatic dispersion and the fiber length. The traditional way of compensating for optical loss in lightwave communication systems has been the rather cumbersome procedure of regeneration. Regeneration includes photon-electron conversion, electrical amplification, retiming, pulse shaping and finally electron-photon conversion. In many applications, direct optical amplification of the light signal would be advantageous. Optical amplifiers can be used in any system that is loss limited: i.e., dispersion effects are the limiting factors [23-26]. This is the case for most systems operating near the dispersion minimum at $1.3\mu\text{m}$, and the coherent lightwave systems with local area networks (LAN), where the main losses are from branching and taps, are also loss limited and can benefit from simple optical amplifiers [27].

Semiconductor laser amplifiers have been studied for a number of years. Significant work at $0.8\text{-}\mu\text{m}$ wavelength was done in the early 80's. Recently major progress has been made in long

wavelength devices. Optical amplifiers with high gain, low gain ripple, low noise, and high saturation output power have been reported. Optical amplifier system applications have also been reported, both applications for preamplifiers and in-line amplifiers [23,24].

Er^{3+} -doped fiber amplifiers are essentially promising because of their inherent matching to fiber lines, high output power, and insensitive to interchannel crosstalk compared to semiconductor laser amplifier (SLA) [25-27]. To date, several works have been reported for multichannel amplification using fiber amplifiers, such as investigations on interchannel modulation and mutual signal-gain saturation as well as demonstrations of 16-channel common amplification [26,27]. They studied an Er^{3+} -doped fiber amplifier for multichannel systems, from the point of clarifying the ultimate capacity and the applicable number of channels.

As optical amplifiers have advanced to the stage that actual system use might be possible in the near future, it is important to know the system consequences, its advantages and limitations. The theoretical as well as experimental investigations of the usefulness of optical amplifiers in lightwave systems are already reported for single channel and multichannel transmission systems [22,26]. When optical amplifiers are used as in-line amplifiers to increase the repeterless transmission distance, the performance of multi-wavelength division multiplexing (WDM)/FDM systems are affected by the combined effect of FWM and accumulated

amplifier's spontaneous emission (ASE) and beat noise components viz. signal-FWM crosstalk, ASE-ASE crosstalk, FWM-ASE crosstalk etc. [19-20]. Although, the amount of crosstalk in WDM optical transmission system due to FWM effect is reported experimentally as well as theoretically, the receiver sensitivity degradation due to the FWM effect is of prime importance. The sensitivity degradation of direct detection FSK system due to FWM is reported in Ref.[22] where optical amplifiers are not considered and the effect of accumulated ASE noise is not taken into account. The degradation of system performance due to FWM in a multiwavelength optical network needs further investigations.

Dense wavelength division multiplexed optical transmission system are very important for future lightwave communications due to inherent enormous information capacity. Optical multi wavelength transport networks (MWTN) have emerged considerable recent interests because of their inherent capability to achieve higher information capacity, greater flexibility, efficient routing, transparent switching, reconfigurability etc.[28-30]. The effect of switch crosstalk and adjacent channel crosstalk, filtering effect, accumulated ASE on the performance of MWTN has been recently addressed [29,30]. However, the performance of closely packed WDM systems is highly vulnerable to the effect of FWM even with dispersion shifted fibers having low dispersion coefficients.

1.5 The objective of this Thesis:

The objectives of this thesis work are:

- (i) To develop a theoretical analysis to evaluate the impact of four-wave mixing (FWM) in optical fiber on the performance of an optical WDM network with CPFSK direct detection receiver.

- (ii) To evaluate the system performance at a bit rate of 2.5 Gb/s and determine the optimum system parameters, viz. optimum fiber span, optimum number of nodes, optimum amplifier bandwidth and channel separation, maximum allowable transmitter power per channel and maximum number of channels that can be transmitted for reliable system performance.

1.6 Brief Introduction to this Thesis:

In chapter 1, a brief introduction and historical background of optical communication systems are discussed. Also the main terms with their definition and features of optical communication systems are presented. A review of recent works in the related field and limitations of optical fiber communication systems are also presented.

In chapter 2, a theoretical analysis for multiwavelength optical transmission system with FSK direct detection receiver

based on MZI (Mach-Zehnder Interferometer) is presented which accounts for the nonlinear effects of optical fibers on the system performance in the presence of accumulated optical amplifier's spontaneous emission (ASE) noise, beat noise components arising out of the beating of the signal, FWM power and ASE in the photodetection process and receiver noise.

Chapter 3 provides the performance results of the optical WDM system described in chapter 2 with FSK direct detection receiver for different sets of values of the receiver and system parameters at a bit rate of 2.5 Gb/s for achieving a bit error rate 10^{-9} . The optimum system parameters are also determined for a reliable system performance.

A brief conclusion and suggestions for future work are presented in chapter 4.

CHAPTER - 2

PERFORMANCE ANALYSIS OF MULTIWAVELENGTH OPTICAL TRANSPORT NETWORK.

2.1 Introduction:

Future telecommunication networks must be capable of adapting to rapid changes in the network traffic requirements. The development of telecommunication networks is constrained by the influenceable interference between the optical high-speed fiber interconnection networks, and the electronic terminals at switch nodes. The vast bandwidth potential of the optical fiber cannot be exploited easily since the existing electronic interface is designed for specific multiplexing schemes and bitrates. Therefore, post installation changes will be required which is expensive. Optical technologies may be employed to provide the required capacity and flexibility. Until now, advanced optical techniques for time switching and frequency switching are still immatured compared to the electronic counterparts, whereas optical space switching and wavelength division multiplexing (WDM) [28-30] provide attractive solutions to some of the improved networking functions required.

Dense wavelength division multiplexing (WDM) or frequency

division multiplexing (FDM) technology is important for increasing the transmission capacity and the network flexibility of fiber transmission system. Many type of optical components for WDM/FDM system have been proposed. Mach-Zehnder interferometer as frequency discriminator for FSK direct detection receiver can be applied to conventional WDM/FDM systems.

In optical WDM/FDM system the generated FWM power in optical fibers is one of the dominant nonlinear effects which causes system performance degradation. The other nonlinear effects arise into the fiber like Stimulated Brillouin Scattering (SBS), Stimulated Raman Scattering (SRS) but they are not so dominant hence neglected in the present analysis of the system performance.

Significant amount of research works have been carried out during the last few years to estimate the amount of FWM power and the crosstalk induced by FWM effect in multi-wavelength optical transmission system [14-16,19-21]. Recently the effects of ASE and crosstalk induced by space switches are investigated in optical multiwavelength transport networks where the channel separation is of the order of nanometers [28-30]. However, the bit error rate (BER) performance of WDM system with direct detection optical FSK receiver is not yet reported incorporating the effect of FWM power, chromatic dispersion etc.

In this chapter, a detail theoretical analysis for WDM system with MZI based Direct detection FSK receiver is provided taking into account the combined effect of FWM power, chromatic dispersion, optical amplifier's spontaneous emission (ASE) noise

etc. on the overall system performance. A single building block of an WDM optical network comprising the wavelength selective elements, optical amplifier, splitter, optical cross point switch etc. is considered for the analysis.

2.2 Four-wave mixing and its mechanism:

Four Wave mixing an important nonlinear process can be explained as follows,

If two signals with different optical frequencies say f_1 and f_2 pass through the amplifier, the electron density is modulated at the beat frequency $|f_1 - f_2|$. This modulation of the electron density modulate the susceptibility of the semiconductor medium $\chi = \chi_n \text{Cos}[2\pi(f_1 - f_2)t]$. The electric fields $\xi_1 \text{Exp}(j2\pi f_1 t)$; $\xi_2 \text{Exp}(j2\pi f_2 t)$ of the two optical signals interact with the susceptibility to create electric polarizations in the amplifier at frequencies $f_1 \pm (f_1 - f_2)$; $f_2 \pm (f_1 - f_2)$. These polarizations act as driving forces in Maxwell's equation to generate components at f_1 , f_2 , $2f_1 - f_2$, $2f_2 - f_1$.

This process not only couples power from the signal waves into the created sidebands but also give a coupling of power from the higher-frequency signal to the lower frequency signal introducing crosstalk which is known as Four-Photon Mixing or Four-Wave Mixing [13,24].

The effect of fiber four-wave mixing(FWM) strongly depends on channel separation and input optical power into the amplifier

[13-14]. It also depends on the number of wavelengths/channels transmitted, fiber chromatic dispersion, wavelengths, fiber span between two nodes and bandwidth of optical multi/demultiplexers. This crosstalk mechanism is a major problem in the IM transmission. As this nonlinear process (FWM) depends on channel separation so when the frequency difference is large enough compared to the inverse of the carrier life time, the carrier can not respond to the beat frequency. Thus little or no nonlinear polarization is generated. The process also dependent on input light intensity i.e. degree of gain saturation in the amplifier. When the amplifier is strongly saturated, the carrier number varies strongly which causes large nonlinear polarization. On the other hand, when the carrier number is considered to be constant, there is therefore little or no nonlinear polarization.

2.3 System Architecture:

An schematic architecture for the optical core network is shown in Fig.2.1 which is similar to that considered in the Ref.[30]. The optical nodes are linked in a mesh configuration where transmission in opposite directions in the network is carried over two separate sub-networks. Optical isolators are assumed to eliminate problems caused by optical reflections. An optical path through the network will typically comprise a number of fiber transmission sections interconnected by optical network nodes incorporating optical space switches, optical amplifiers and WDM components [29-30]. This network forms a high capacity

optical transport layer of simple functionality with access to an electronic transport layer of limited bandwidth, capable of providing a number of network management functions, drop-insert of new channels, etc.. Each module in the optical network consists of a network node and a length of fiber. If operation of the single network elements is independent of the overall network architecture, this approach allows simple overall network configuration and ease of upgrade and extensions.

In Fig. 2.2 a single network module (building block) is illustrated along with an schematic of an optical path through the network [30]. An optical building block comprises wavelength selective elements for improved capacity and flexibility, amplifiers for signal level restoration, a splitter and a small switch for path protection, an optical crosspoint switch matrix, and a length of fiber for network node interconnection. The signals at the input and at the output of a network building block are to maintained at the same level.

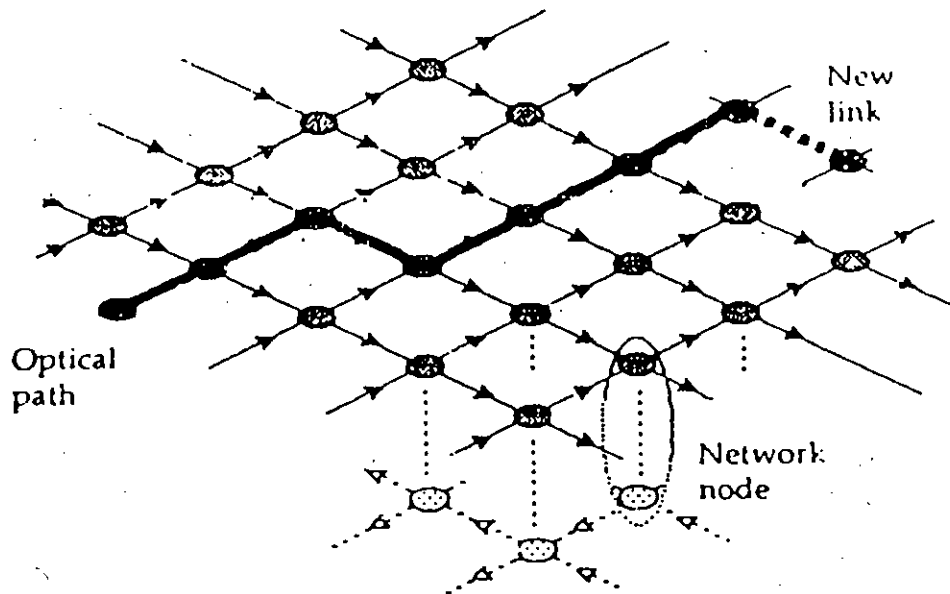


Fig.2.1 An schematic architecture of an optical mesh network.

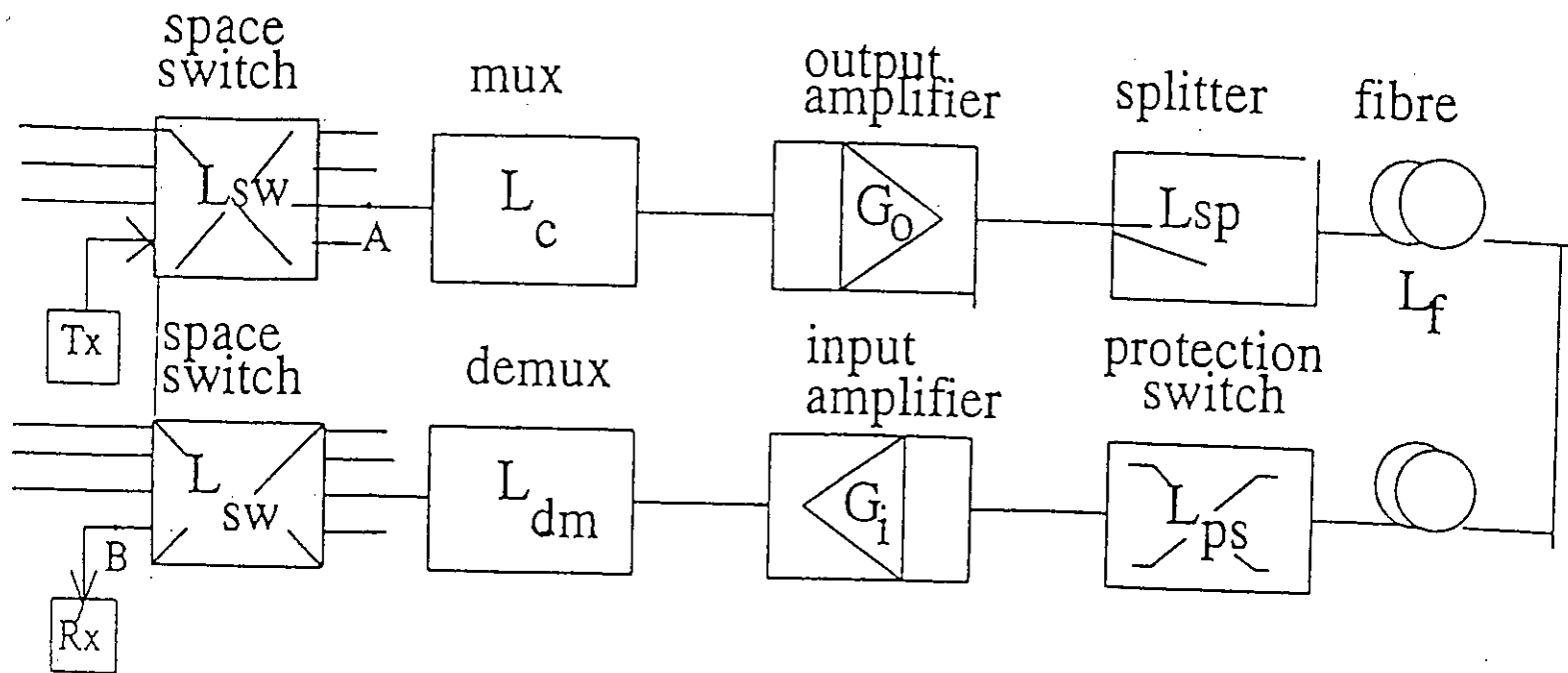


Fig.2.2 A single network module (building block)

2.4 The Optical Transmitter/Receiver Model:

The dimension of an optical network is limited by a number of effects, such as laser phase noise, Amplifier's Spontaneous Emission (ASE), laser saturation, reflection, jitter accumulation, signal bandwidth narrowing caused by filter concatenation and as well as nonlinear effects already mentioned before.

The transmitter and receiver models considered in the analysis is shown in Fig. 2.3. For each channel we consider CPFSK modulation of the transmitter DFB laser using direct frequency modulation of its driving current.

In the receiver we considered direct detection (DD) reception using a Mach-Zehnder interferometer (MZI) as an optical frequency discriminator (OFD). The model of the receiver is shown in Fig. 2.3(b). The light source used by the transmitter is assumed to be a single-mode laser. The optical signal is detected by two PIN photodetectors to produce the electrical signal. During the conversion process, Gaussian noise is added in two ways, (i) shot noise produced in the process of photodetection, (ii) thermal noise introduced by the circuitry following the photodetector, and (iii) beat noise terms arising out from the beating of the signal, FWM signal and optical amplifier's spontaneous emission (ASE) noise in the photodetection process.

With certain conditions maintained, the polarity of the output signal, after passing through a low pass filter, contains the

bit information. Data decision is made by using the polarity of this output signal.

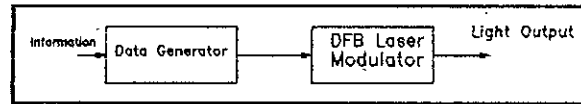


Fig. 2.3(a) Block diagram of an optical transmitter.

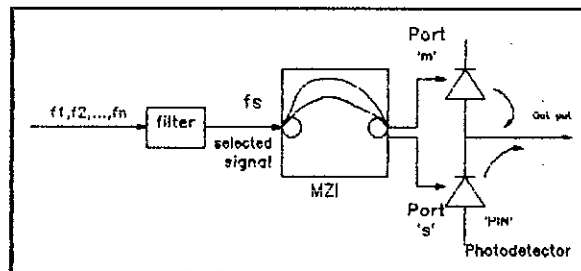


Fig. 2.3(b) A typical model of MZI based optical CPFSK DD receiver.

The system employed here has few distinctive advantages over coherent detection as follows,

- (i) It does not require any sophisticated and complicated wideband IF circuits.
- (ii) The receiver design is simple and less costly.
- (iii) For multichannel application, both MZI and FPI can be used as tunable filter and optical frequency discriminator.
- (iv) MZI can provide easy tunability in multichannel system compared to heterodyne system which requires LDs with tuning range and narrow linewidth.
- (v) The OFDs like MZI/FPI are built with passive components

. These are less costly compared to heterodyne system.

2.4.1 The Mach-Zehnder Interferometer:

In our multi-wavelength transport network, MZI is employed as the optical frequency discriminator (OFD) in the receiver model. Because, integrated MZI, consisting of silica based waveguide, is a very promising device as an OFD in WDM/FDM optical reception system [31]. It also acts as a channel selective filter and modulator. There is also FPI but MZI has some advantages over FPI like [31];

- (i) MZI periodic filters have high frequency selectivity without mechanical actuators. FP etalon filters require very high finesse and piezoelectric transducer driver or mechanical actuators for channel selection.
- (ii) MZI is 3 dB more power efficient than FPI.
- (iii) Transmission capacity can be increased by increasing the number of channels with serially connected MZI.
- (iv) Monolithic integration of MZI with laser source and operation with low driving power is possible.

The transmittances of the two port of an MZI as shown in Fig.2.4 are,

$$T_1(f) = \sin^2\left(\frac{\pi f}{4\Delta f}\right)$$

and,

$$T_2(f) = \cos^2\left(\frac{\pi f}{4\Delta f}\right)$$

where $2\Delta f$ is the separation between the "mark" and "space" frequencies of the FSK signal that is $2\Delta f$ is the peak frequency deviation.

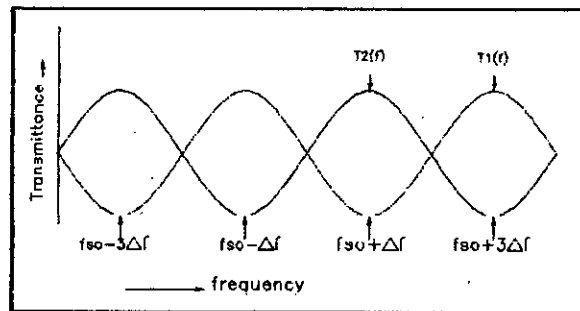


Fig.2.4 Transmittance of a Mach-Zehnder Interferometer(MZI).

For an MZI used as an OFD, $\Delta f = f_s / (2n + 1)$, f_s is the carrier frequency of the FSK signal and n is an integer. The 'mark' and 'space' of FSK signals are represented by f_1 and f_2 respectively where, $f_1 = f_s + \Delta f$ and $f_2 = f_s - \Delta f$.

Therefore, when "mark" is transmitted,

$$T_1(f_1) = 1 \quad \text{and} \quad T_2(f_2) = 0$$

Similarly when "space" is transmitted,

$$T_1(f_1) = 0 \quad \text{and} \quad T_2(f_2) = 1$$

Thus, two different signals f_1 and f_2 can be extracted from the two output ports of MZI [40].

2.5 Theoretical analysis of multiwavelength optical Transmission system:

2.5.1 The Optical Signal:

The optical FSK signal at the output of the laser transmitter can be expressed as,

$$e_s(t) = \sqrt{2P_{in}} e^{j[\omega_s t + \phi_s(t) + \phi_n(t)]} \quad (2.1)$$

where, P_{in} is the transmitted optical signal power.

$\omega_s = 2\pi f_s$; is the angular frequency of the optical carrier

, $\phi_s(t)$ is the modulated (FSK) phase and $\phi_n(t)$

represents the phase noise of transmitting laser. For an ideal

laser with zero linewidth $\phi_n(t) = 0$.

The modulated phase $\phi_s(t)$ is given by,

$$\phi_s(t) = 2\pi\Delta f \int_{-\infty}^t \sum_{k=-\infty}^{\infty} a_k \cdot p(t-kT) dt \quad (2.2)$$

where, $p(t)$ is the pulse shape, a_k is the k -th information bit, f_d is the peak frequency deviation and T is the bit period.

The signal power at the input of the MZI is written as,

$$\begin{aligned} P_s &= P_{in} L_m G_1 L_f G_2 L_{sp} L_{ps} L_{sw} \\ &= P_{in} G_T \end{aligned} \quad (2.3)$$

Here, $G_T = L_m G_1 L_f G_2 L_{sp} L_{ps} L_{sw}$, is the total gain, and the different other parameters are defined as follows,

- L_m = Loss in the Multiplexer (Combiner).
- G_1 = Gain of the first optical amplifier.
- L_f = Loss in the fiber.
- G_2 = Gain of the second optical amplifier.
- L_{sp} = Loss in the splitter.
- L_{ps} = Loss in the protection switch.
- L_{sw} = Loss in the optical space switch.

2.5.2 The FWM Signal:

If the Four-wave mixing (FWM) power generated within the

fiber, which falls on the desired signal channel frequency, is represented by P_{pqr} with frequency f_{pqr} , then the FWM signal is given by [8,14-15,20,22],

$$e_{FWM}(t) = \sum_{p,q,r} \sqrt{2P_{pqr}} e^{j[2\pi f_{pqr}t + \theta_{pqr}]}$$

(2.4)

Simply it can be expressed as,

$$e_{FWM}(t) = \sum_{p,q,r} \sqrt{2P_{pqr}} \cos[2\pi f_{pqr}t + \phi_{pqr}]$$

(2.5)

$$\begin{aligned} \text{where, } f_{pqr} &= f_p + f_q - f_r . \\ &= (f_{p0} \pm \Delta f) + (f_{q0} \pm \Delta f) - (f_{r0} \pm \Delta f) \\ &= f_{s0} + \Omega . \end{aligned}$$

Here, $\Omega = \pm \Delta f$ or $\pm 3\Delta f$. The value of Ω is dependent on whether the other channels are 'mark' or 'space' and its sign will depend on nondegenerate case ($p \neq q \neq r$) or partially degenerate case ($p = q + r$).

ϕ_{pqr} is the random phase of FWM signal and represented as, $\phi_{pqr} = \phi_p + \phi_q - \phi_r$. And f_p , f_q and f_r represents the carrier frequency of the p-th, q-th, and r-th channel respectively and f_{s0} is the optical carrier frequency. The expression for P_{pqr} is given in Appendix A.

2.5.3 The Combined Optical Field:

The combined optical field at the output of the fiber that is at the input of the MZI can be expressed as,

$$\begin{aligned}
 E(t) = & \sqrt{2P_s} \cdot \text{Exp} j [2\pi f_s t + \phi_s(t) + \phi_n(t)] \\
 & + \sum_{p,q,r} \sqrt{2P_{pqr}} \cdot \text{Exp} j [2\pi f_{pqr} t + \phi_{pqr}(t)] \\
 & + e_{ASE}(t)
 \end{aligned}
 \tag{2.6}$$

where, $e_{ASB}(t)$ is the optical amplifier's spontaneous emission signal which is given by [23],

$$e_{ASE}(t) = \sum_{K=-M}^M \sqrt{2N_0 \delta v} e^{j[\omega_s t + 2\pi k \delta v t + \Omega_k]}
 \tag{2.7}$$

where $N_0 = N_{sp} (G - 1) h\nu$ is the power spectral density of ASE signal, N_{sp} is the spontaneous emission factor, $h\nu$ is the photon energy, δv is the frequency separation between the discrete components of $e_{ASB}(t)$ such that M becomes as integer $M = B_0/2\delta v$, B_0 is the bandwidth of optical amplifier, and G is

the amplifier, s gain in which the ASE noise is generated and Ω_k is the random phase for each component of the spontaneous emission [23].

Let us assumed that $\phi_s(t)$ is uniformly distributed phase. If 'mark' is transmitted, by setting the value of Ω , we get from equation (2.4) with ,

$$\begin{aligned} f_s &= f_{s0} + \Delta f \text{ for "mark", and} \\ &= f_{s0} - \Delta f \text{ for "space"} \end{aligned}$$

The signal is now expressed as,

$$\begin{aligned} E(t) &= \sqrt{2P_s} \cdot e^{j[2\pi(f_{s0} + \Delta f)t + \phi_s(t) + \phi_{II}]} \\ &+ \sum_I \sqrt{2P_{pqr}} e^{j[2\pi(f_{s0} + \Delta f)t + \phi_{pqr}]} \\ &+ \sum_{III} \sqrt{2P_{pqr}} e^{j[2\pi(f_{s0} - 3\Delta f)t + \phi_{pqr}]} \\ &+ \sum_k \sqrt{2P_{pqr}} e^{j[2\pi(f_{s0} \pm k\Delta f)t + \phi_{pqr}]} \\ &+ e_{ASE}(t) \end{aligned} \tag{2.8}$$

The subscript Σ_I and Σ_{III} and Σ_k of the equation (2.8) represent the summation for the signals of FWM lights at frequencies of $(f_{s0} + \Delta f)$, $(f_{s0} - 3\Delta f)$ and $(f_{s0} \pm k\Delta f)$ respectively. The value of k will be greater than 3 but odd numbers and its sign can be determined accordingly. The third and fourth terms of that equation can be neglected.

The multiplexed optical FSK signal and generated FWM signal coupled into an optical filter, which selects one of the multiplexed signal lights. This selected signal light is coupled into a Mach-Zehnder Type frequency discriminator which converts frequency modulated light into intensity modulated light. When the signal has the "mark" and "Space" frequency, it appears at port "m" and "s" of the frequency discriminator, respectively. Output from the MZI is detected by dual PIN detectors and demodulated.

Hence adding noise terms (ASE noise) and taking the real parts of the optical fields and neglecting the higher frequency components we get the MZI input signal as,

$$\begin{aligned}
 E(t) = & \sqrt{2P_s} \cos[2\pi(f_{s0} + \Delta f)t + \phi_0] \\
 & + \sum \sqrt{2P_{pqr}} \cos[2\pi(f_{s0} + \Delta f)t + \phi_{pqr} - \phi_0 + \phi_0] \\
 & + N_c(t) \cos[2\pi(f_{s0} + \Delta f)t + \phi_0] \\
 & - jN_s(t) \sin[2\pi(f_{s0} + \Delta f)t + \phi_0]
 \end{aligned}
 \tag{2.9}$$

Where $\phi_0 = \phi_s(t) + \phi_n$. But here we assumed $\phi_n = 0$. Now simplifying the above expression we get the MZI input is,

$$\begin{aligned}
E(t) = & \left[\sqrt{2P_s} + \sum \sqrt{2P_{pqx}} \cdot \text{Cos}(\phi') + N_c(t) \right] \text{Cos}[2\pi(f_{so} + \Delta f)t + \phi_o] \\
& + \left[\sum \sqrt{2P_{pqx}} \text{Sin}(\phi') - N_s(t) \right] \text{Sin}[2\pi(f_{so} + \Delta f)t + \phi_o]
\end{aligned}
\tag{2.10}$$

where $\phi' = \phi_{pqx} - \phi_o$.

or, the equation can be written as,

$$E(t) = R \text{Cos}[2\pi(f_{so} + \Delta f)t + \phi_o + \Psi_{S-FWM}]
\tag{2.11}$$

where,

$$R = \sqrt{\left[\sqrt{2P_s} + \sum \sqrt{2P_{pqx}} \text{Cos}(\phi') + N_c(t) \right]^2 + \left[\sum \sqrt{2P_{pqx}} \text{Sin}(\phi') - N_s(t) \right]^2}
\tag{2.12}$$

and,

$$\Psi_{S-FWM} = \tan^{-1} \left(\frac{\sum \sqrt{2P_{pqx}} \text{Sin}(\phi') - N_s(t)}{\sqrt{2P_s} + \sum \sqrt{2P_{pqx}} \text{Cos}(\phi') + N_c(t)} \right)
\tag{2.13}$$

The term Ψ_{S-FWM} is a random variable with variance,

$$\sigma^2 = \sum P_{pqx} + \sigma_{ASE}^2$$

Where,

$$\sigma_{ASE}^2 = G_T h\nu \eta_{sp}' B_0$$

, B_0 is the optical filter bandwidth, $h\nu$ is the photon energy, η_{sp}' is the accumulated spontaneous emission factor and its expression is provided in the appendix B.

Following Ref.[32], the probability density function of Ψ_{S-FWM} can be written as ,

$$P(\Psi_{S-FWM}) = \int_0^{\infty} \left(-\frac{dX}{\pi} X \text{Exp}[-(X^2 + \rho - 2X\sqrt{\rho} \text{Cos}(\Psi_{S-FWM}))] \right) \quad (2.14)$$

where ,

$$\rho = \frac{P_s}{\sum P_{pqr} + \sigma_{ASE}^2} \quad (2.15)$$

The optical fields at the output of the two branches of MZI are,

$$E_1(t) = \frac{1}{2} [E(t - \tau_a) - E(t - \tau_b)] \quad (2.16)$$

$$E_2(t) = \frac{1}{2}[E(t - \tau_a) + E(t - \tau_b)]$$

(2.17)

where, τ_a and τ_b are the time delays in the two arms of the MZI and $(\tau_a - \tau_b) = \tau$. Without loss of generality we can take $\tau_a = 0$, then $\tau_b = \tau$. Using equation (2.8) and (2.15), the output currents of two photodetectors of MZI are,

$$i_1(t) = R_d |E_1(t)|^2$$

(2.18)

$$i_2(t) = R_d |E_2(t)|^2$$

(2.19)

where R_d is the responsivity of the photodetectors. Using equation (2.16), (2.18) and (2.17), (2.19) we get,

$$i_1(t) = \frac{R_d P_s'}{2} \left[1 + \cos[2\pi f_{so}\tau + 2\pi\Delta f \int_{t-\tau}^t \sum a_k \cdot P(t-kT) dt + \Delta\psi_{S-PWM}(t, \tau)] \right]$$

(2.20)

and,

$$i_2(t) = \frac{R_d P_s'}{2} \left[1 - \cos[2\pi f_{so}\tau + 2\pi\Delta f \int_{t-\tau}^t \sum a_k \cdot P(t-kT) dt + \Delta\psi_{S-PWM}(t, \tau)] \right]$$

(2.21)

$$P_s' = 2P_s + 2 \sum P_{pqr} + \sigma_{ASE}^2 \quad (2.22)$$

and the combined phase $\psi_{S-FWM}(t, \tau)$, which is expressed as,

$$\begin{aligned} \Delta\psi_{S-FWM}(t, \tau) &= \int_{t-\tau}^t \psi_{S-FWM} dt \\ &= \psi_{S-FWM}(t) - \psi_{S-FWM}(t-\tau) \end{aligned} \quad (2.23)$$

If we assume that $\psi_{S-FWM}(t)$ and $\psi_{S-FWM}(t - \tau)$ are independent which means that $N(t)$ and $N(t - \tau)$ and $\phi_{pqr}(t)$ and $\phi_{pqr}(t - \tau)$ are uncorrelated for the MZI.

2.5.4 The Bit Error Rate Calculation:

The probability density function (pdf) of $\Delta\psi_{S-FWM}$ can be obtained by taking convolution of the pdf of $\psi_{S-FWM}(t)$ and $\psi_{S-FWM}(t - \tau)$ that is already given in equation (2.14), that is,

$$p(\Delta\psi_{S-FWM}) = p(\psi_{S-FWM}(t)) * p(\psi_{S-FWM}(t - \tau)) \quad (2.24)$$

With some mathematical manipulation analytical expression for $p(\Delta\psi_{S-FWM})$ can be given by [32],

$$p(\Delta\psi) = \frac{e^{-U}}{4\pi} \int_0^\pi [1 + U + U \sin(\alpha) \cos(\Delta\psi_{S-FWM})] e^{U \sin(\alpha) \cos(\Delta\psi_{S-FWM})} \sin(\alpha) d\alpha \quad (2.25)$$

where, $|\Delta\psi| \leq \pi$. and,

$$U = \rho = \frac{P_s}{\sum P_{pqr} + \sigma_{ASE}^2} \quad (2.26)$$

Assuming that a 'mark' is transmitted i.e. $a_0 = 1$ and fulfilling the following demodulation conditions,

$2\pi(\Delta f)\tau = (2n+1)\pi/2$.(Here n is an integer). That is,

$2\pi(\Delta f)\tau = \pi/2$.The 'mark' signal current is given by,

$$i_m(t) = R_d P_s' \cos(\Delta\psi_{S-FWM})$$

Similarly for 'space' the signal current is,

$$i_s(t) = -R_d P_s' \cos(\Delta\psi_{S-FWM})$$

In the above equations $\tau = T/2h$,Where, $h = 2(\Delta f)\tau$ is the modulation index.

The total noise power σ^2 at the balanced photodetector output is given by,

$$\begin{aligned} \sigma^2 = & P_{shot} + P_{th} + P_{FWM-sp} + P_{ssp} \\ & + P_{s-FWM} + P_{sp-sp} + P_{c-sp} + P_{ASE} \end{aligned}$$

(2.27)

Where P_{FWM-sp} , represents the FWM-spontaneous emission beat noise power, P_{ssp} is the power of signal-spontaneous emission beat noise, P_{s-FWM} is the signal-FWM beat noise power and P_{sp-sp} is the spontaneous-spontaneous beat noise power, P_{c-sp} is the adjacent channel crosstalk-spontaneous emission beat noise power and P_{ASE} is the amplifier's spontaneous emission power. The expressions for these above noise powers are given in Appendix B.

For a given value of $\Delta\psi_{s-FWM}(t, \tau) = \Delta\psi$ the signal to noise ratio at the output of the receiver is given by,

$$\begin{aligned} Q &= \frac{i_m - i_s}{\sigma_m + \sigma_s} = \frac{2i_m}{2\sigma_m} \\ &= \frac{2R_d P_s' \text{Cos}(\Delta\psi)}{\sigma} \end{aligned}$$

(2.28)

Conditioning on $\Delta\psi$, the conditional bit error rate for the receiver is [33],

$$\begin{aligned}
p(e/\Delta\psi) &= BER(\Delta\psi) \\
&= \frac{1}{2} \operatorname{erfc}\left(\frac{Q}{\sqrt{2}}\right)
\end{aligned}$$

Where, $\operatorname{erfc}(x)$ represents the complimentary error function defined as,

$$\begin{aligned}
\operatorname{erfc}(x) &= 1 - \operatorname{erf}(x) \\
&= \frac{2}{\sqrt{\pi}} \int_{-\infty}^{\infty} e^{-x^2} dx
\end{aligned}$$

(2.29)

The unconditional bit error rate (BER) can be obtained by averaging the conditional bit error rate over the distribution of $\Delta\psi$. Then the BER is expressed as,

$$BER = \sum_n \int_{-\pi}^{\pi} \frac{1}{2} \operatorname{erfc}\left(\frac{Q}{\sqrt{2}}\right) p(\Delta\psi + 2n\pi) d(\Delta\psi)$$

(2.30)

where, n is an integer. If $n = 0$ then the bit error rate (BER) simply will be as,

$$BER = \int_{-\pi}^{\pi} \frac{1}{2} \operatorname{erfc}\left(\frac{Q}{\sqrt{2}}\right) p(\Delta\psi) d(\Delta\psi)$$

(2.31)

CHAPTER - 3

RESULTS AND DISCUSSIONS

Following the theoretical analysis presented in chapter 2, the theoretical performance results for multiwavelength optical transport system is evaluated at a bit rate of 2.5 Gb/s considering the FWM effect for several sets of values of the receiver and system parameters. The parameters used in the theoretical computations are:

Bit rate, $B_r = 2.5$ Gb/s

Fiber attenuation, $\alpha = 0.2$ dB/Km

Fiber chromatic dispersion, $D_c = 1$ ps/nm-Km

Optical wavelength, $\lambda = 1550$ nm

Responsivity factor, $R_d = 0.85$

Loss of WDM MUX, $L_m = -4.0$ dB

Loss of splitter, $L_s = -3.0$ dB

Loss of fiber protection switch, $L_{ps} = -6.0$ dB

Loss of WDM DMUX, $L_{dm} = -4.0$ dB

Loss of optical space switch, $L_{sw} = -10.0$ dB

Gain of optical amplifier in the head-end, $G_1 = 18.0$ dB

Gain of optical amplifier in the front-end, $G_2 = -G_1 - L_T$ (dB)

Bandwidth of optical filter, $B_{FP} = 4.0B_r$

Bandwidth of preamplifier, $B_a = 0.7B_r$

Fiber core diameter, $W = 0.5 \times 11^{-6} \text{ m}$

Refractive index of fiber, $n = 1.45$

Nonlinear susceptibility, $\chi = 5 \times 10^{-14} \text{ m}^3/\text{watt-sec.}$

Thermal noise current spectral density, $I_{th} = 10^{-12} \text{ A}/\sqrt{\text{Hz}}$

The bit error rate (BER) performance results of optical MWTN in the presence of FWM effect with CPFSK modulation and MZI based direct detection receiver is shown in Fig.3.1 as a function of the number of nodes M for several values of input transmitter power $P_{in} = -10, -8, -4, -2 \text{ dBm}$ when fiber span $L = 20 \text{ Km}$ and number of WDM channels $N = 11$ and optical amplifier's bandwidth $B_a = 15 \text{ GHz}$. The plots illustrate how the bit error rate varies with the number of nodes. It is found that for a given input power, the error rate increases with increasing value of the number of nodes due to accumulation of optical amplifier's spontaneous emission (ASE) from one node to another. At an specified BER, the allowable number of nodes is more at higher input power. For example, at $\text{BER} = 10^{-9}$ the allowable number of nodes is around 50 when $P_{in} = -10 \text{ dBm}$, when P_{in} is increased to -4.0 dBm , the number of allowable nodes reaches around 175.

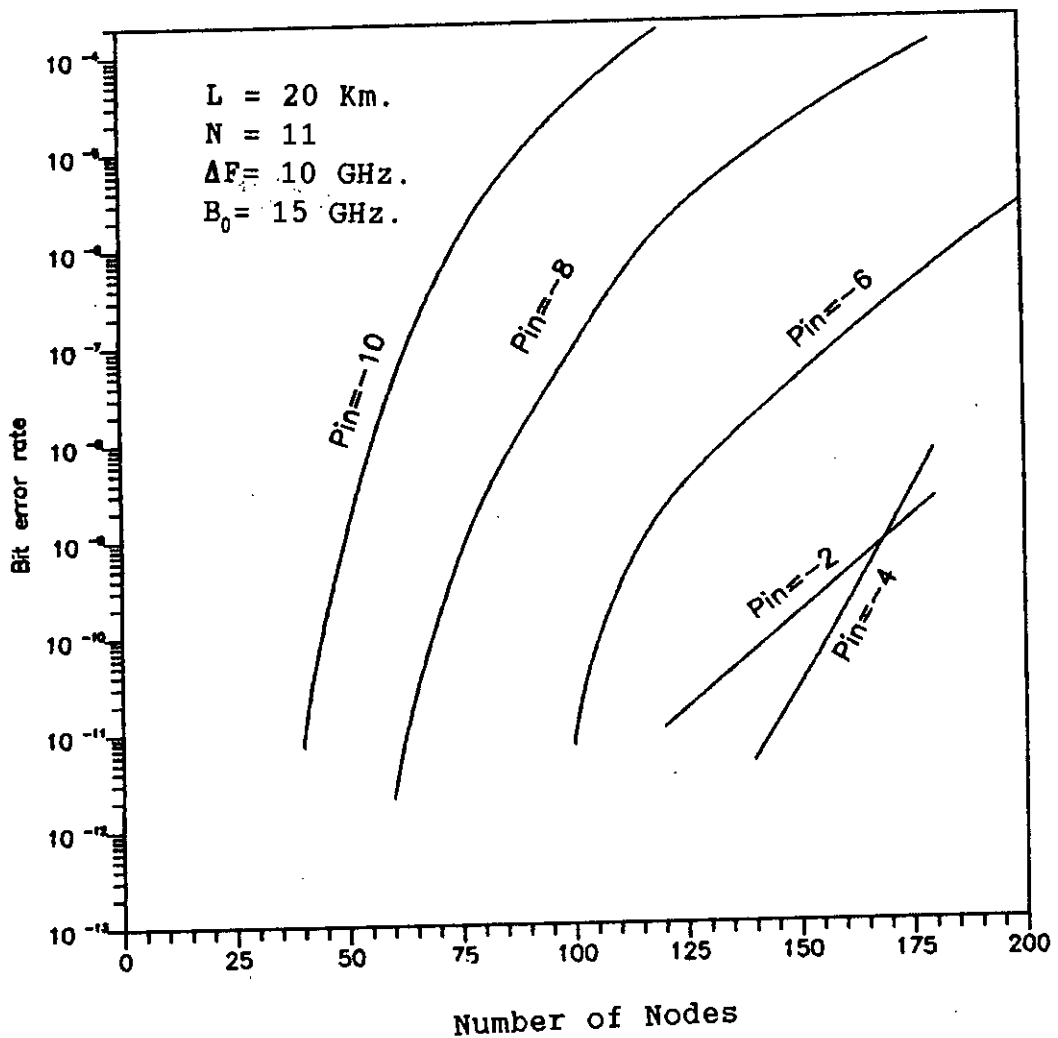


Fig.3.1 Bit error rate performance of optical multiwavelength transport network at a bit rate of 2.5 Gb/s as a function of the number of nodes M when number of channels $N=11$, fiber span $L=20$ Km, optical bandwidth $B_0=15$ GHz, $\Delta F=10$ GHz for different values of the optical transmitter power P_{in} (dBm).

When the number of channels is increased to 51 and 101, the BER performance results are shown in Fig.3.2 and Fig.3.3 respectively for the same values of fiber span L , optical bandwidth B_o and channel separation ΔF as in Fig.3.1. Comparison of these curves reveal that the system performance is degraded and the achievable number of nodes at $BER=10^{-9}$ is significantly reduced due to increased FWM power and associated beat noise components. For example, it is seen that the number of nodes corresponding to $BER=10^{-9}$ is around 175 for $N=11$ whereas it reduces to around 145 when N is increased to 101 for $P_{in}=-4$ dBm. The effect of FWM is more prominent at higher values of input power.

When the fiber span is increased to 50 Km, the performance results are depicted in Fig.3.4 for $N=51$. Comparing with Fig.3.2 it becomes evident that for the same input power, the number of allowable nodes is drastically reduced due to increased fiber span. When L is increased to 100 Km, the number of allowable nodes are further reduced as is evident from Fig.3.5. This is due to increased ASE with increased amplifier gain to meet the additional fiber loss due to increased fiber span and increased associated beat noise components viz. $FWM*ASE$, $Signal*ASE$, $ASE*ASE$ beat noise powers.

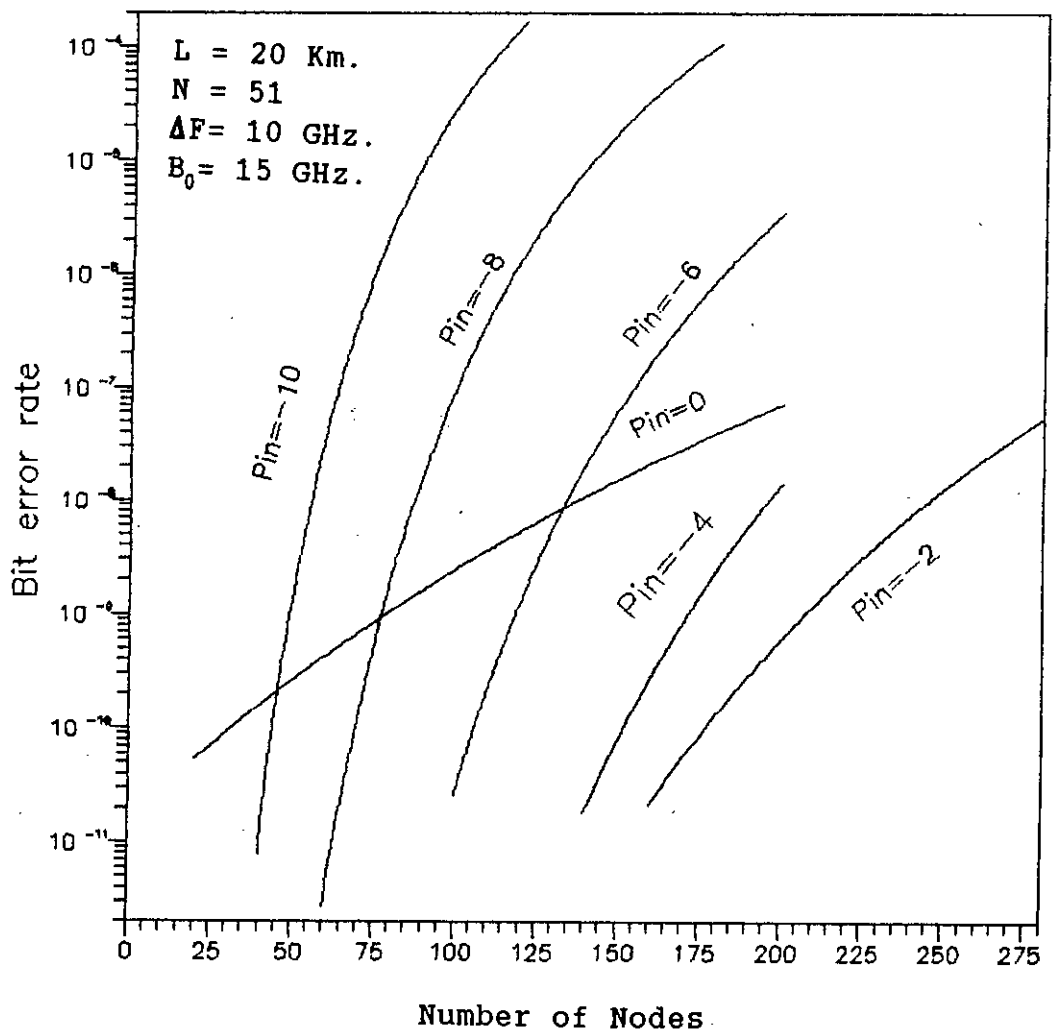


Fig.3.2 Bit error rate performance of optical MWTN at a bit rate of 2.5 Gb/s as a function of the number of nodes M when number of channels $N=51$, fiber span $L=20 \text{ Km}$, optical bandwidth $B_0=15 \text{ GHz}$, $\Delta F=10 \text{ GHz}$ for different values of the optical transmitter power P_{in} (dBm).

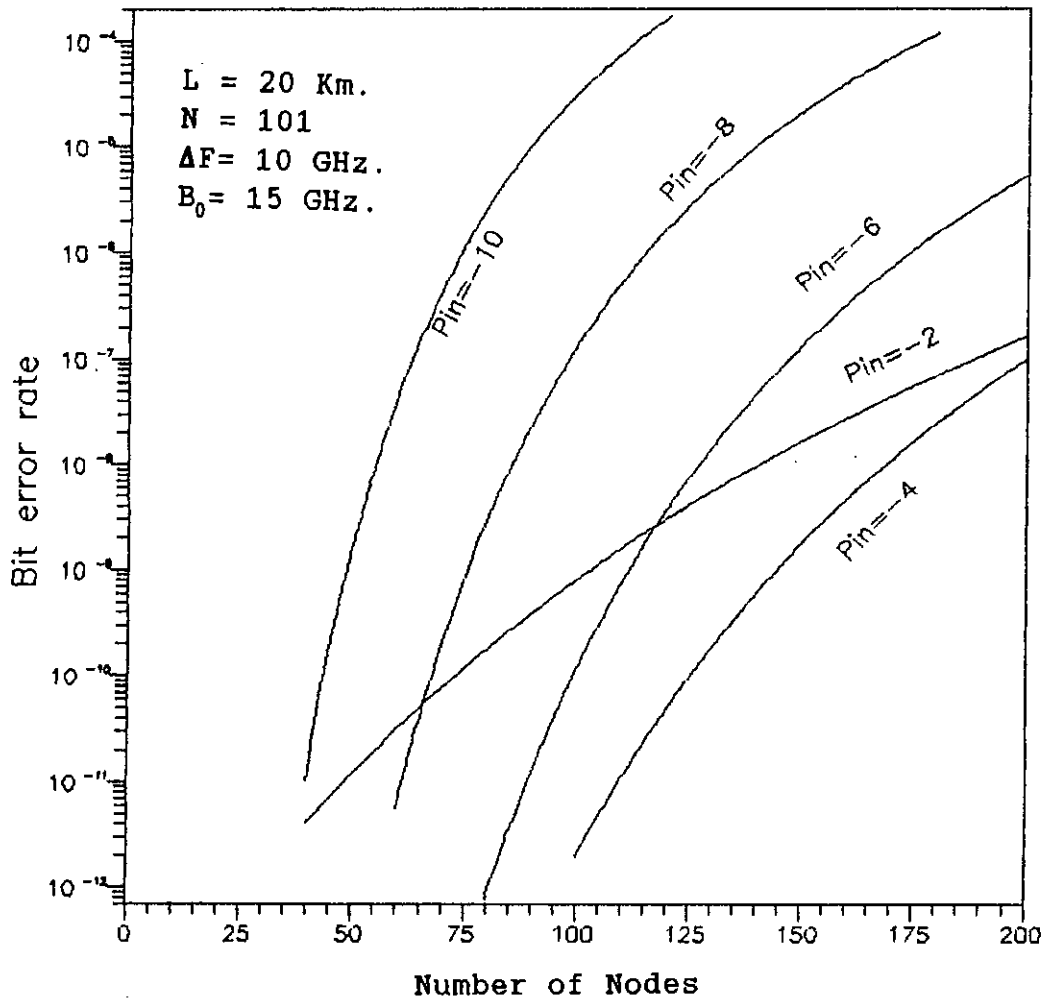


Fig.3.3 Bit error rate performance of optical MWTN at a bit rate of 2.5 Gb/s as a function of the number of nodes M when number of channels $N=101$, fiber span $L=20$ Km, optical bandwidth $B_0=15$ GHz, $\Delta F=10$ GHz for different values of the optical transmitter power P_{in} (dBm).

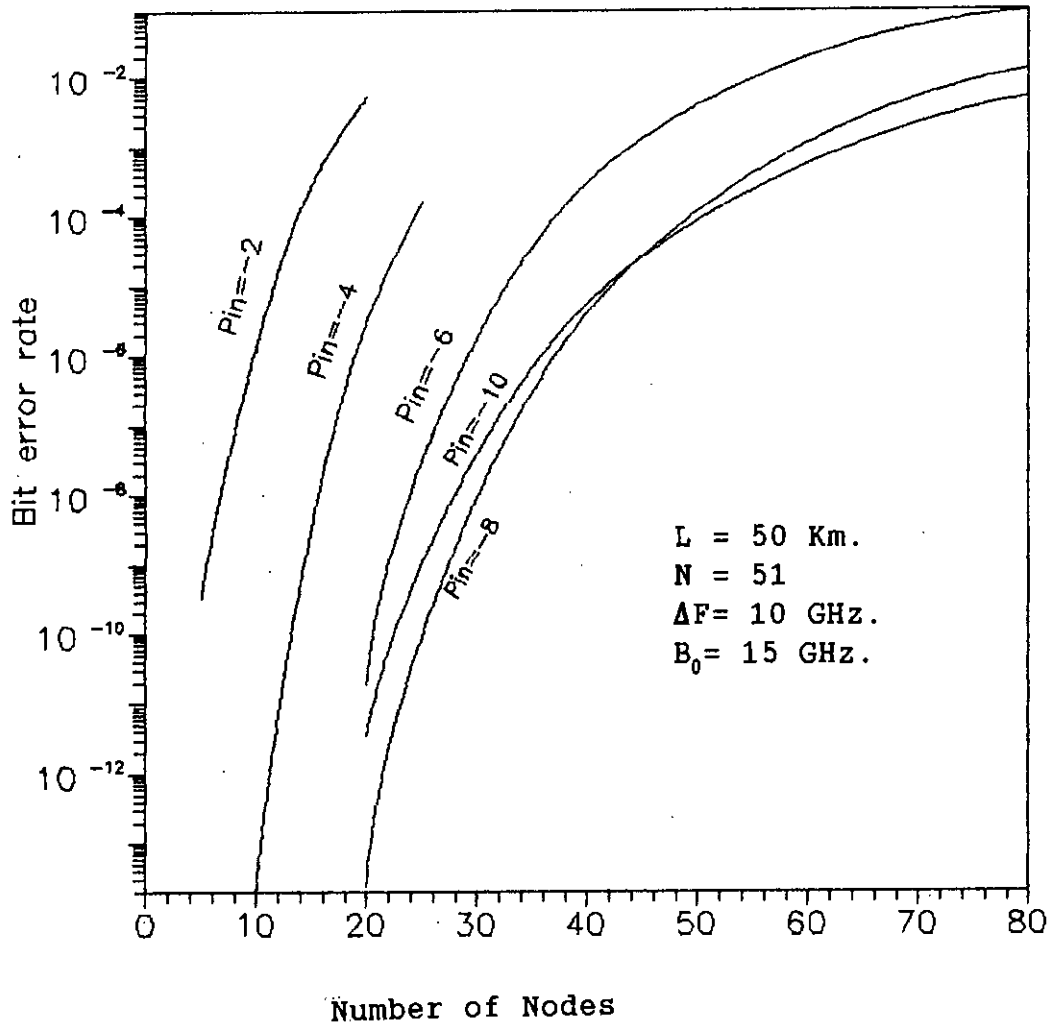


Fig.3.4 Bit error rate performance of optical MWTN at a bit rate of 2.5 Gb/s as a function of the number of nodes M when number of channels $N=51$, fiber span $L=50$ Km, $B_0=15$ GHz, $\Delta F=10$ GHz for different values of the optical transmitter power P_{in} (dBm).

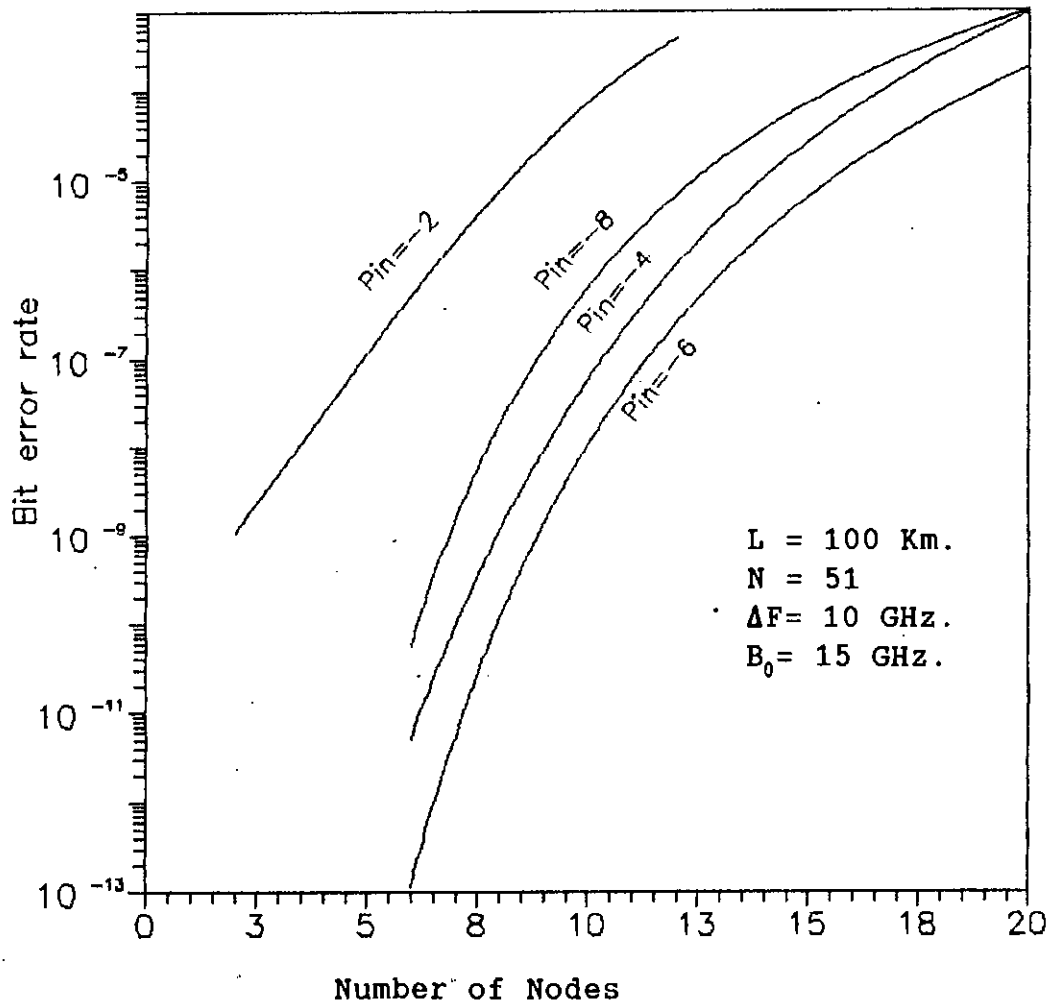


Fig.3.5 Bit error rate performance of optical MWTN at a bit rate of 2.5 Gb/s as a function of the number of nodes M when number of channels $N=51$, fiber span $L=100 \text{ Km}$, $B_0=15 \text{ GHz}$, $\Delta F=10 \text{ GHz}$ for different values of the optical transmitter power P_{in} (dBm).

For a given input transmitter power, when the channel separation is increased to 25 GHz, the performance results are shown in Fig. 3.6 as a function of BER versus number of nodes for $N=11, 51, 101$ for $\Delta F=25$ GHz, $B_o=15$ GHz and $L=20$ Km. It becomes evident that at a given $BER=10^{-9}$, the number of achievable nodes considerably decreases with increase of the number of channels. Similar observations are also found in Fig. 3.7 and Fig. 3.8 for $L=50$ Km and 100 Km. Comparison of Fig. 3.6 and Fig. 3.1 shows that the number of achievable nodes is higher in case of higher channel separation due to reduction in FWM effect for a given values of N .

When the optical bandwidth B_o is increased to 25 GHz and the channel separation is 25 GHz, the performance results are depicted in Fig. 3.9, Fig. 3.10 and Fig. 3.11 for $L=20, 50, 100$ Km respectively. Comparing Fig. 3.6 and Fig. 3.9 we note that increase of optical bandwidth causes a decrease in the number of nodes. This is due to increase in the FWM power and associated noise powers at increased optical bandwidth.

The plots of allowable number of nodes M at $BER = 10^{-9}$ as a function of input power P_{in} (dBm) is shown in Fig. 3.12 for three values of the number of channels $N = 11, 51$ and

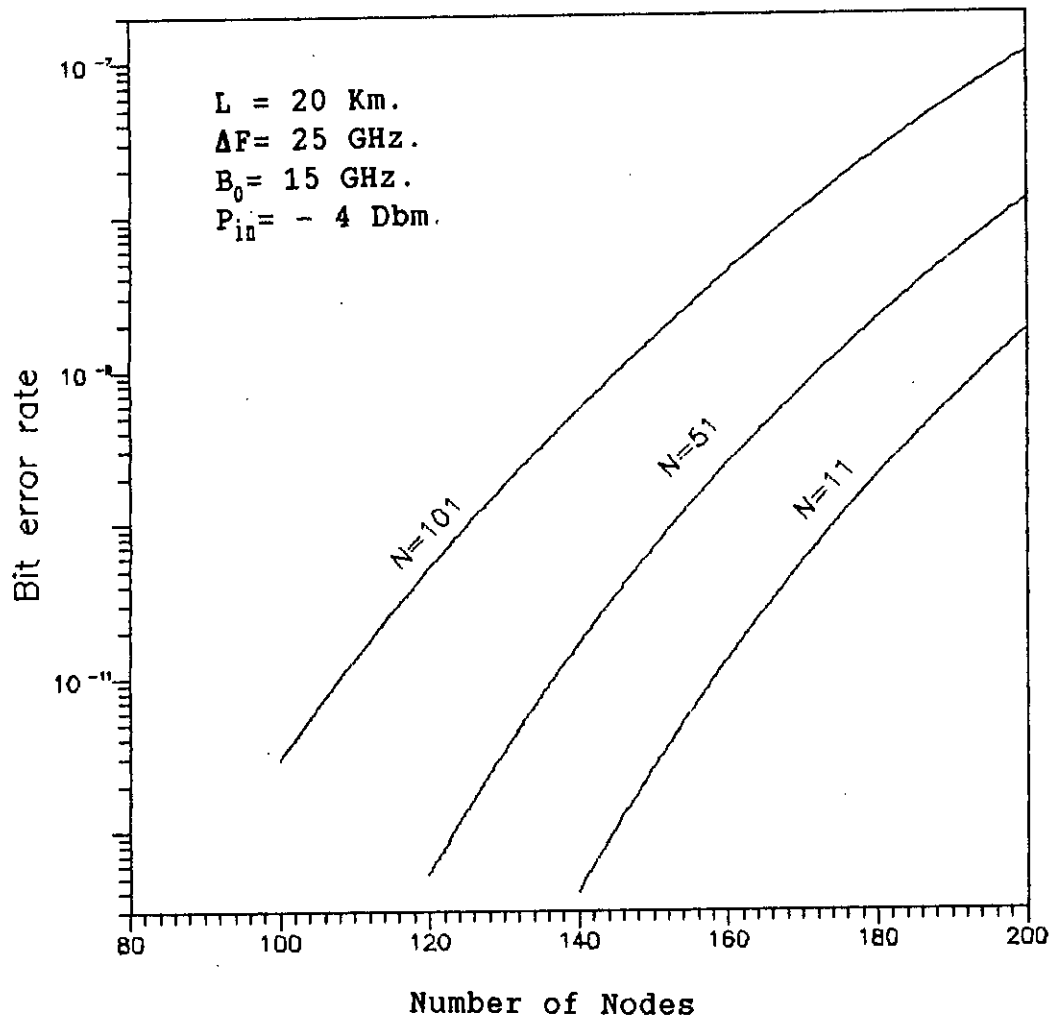


Fig.3.6 Bit error rate performance of optical MWTN versus number of nodes M , at a bit rate of 2.5 Gb/s for transmitter power $P_{in} = -4 \text{ dBm}$ and number of channels $N=11, 51, 101$ with $L=20 \text{ Km}$ and $B_0=15 \text{ GHz}, \Delta F=25 \text{ GHz}$.

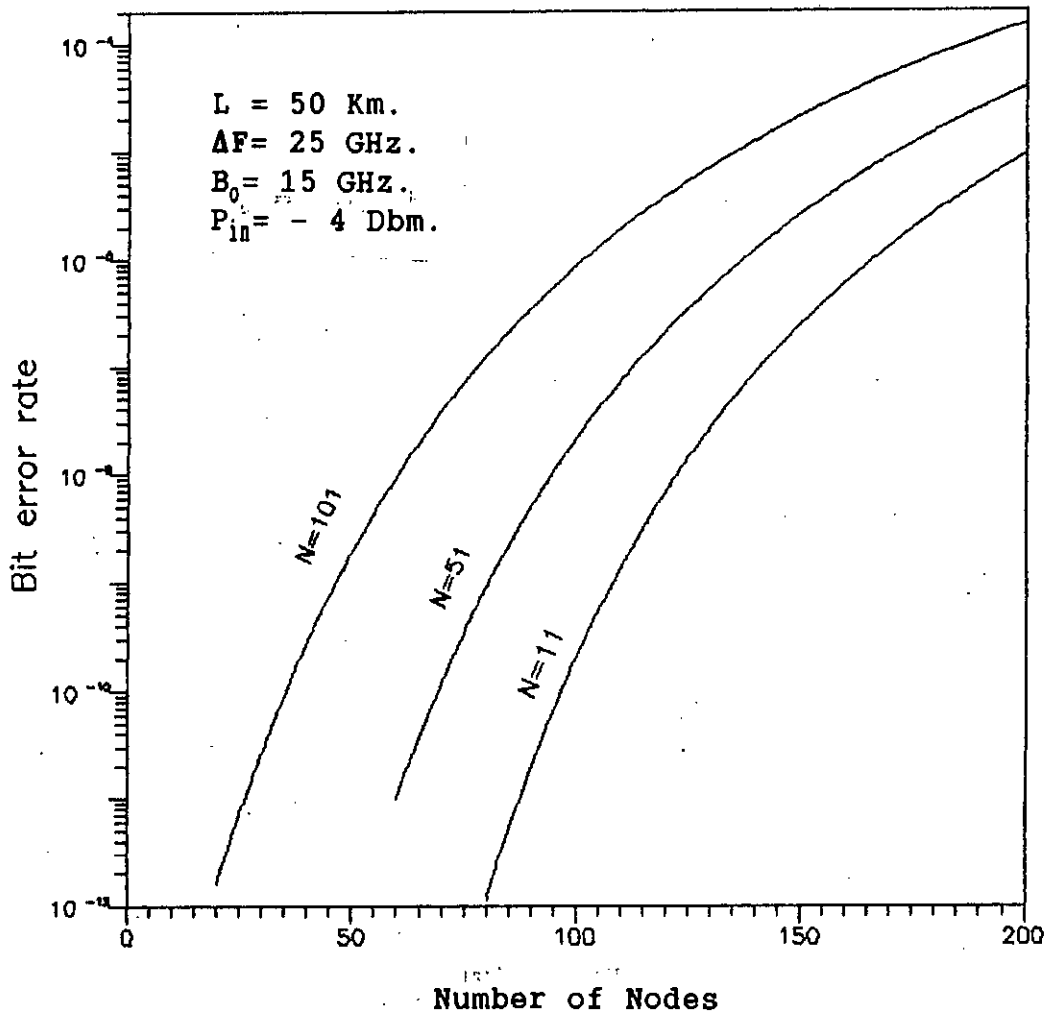


Fig.3.7 Bit error rate performance of optical MWTN versus number of nodes M , at a bit rate of 2.5 Gb/s for transmitter power $P_{in} = -4 \text{ dBm}$ and number of channels $N=11, 51, 101$ with $L=50 \text{ Km}$ and $B_0=15 \text{ GHz}$, $\Delta F=25 \text{ GHz}$.

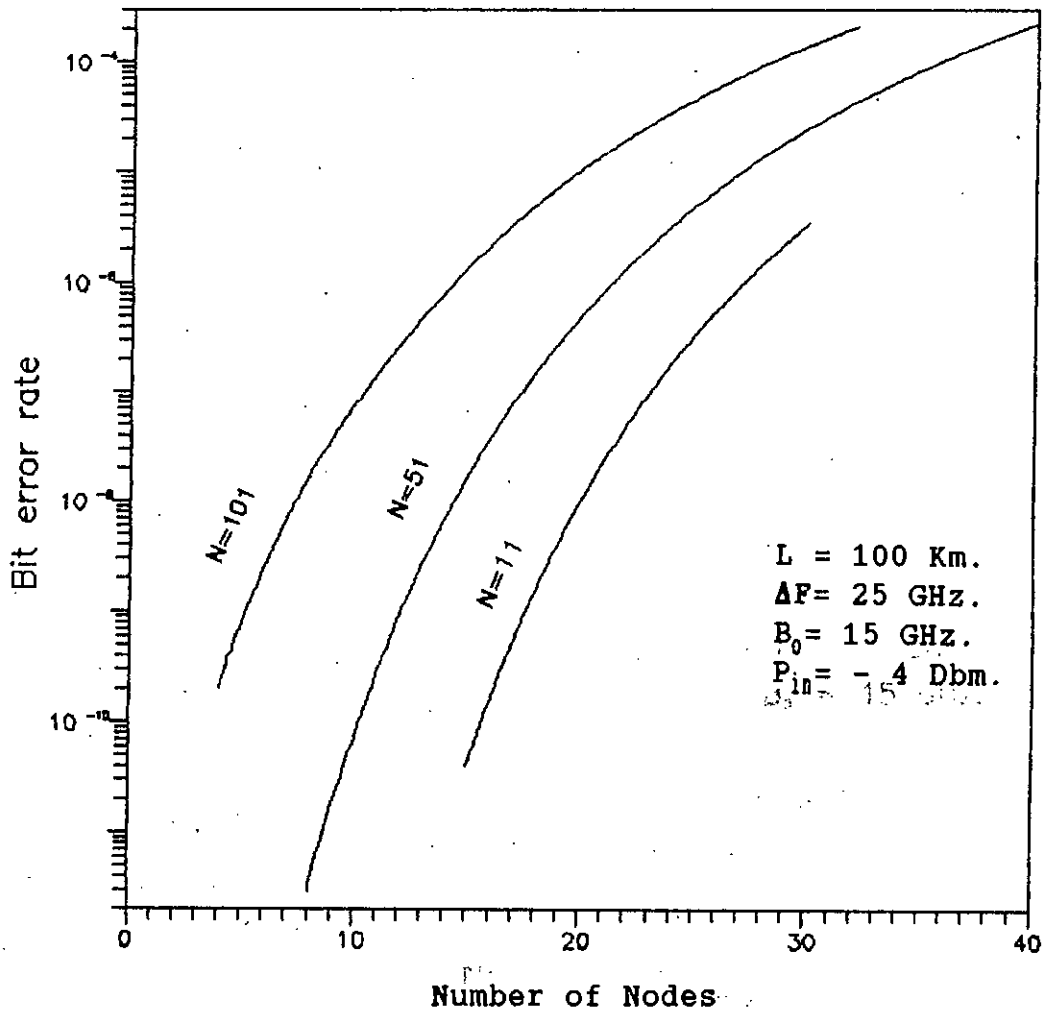


Fig.3.8 Bit error rate performance of optical MWTN versus number of nodes M , at a bit rate of 2.5 Gb/s for transmitter power $P_{in} = -4 \text{ dBm}$ and number of channels $N=11, 51, 101$ with $L=100 \text{ Km}$ and $B_0=15 \text{ GHz}, \Delta F=25 \text{ GHz}$.

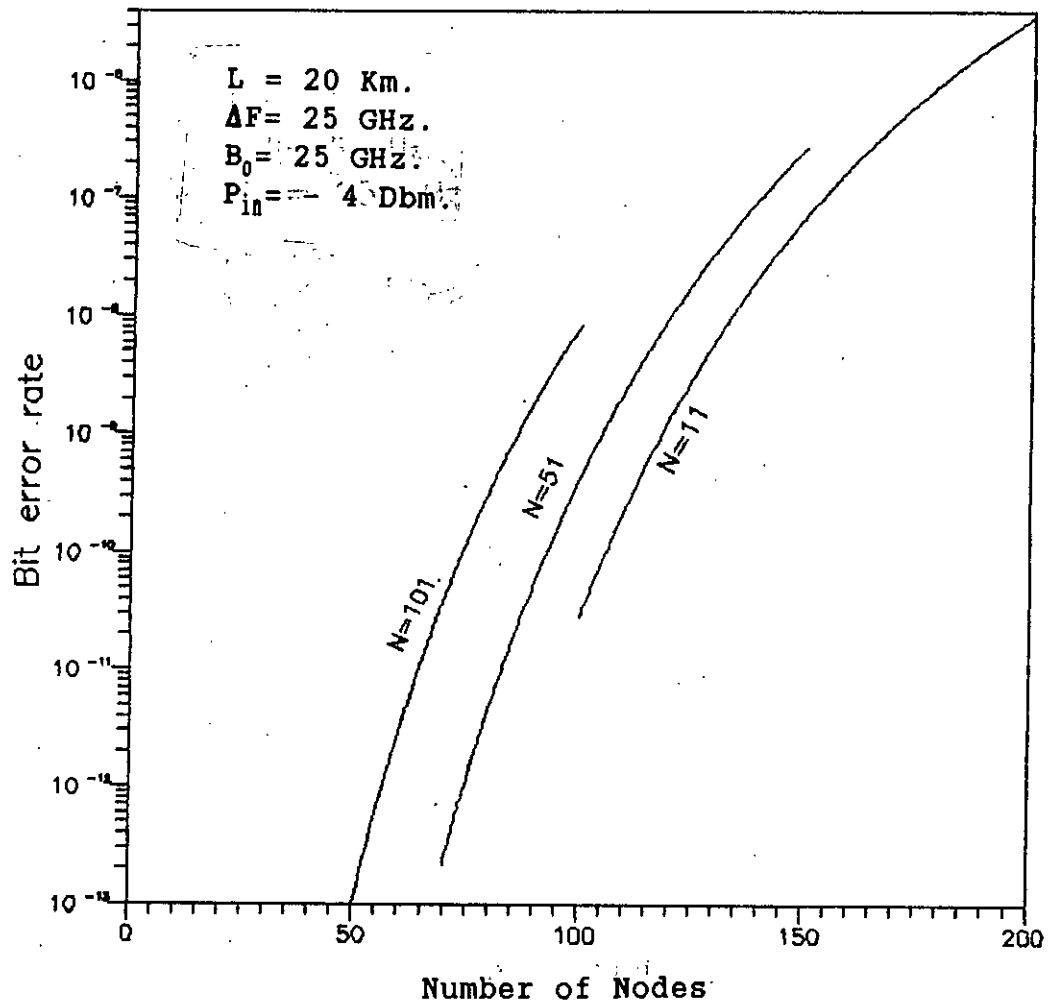


Fig.3.9 Bit error rate performance of optical MWTN versus number of nodes M , at a bit rate of 2.5 Gb/s for transmitter power $P_{in} = -4 \text{ dBm}$ and number of channels $N=11, 51, 101$ with $L=20 \text{ Km}$ and $B_0=25 \text{ GHz}, \Delta F=25 \text{ GHz}$.

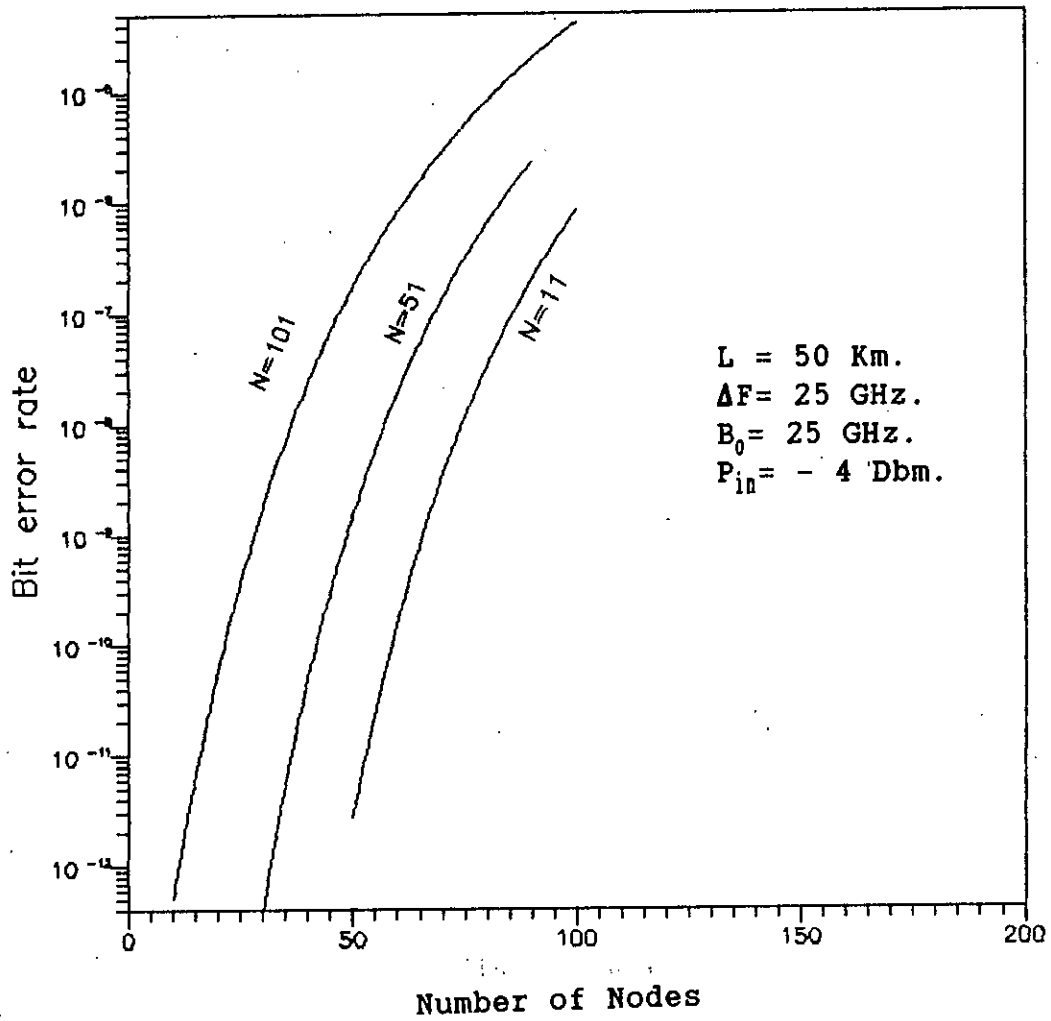


Fig.3.10 Bit error rate performance of optical MWTN versus number of nodes M , at a bit rate of 2.5 Gb/s for transmitter power $P_{in} = -4 \text{ dBm}$ and number of channels $N=11, 51, 101$ with $L=50 \text{ Km}$ and $B_0=25 \text{ GHz}, \Delta F=25 \text{ GHz}$.

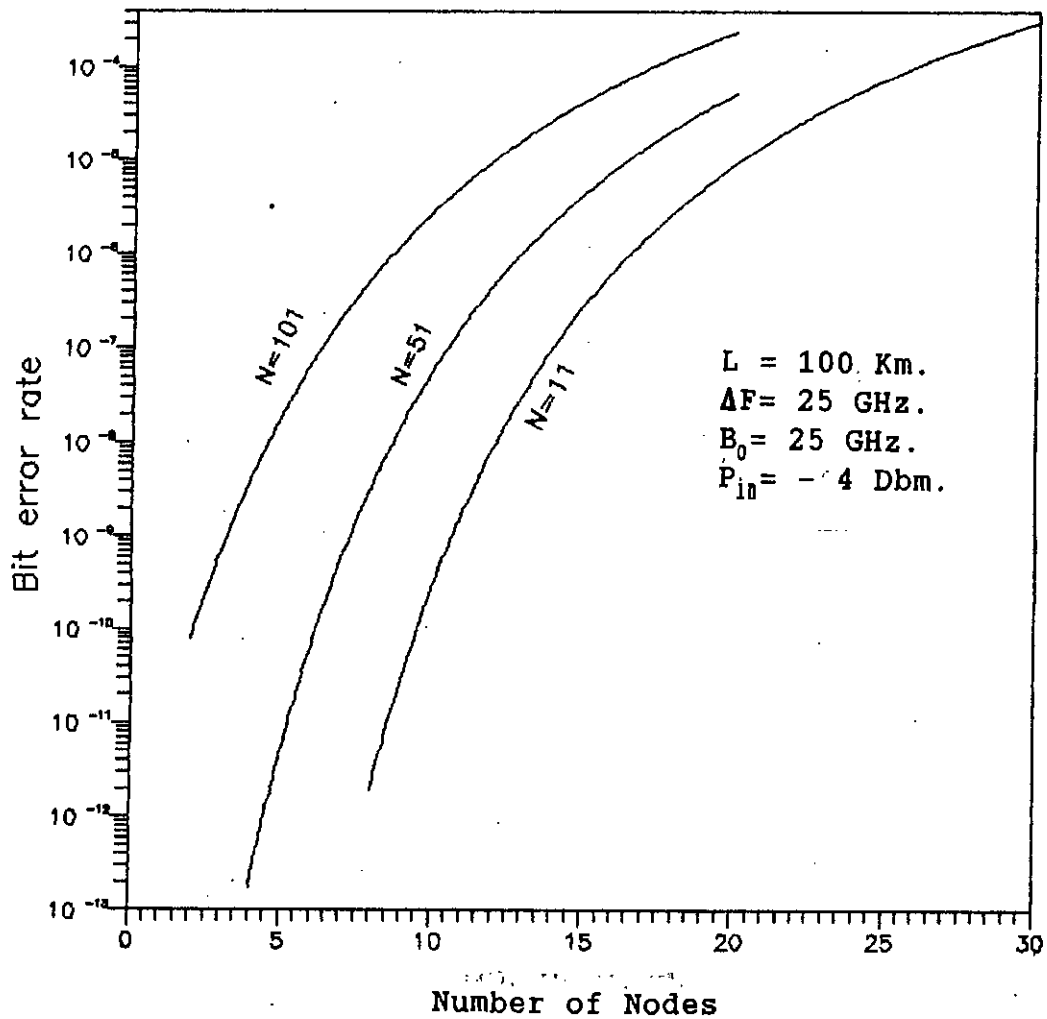


Fig.3.11 Bit error rate performance of optical MWTN versus number of nodes M , at a bit rate of 2.5 Gb/s for transmitter power $P_{in} = -4 \text{ dBm}$ and number of channels $N=11, 51, 101$ with $L=100 \text{ Km}$ and $B_0=25 \text{ GHz}, \Delta F=25 \text{ GHz}$.

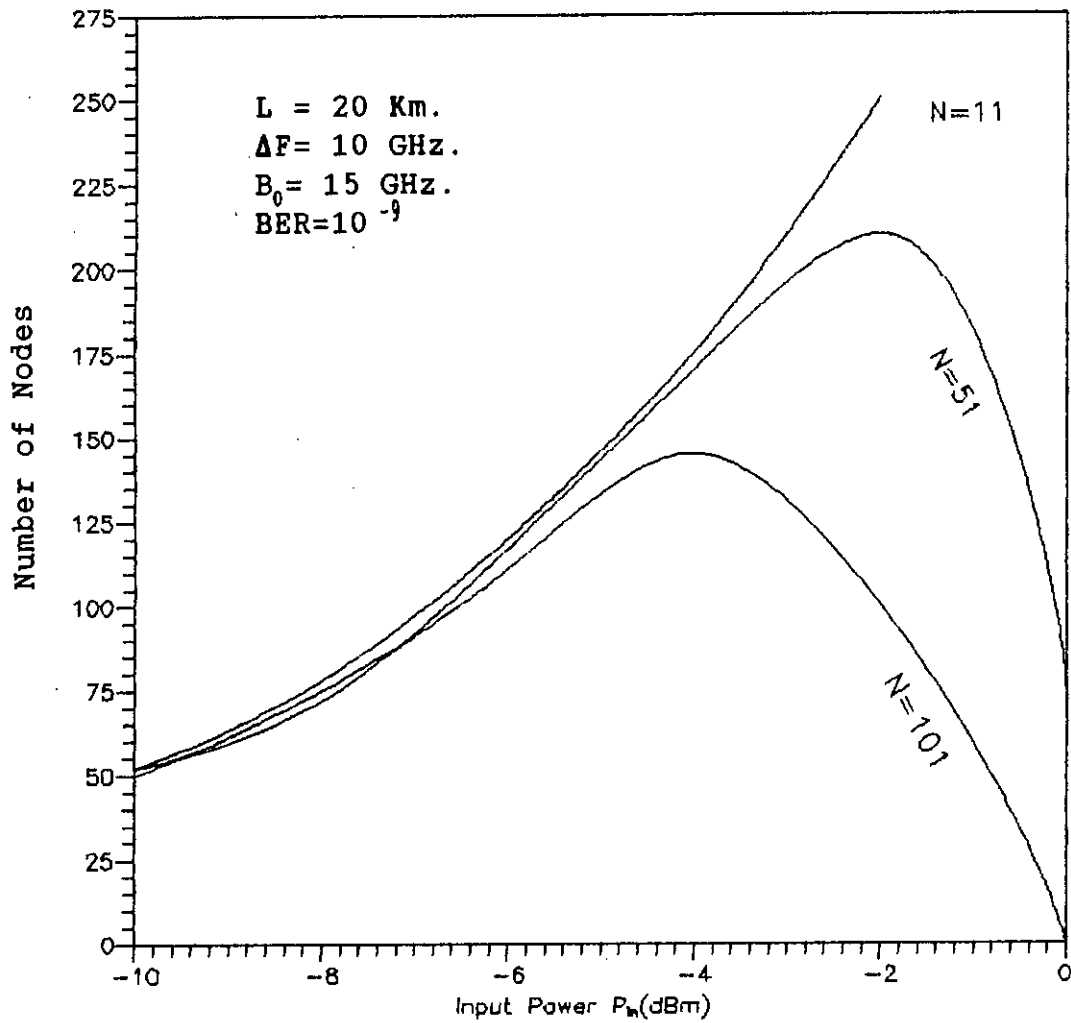


Fig.3.12 Variation of the allowable number of nodes M at $\text{BER} = 10^{-9}$ versus the transmitter power P_{in} (dBm) in the presence of FWM effect when the number of channels $N=11, 51$ and 101 and channel separation $\Delta F=10 \text{ GHz}$, $B_0=15 \text{ GHz}$ and fiber span, $L=20 \text{ Km}$.

101, when $L = 20$ Km, $B_s = 15$ GHz. The plots depict that the number of nodes increases with P_{in} but up to a certain limit where it reaches a maximum value corresponding to a given value of P_{in} and then decreases. This is due to the fact that as the input power increases, the receiver sensitivity and hence the allowable number of nodes increases and the receiver performance is limited by ASE and associated beat noise components. At increased P_{in} , the FWM power drastically increases with P_{in}^2 and as a consequence the system performance degrades and the allowable number of nodes is greatly reduced. Thus, there is a maximum value of the allowable number of nodes for a given value of the number of channels N which can be termed as M_{max} . The maximum value of M i.e., M_{max} is further reduced at increased values of the number of channels N . It is also evident that the maximum number of nodes M_{max} occurs corresponding to a maximum allowable input power $P_{in,max}$. The value of $P_{in,max}$ is less when the number of channels is increased.

Similar plots of allowable number of nodes M versus P_{in} (dBm) for higher fiber span e.g., $L = 50$ Km and 100 Km are provided in Fig.3.13 and Fig.3.14. Comparing these curves with Fig.3.12 we found that the maximum allowable

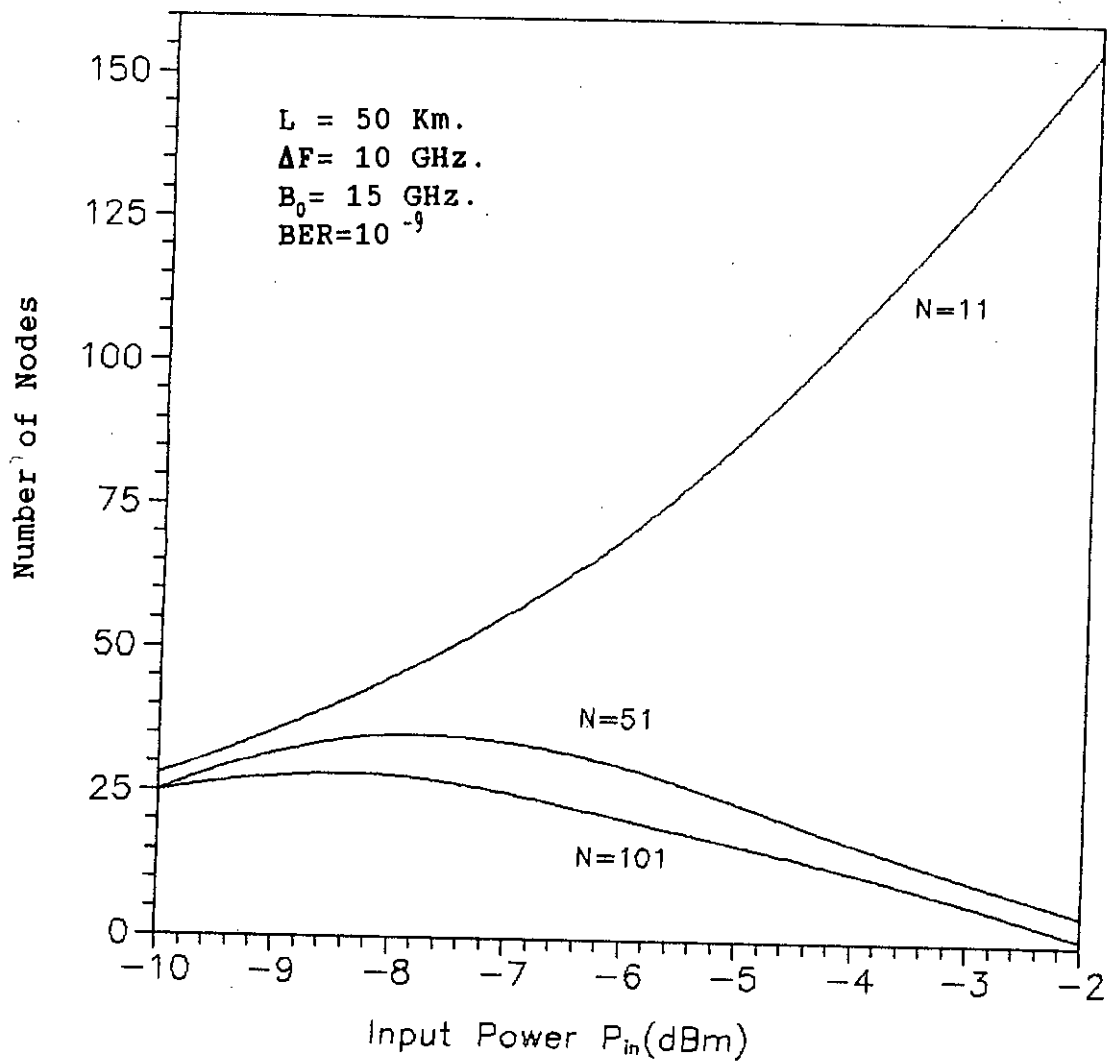


Fig.3.13 Variation of the allowable number of nodes M at $\text{BER} = 10^{-9}$ versus the transmitter power P_{iD} (dBm) in the presence of FWM effect when the number of channels $N=11, 51$ and 101 and channel separation $\Delta F=10 \text{ GHz}$, $B_0=15 \text{ GHz}$ and fiber span, $L=50 \text{ Km}$.

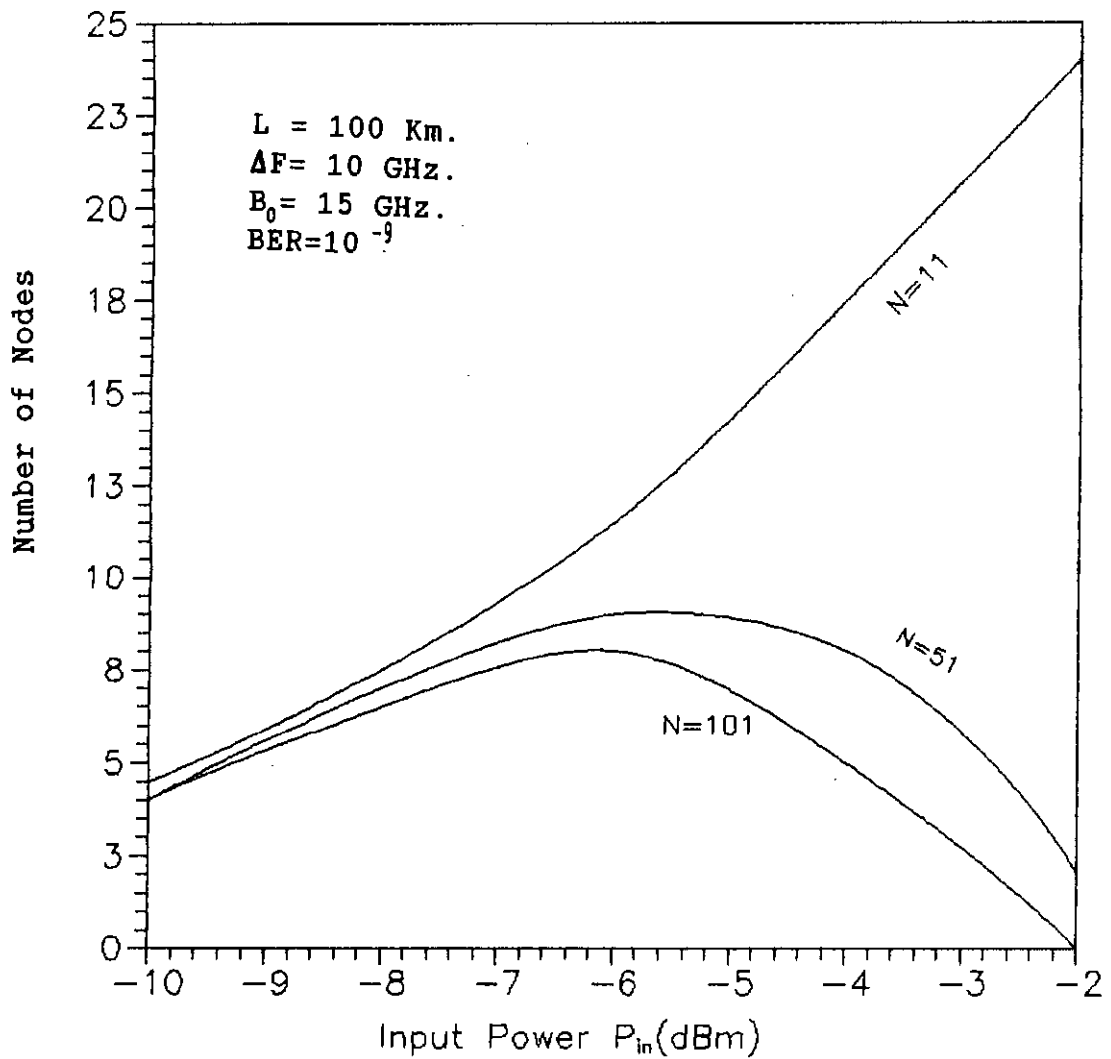


Fig.3.14 Variation of the allowable number of nodes M at $\text{BER}=10^{-9}$ versus the transmitter power P_{in} (dBm) in the presence of FWM effect when the number of channels $N=11, 51$ and 101 and channel separation $\Delta F=10 \text{ GHz}$, $B_0=15 \text{ GHz}$ and fiber span, $L=100 \text{ Km.}$

When the optical channel separation ΔF is increased, the plots of the allowable number of nodes M , corresponding to $BER = 10^{-9}$, versus P_{in} (dBm) for a given fiber span ($L = 20$ Km) is illustrated in Fig.3.15 and Fig.3.16 for $\Delta F = 25$ and 50 GHz respectively. Comparing these with Fig.3.12 it is noticed that there is a considerable increase in the number of allowable nodes as ΔF is increased from 10 GHz to 25 . However, when the channel separation ΔF is further increased to 50 GHz the number of nodes is greatly reduced. Thus, the results indicate that there is an optimum value of channel separation at which the effect of FWM is minimum. Similar observations are also noticed in Fig.3.17 and Fig.3.18 for $L=50$ Km.

In Fig.3.19 the allowable number of nodes at $BER = 10^{-9}$ is plotted as a function of the number of channels N when $L=20$ Km and $B_o = 15$ GHz for several input transmitter power P_{in} (dBm). It is noticed that at a given input power, the number of nodes reduces with increasing values of the number of channels due to increased FWM effect. The rate at which the number of nodes M decreases depends on input power P_{in} . The reduction is more rapid at higher optical input power and at low value of input power number of nodes M is almost independent of number of channels N . Similar curves of M versus N for higher span length L and higher optical bandwidth B_o are shown in Fig.3.20 and

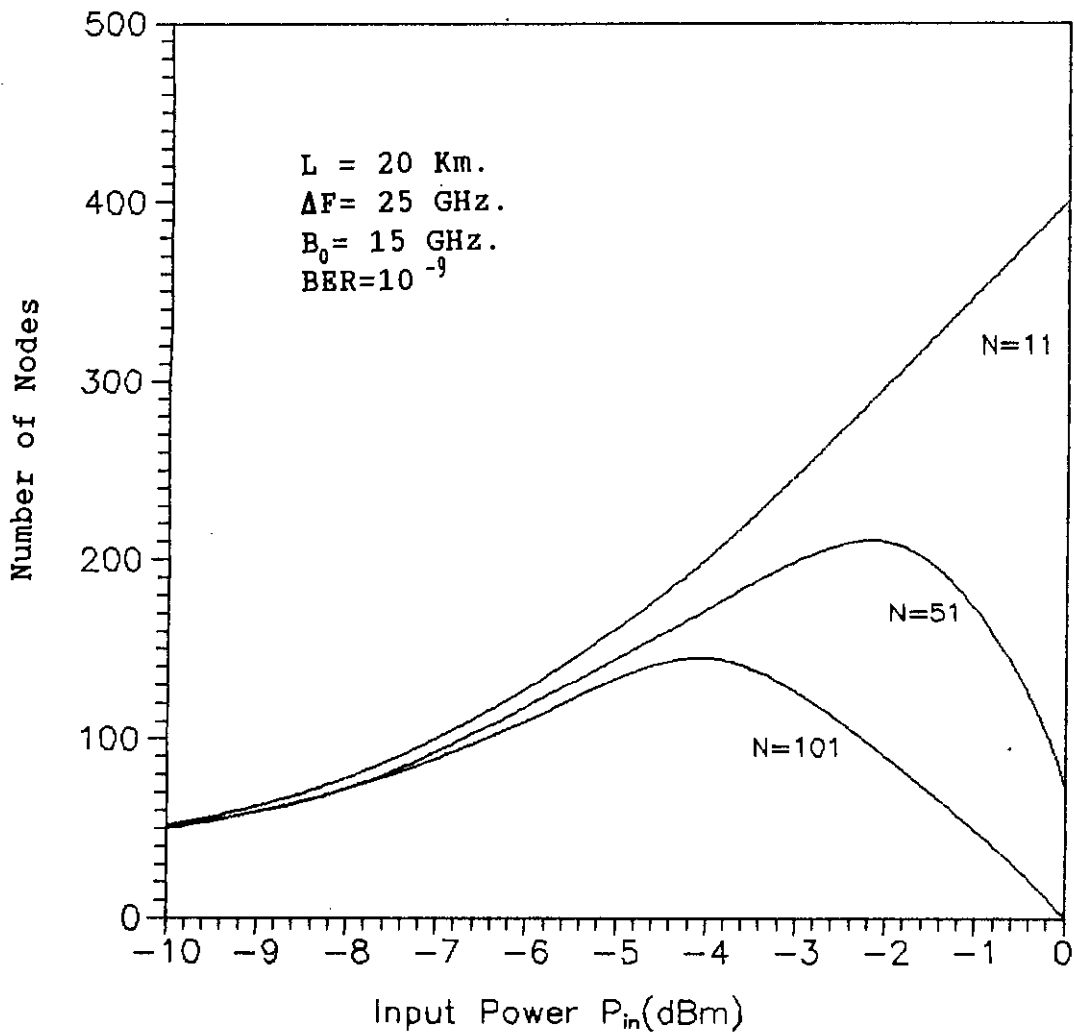


Fig.3.15 Variation of the allowable number of nodes M at $\text{BER} = 10^{-9}$ versus the transmitter power P_{in} (dBm) in the presence of FWM effect when the number of channels $N=11, 51$ and 101 and channel separation $\Delta F=25 \text{ GHz}$, $B_0=15 \text{ GHz}$ and fiber span, $L=20 \text{ Km}$.

90300

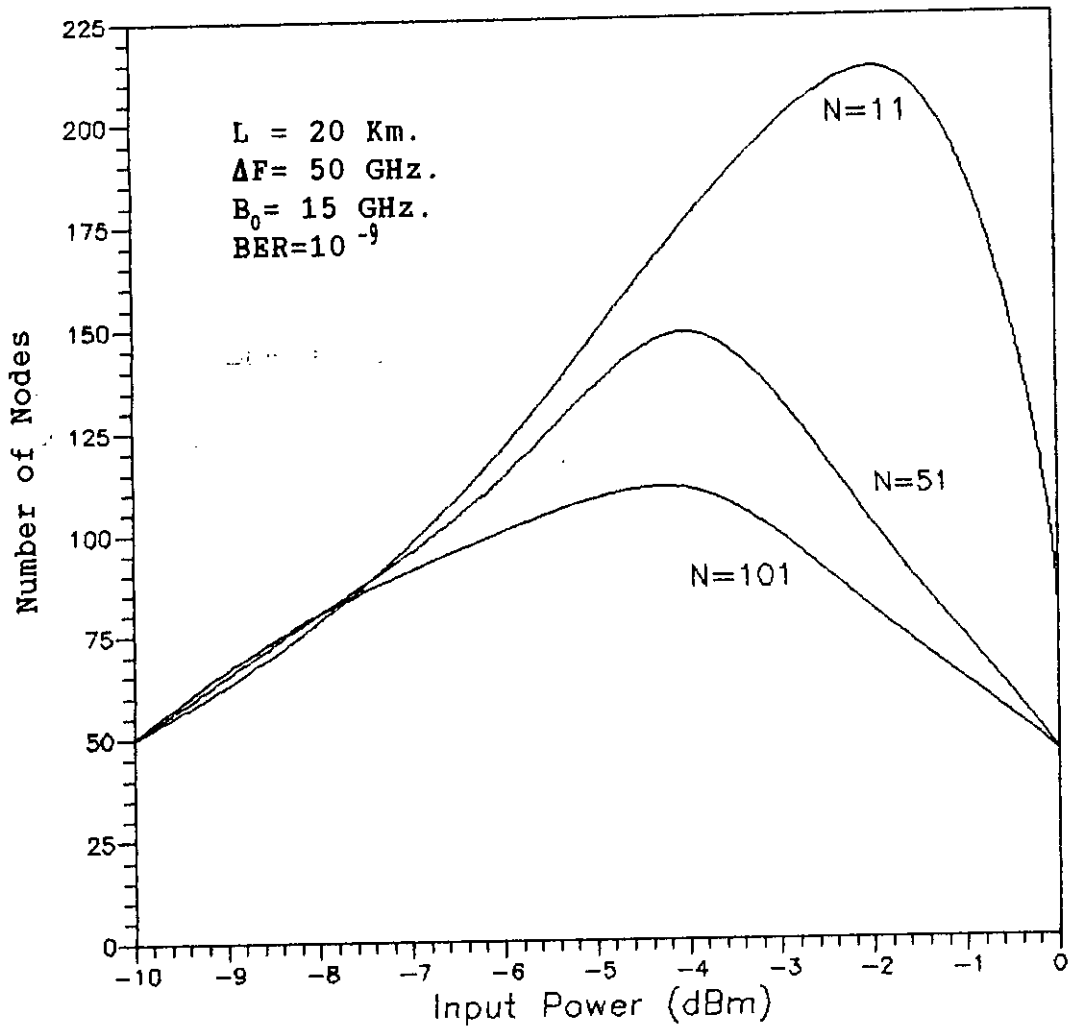


Fig.3.16 Variation of the allowable number of nodes M at $BER=10^{-9}$ versus the transmitter power P_{in} (dBm) in the presence of FWM effect when the number of channels $N=11, 51$ and 101 and channel separation $\Delta F=50$ GHz, $B_0=15$ GHz and fiber span, $L=20$ Km.

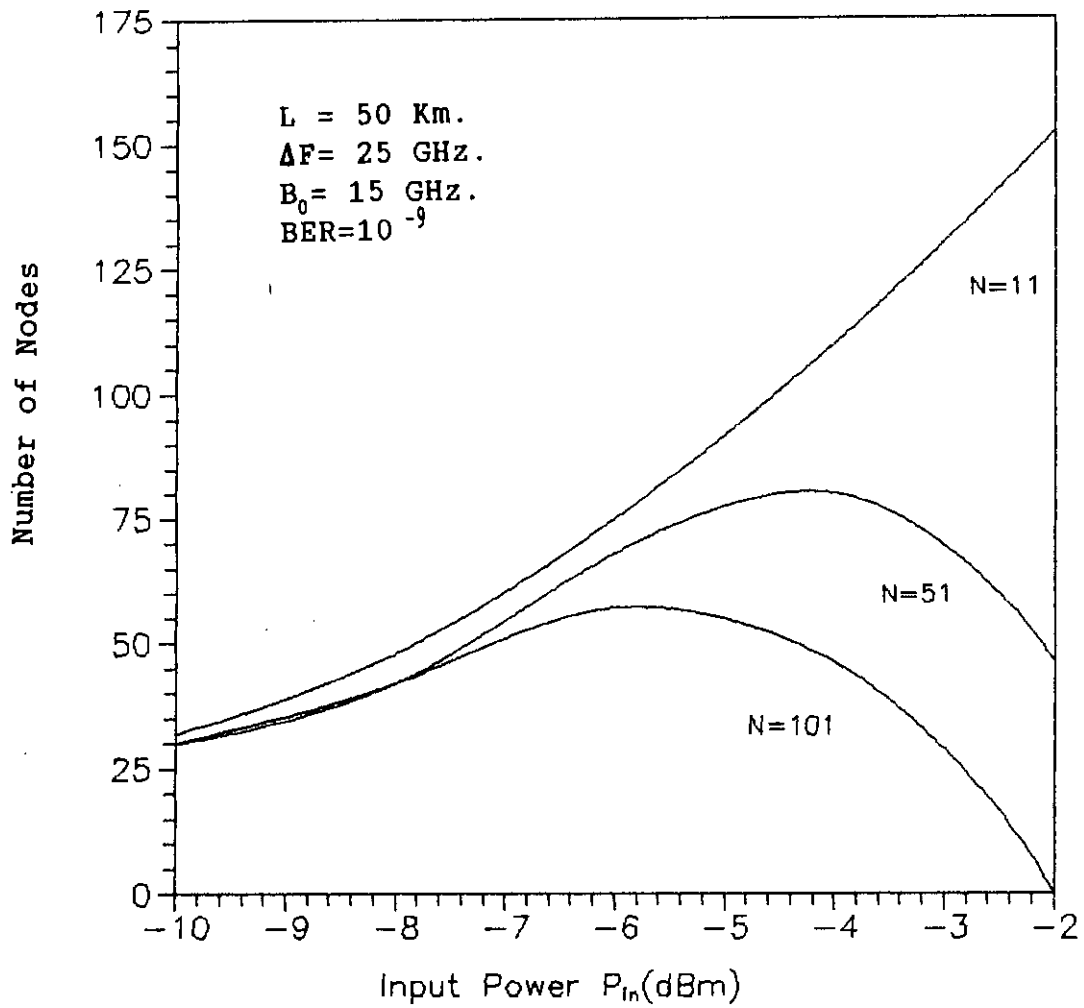


Fig.3.17 Variation of the allowable number of nodes M at $\text{BER} = 10^{-9}$ versus the transmitter power P_{in} (dBm) in the presence of FWM effect when the number of channels $N = 11, 51$ and 101 and channel separation $\Delta F = 25 \text{ GHz}$, $B_0 = 15 \text{ GHz}$ and fiber span, $L = 50 \text{ Km}$.

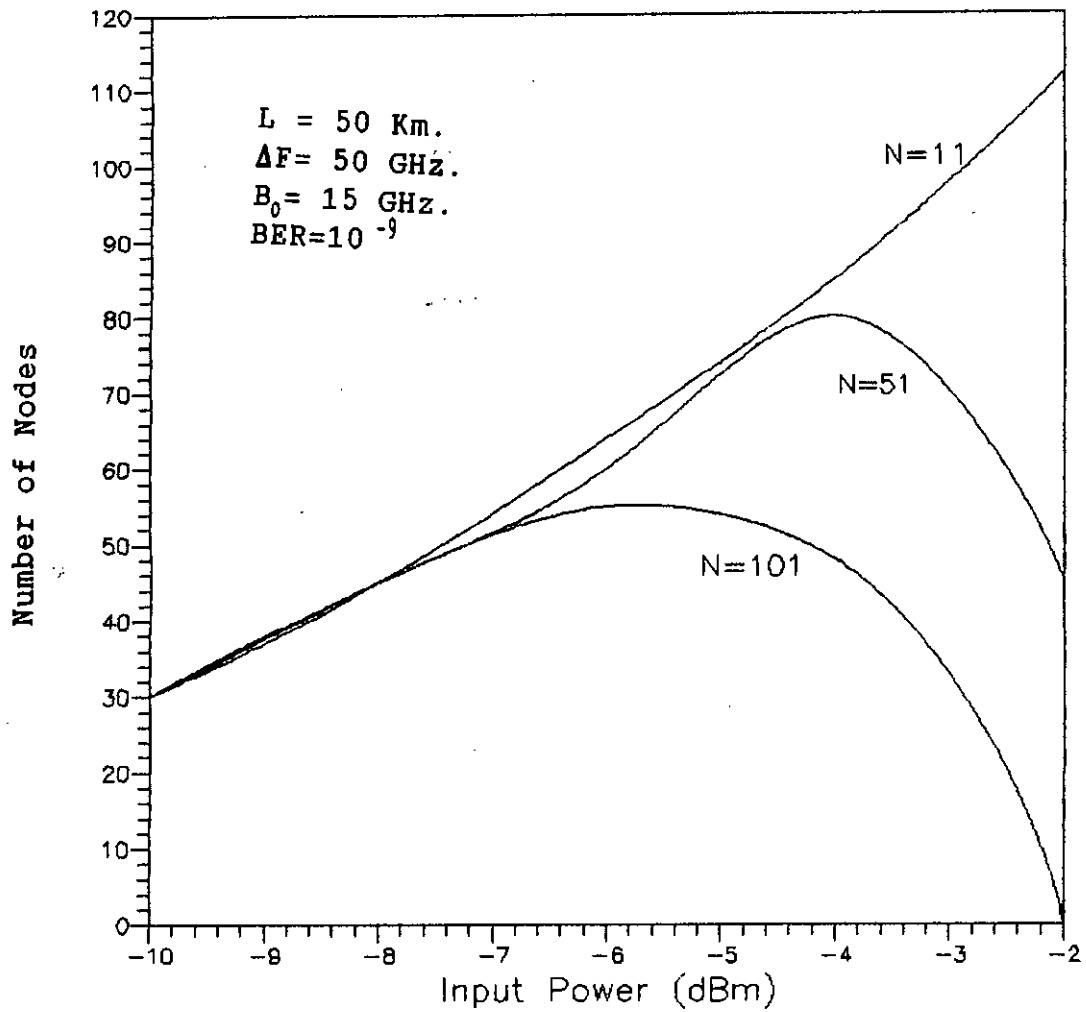


Fig.3.18 Variation of the allowable number of nodes M at $BER=10^{-9}$ versus the transmitter power P_{in} (dBm) in the presence of FWM effect when the number of channels $N=11, 51$ and 101 and channel separation $\Delta F=50 \text{ GHz}$, $B_0 = 15 \text{ GHz}$ and fiber span, $L=50 \text{ Km}$.

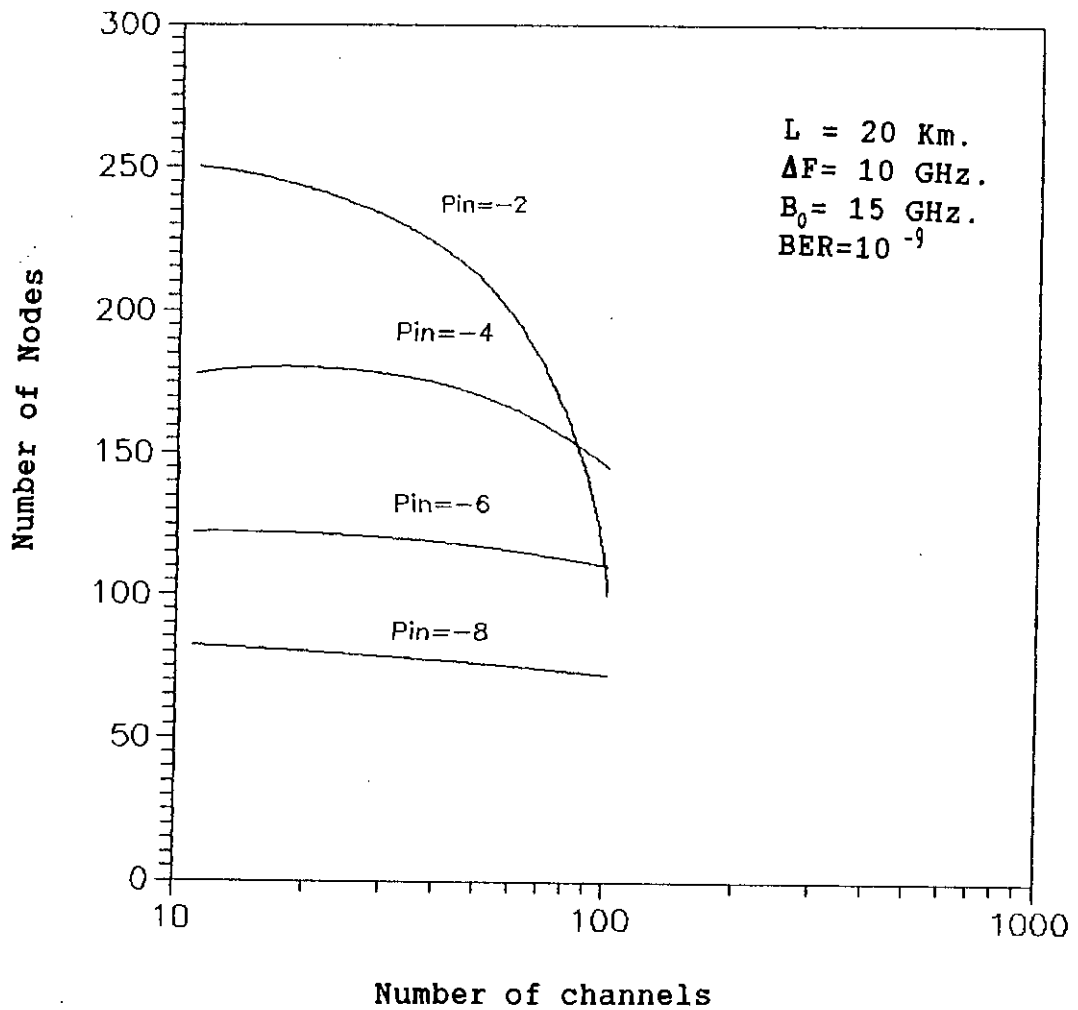


Fig.3.19 Plots of allowable number of nodes M in presence of FWM effect at a bit error rate of 10^{-9} as a function of the number of WDM channels N , when channel separation $\Delta F = 10 \text{ GHz}$, $B_0 = 15 \text{ GHz}$ and $L = 20 \text{ Km}$ for different values of transmitter power P_{in} (dBm).

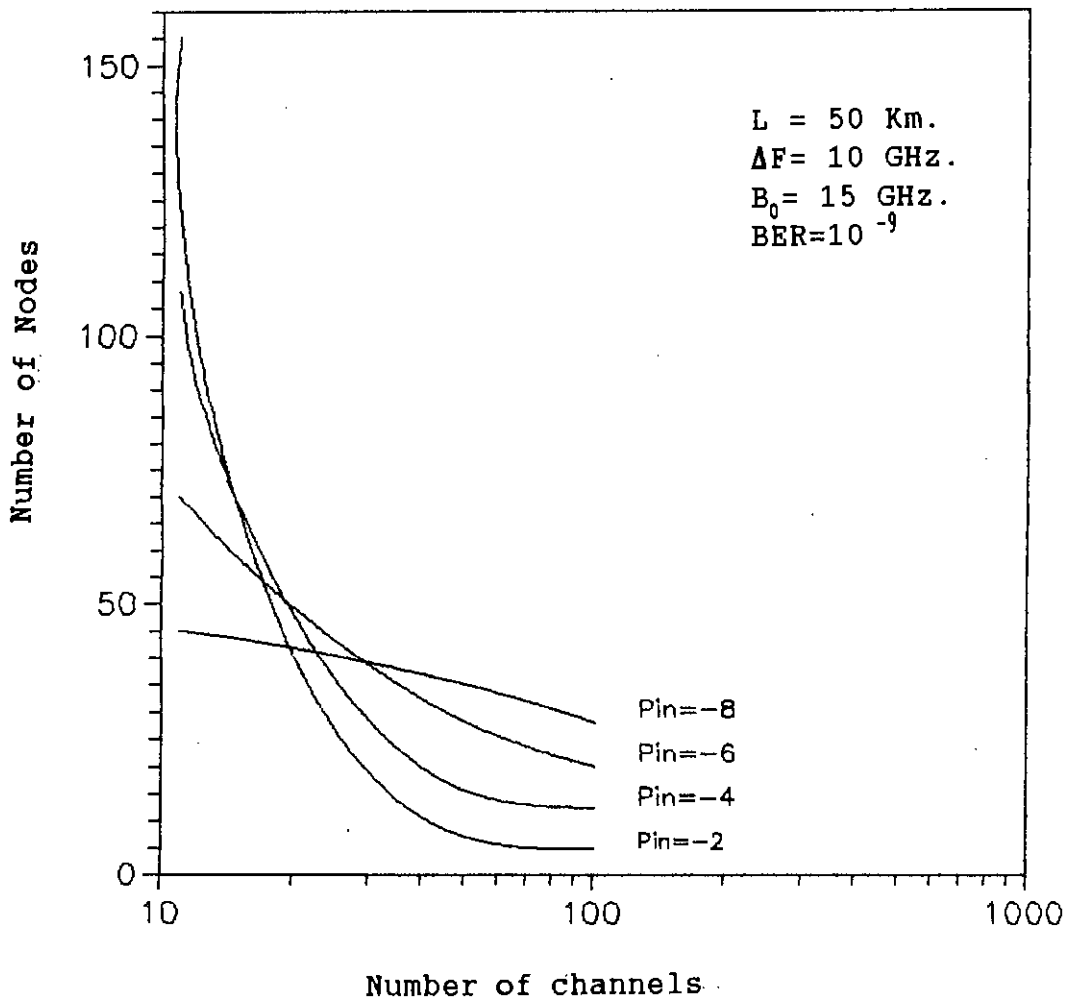


Fig.3.20 Plots of allowable number of nodes M in presence of FWM effect at a bit error rate of 10^{-9} as a function of the number of WDM channels N , when channel separation $\Delta F = 10 \text{ GHz}$, $B_0 = 15 \text{ GHz}$ and $L = 50 \text{ Km}$ for different values of transmitter power P_{in} (dBm).

Fig.3.21 . The figures reveal similar behavior and indicate how the number of allowable nodes is greatly reduced due to increased fiber length and/or increased optical bandwidth.

The maximum achievable number of nodes at $BER = 10^{-9}$ and given value of the channel separation ΔF is plotted against the number of channels in Fig.3.22 and Fig.3.23 and Fig.3.24 with fiber span length L as a parameter for $\Delta F=10,25,50$ GHz respectively. These curves illustrate the dependence of FWM effect (and/or maximum allowable number of nodes M_{max}) on the number of channels and channel separation. It becomes clear that as the number of channels increases, the value of M_{max} decreases exponentially.

Fig.3.25 depicts the variation of maximum allowable input power $P_{in(max)}$ with optical bandwidth B_o for number of channels $N=11,51$ and 101 . Again it is clearly noticed that $P_{in(max)}$ decreases with increased optical bandwidth.

In Fig.3.26, the maximum input power $P_{in} (Max)$ corresponding to maximum achievable number of WDM channels is plotted as a function of number of channels N for $B_o = 15, 25$ and 50 GHz, $\Delta F= 25$ GHz and $L = 50$ Km. This figure reveals that $P_{in(max)}$ is reduced greatly at higher values of N , and higher

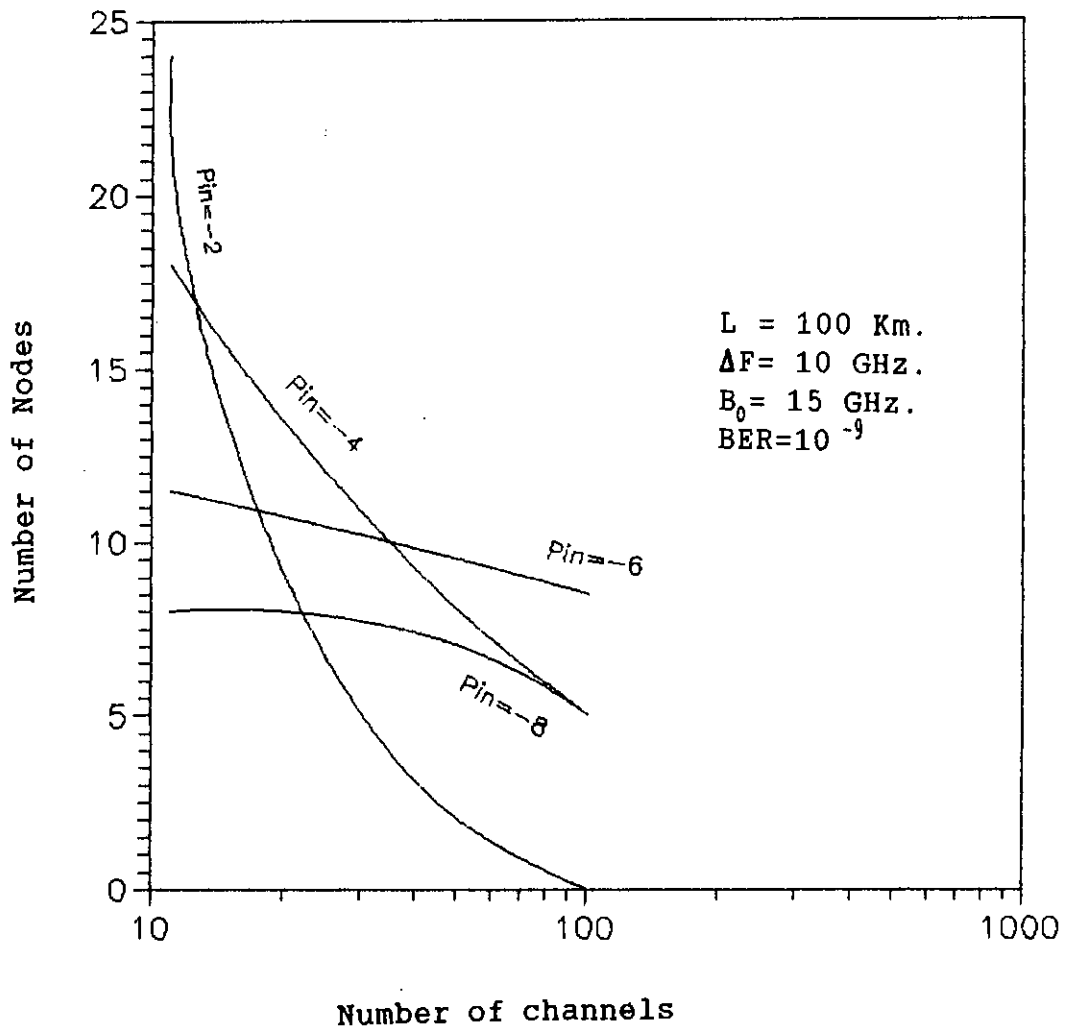


Fig.3.21 Plots of allowable number of nodes M in presence of FWM effect at a bit error rate of 10^{-9} as a function of the number of WDM channels N , when channel separation $\Delta F=10$ GHz, $B_0=15$ GHz and $L=100$ Km for different values of transmitter power P_{in} (dBm).

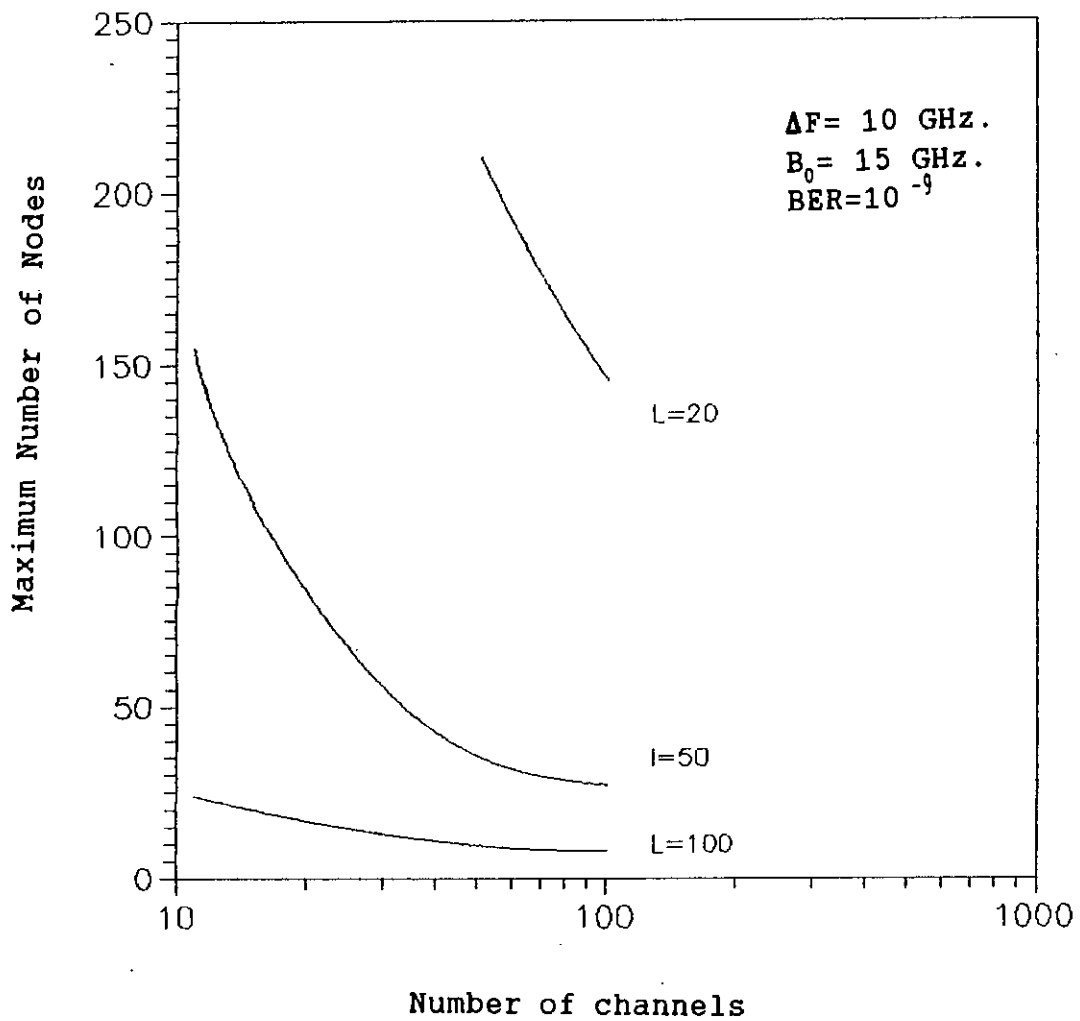


Fig.3.22 Plots of allowable maximum number of nodes M in presence of FWM effect at a bit error rate of 10^{-9} as a function of the number of WDM channels N , when channel separation $\Delta F=10 \text{ GHz}$, $B_0=15 \text{ GHz}$ and for $L=20, 50, 100 \text{ Km}$.

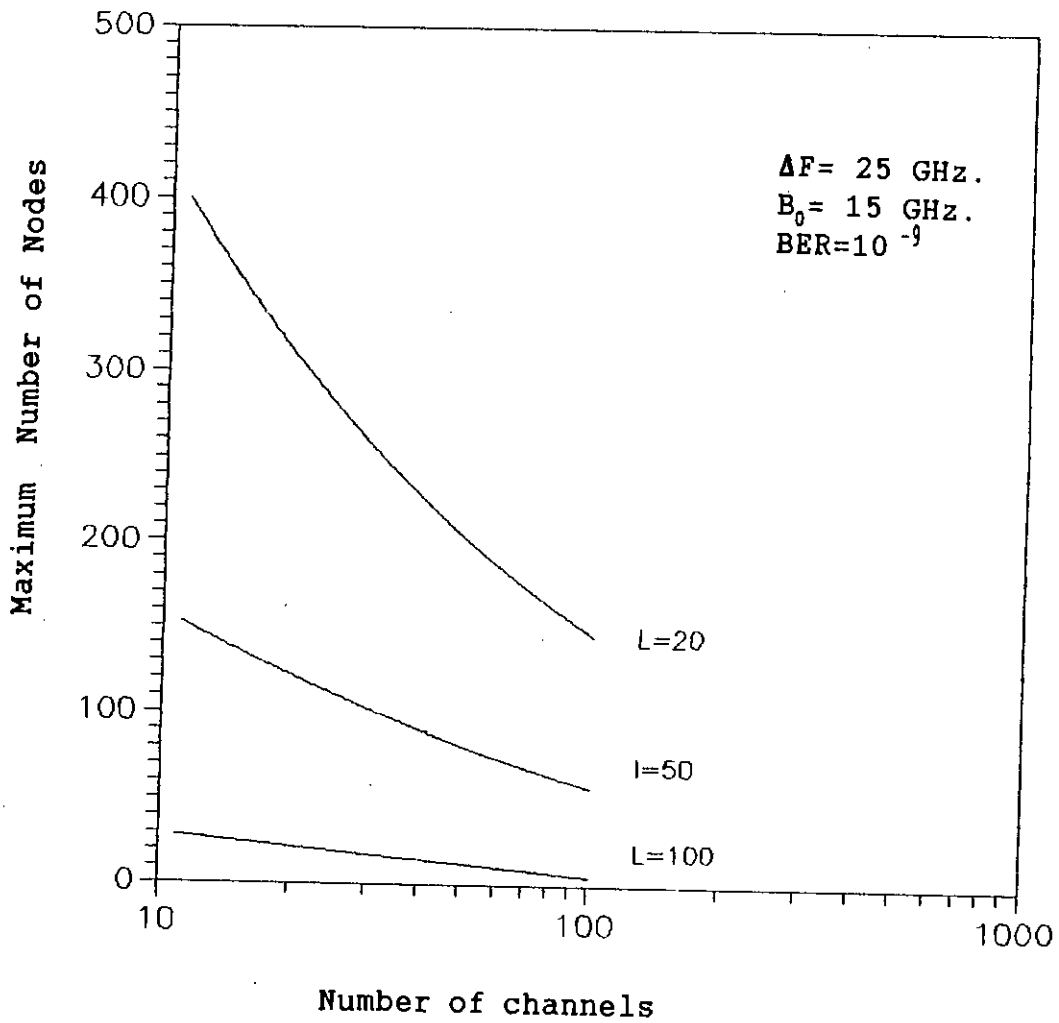


Fig.3.23 Plots of allowable maximum number of nodes M in presence of FWM effect at a bit error rate of 10^{-9} as a function of the number of WDM channels N , when channel separation $\Delta F=25 \text{ GHz}$, $B_0=15 \text{ GHz}$ and for $L=20, 50, 100 \text{ Km}$.

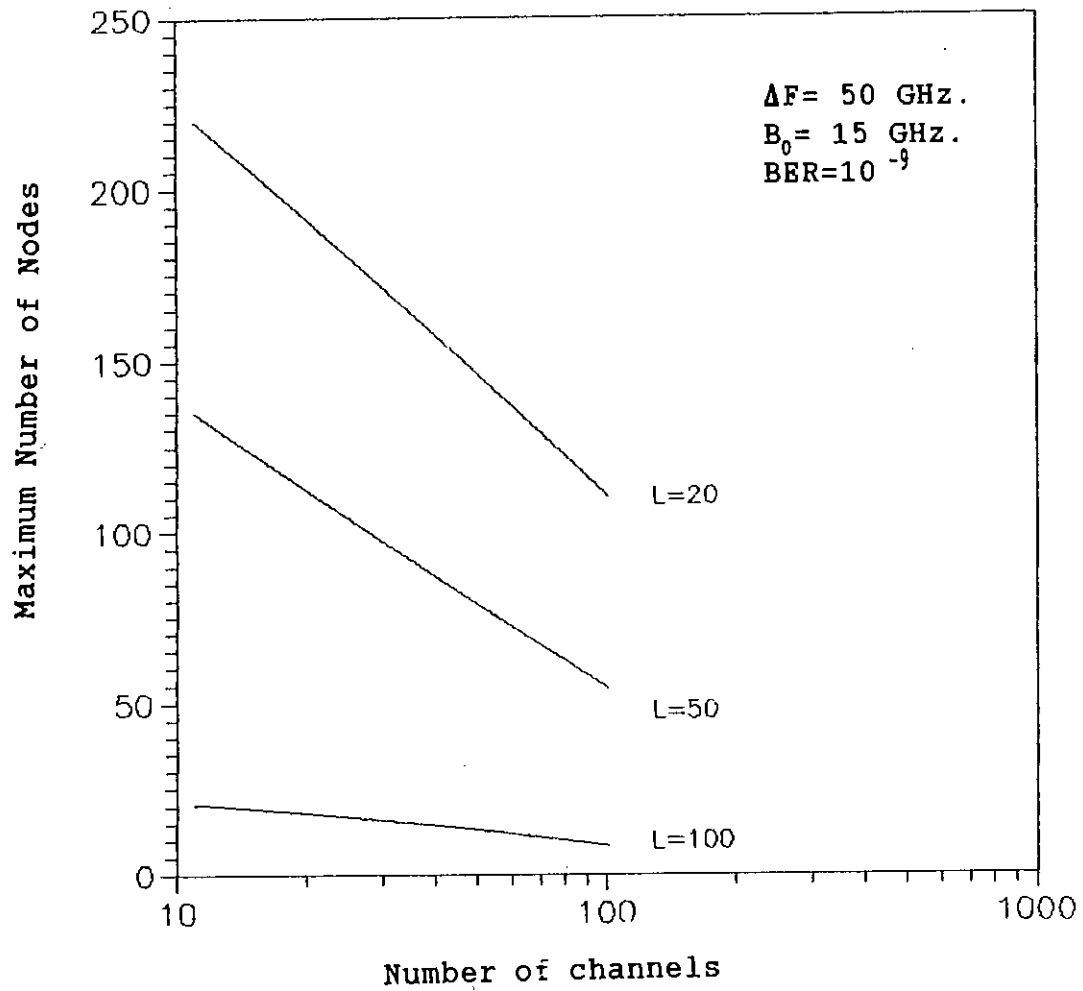


Fig.3.24 Plots of allowable maximum number of nodes M in presence of FWM effect at a bit error rate of 10^{-9} as a function of the number of WDM channels N , when channel separation $\Delta F=50 \text{ GHz}$, $B_0=15 \text{ GHz}$ and for $L=20, 50, 100 \text{ Km}$.

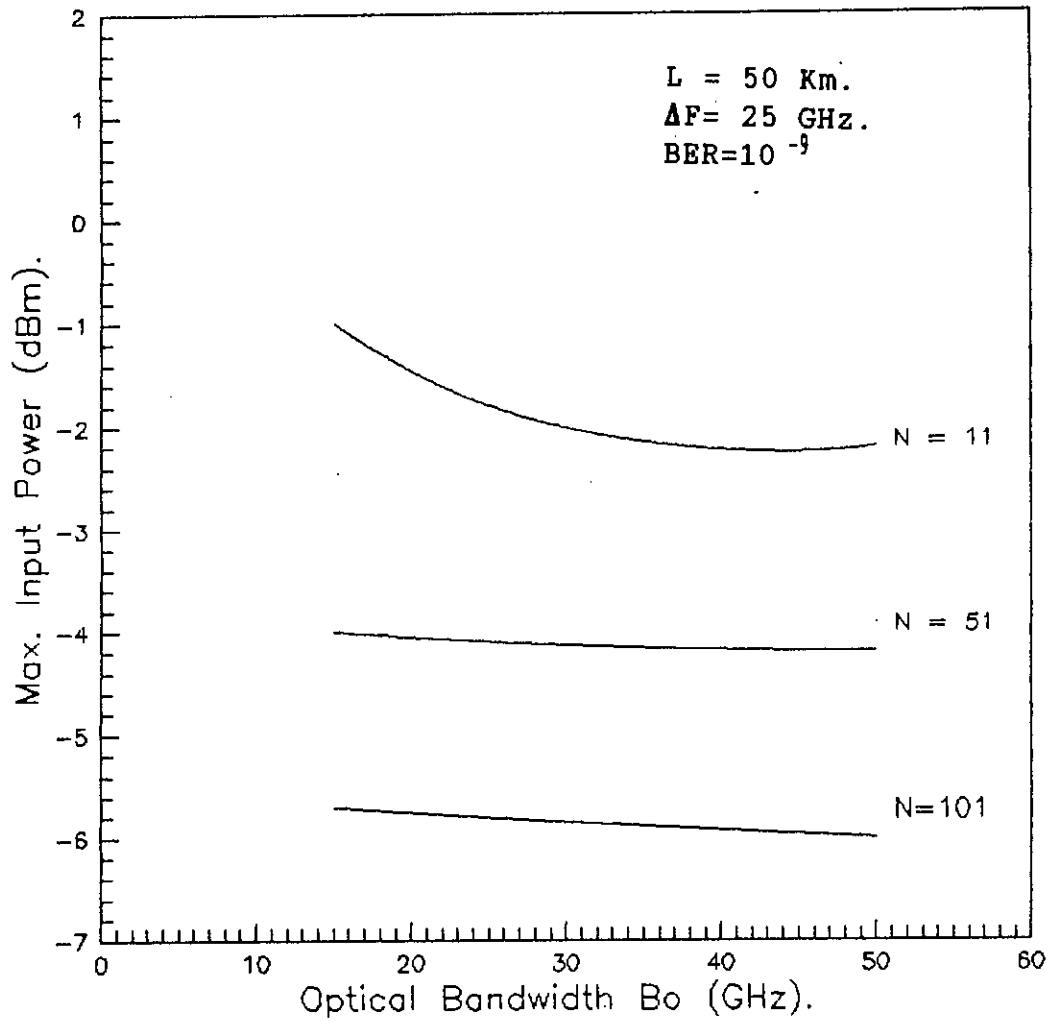


Fig.3.25 Plots of maximum allowable laser transmitter power $P_{in(max)}$ (dBm) at $\text{BER} = 10^{-9}$ versus optical bandwidth B_0 (GHz) in the presence of FWM effect when fiber span $L = 50 \text{ Km}$ and channel separation $\Delta F = 25 \text{ GHz}$ for number of channels $N = 11, 51, 101$

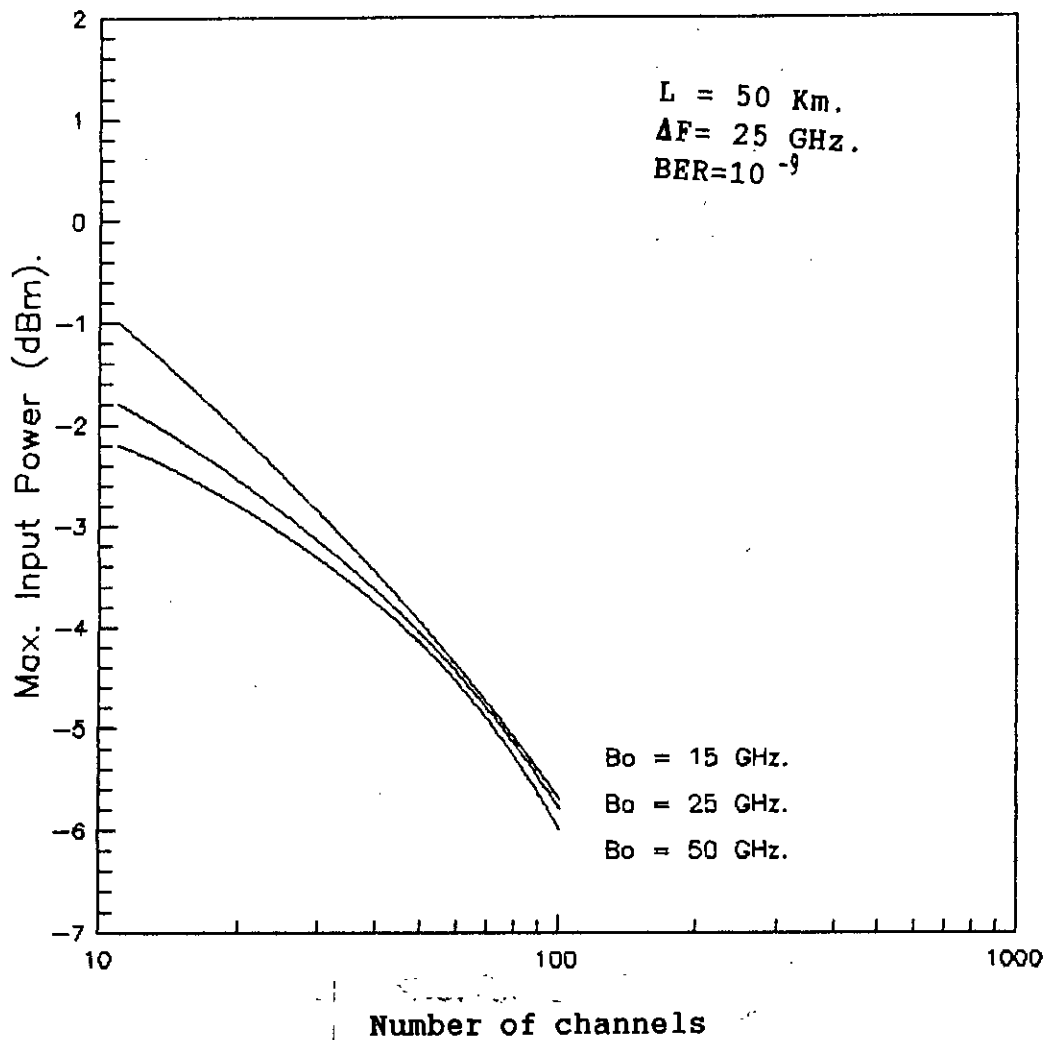


Fig.3.26 Plots of maximum allowable laser transmitter power $P_{in(max)}$ (dBm) at $BER=10^{-9}$ versus number of WDM channel N , in the presence of FWM effect when fiber span $L=50 \text{ Km}$ and channel separation $\Delta F=25 \text{ GHz}$ for optical bandwidth $B_0 = 15, 25, 50 \text{ GHz}$

optical bandwidth.

Fig.3.27 depicts the variation of number of nodes at $BER=10^{-9}$ as a function of channel separation ΔF (GHz) with P_{in} as a parameter for $N=11$ and $L=50$ Km. Similar plots are shown in Fig.3.28 and Fig.3.29 for $N=51$ and 101 respectively. The figure show that the number of achievable nodes increases with ΔF and attains a maximum value and then decreases. Correspond to the maximum achievable number of nodes there is an optimum channel separation. The nature of the curve is due to the dependence of FWM phase $\Delta\beta$ on the channel separation ΔF . The optimum channel separation is higher at smaller values of transmitter power P_{in} (dBm) and is less at higher values of P_{in} . This is due to the fact that the FWM effect is more prominent at higher input power and hence smaller channel separation is required for optimum system performance.

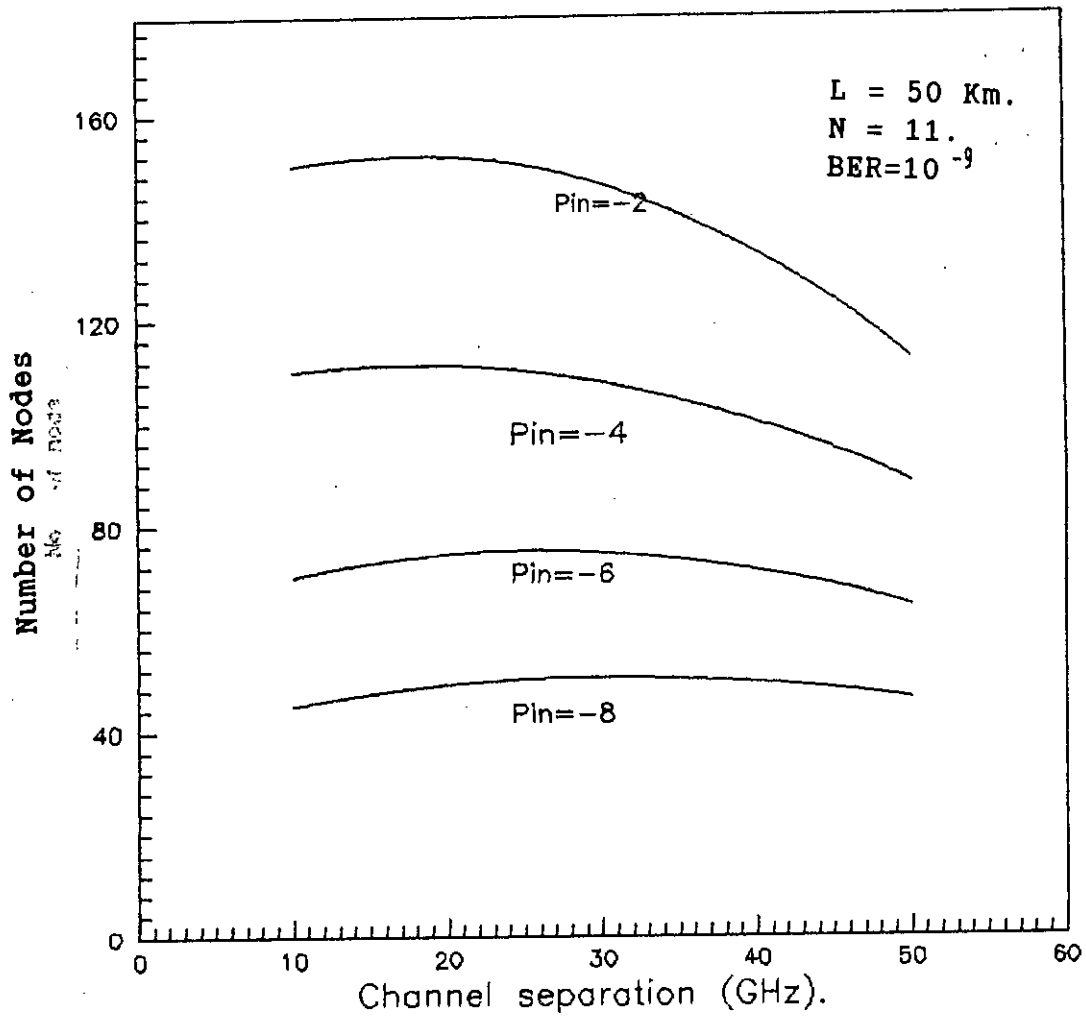


Fig.3.27 Plots of the allowable number of nodes M at $BER=10^{-9}$ as a function of channel separation ΔF (GHz) in the presence of FWM effect when the number of WDM channels $N=11$ and fiber span $L=50 \text{ Km}$ for different input power (dBm).

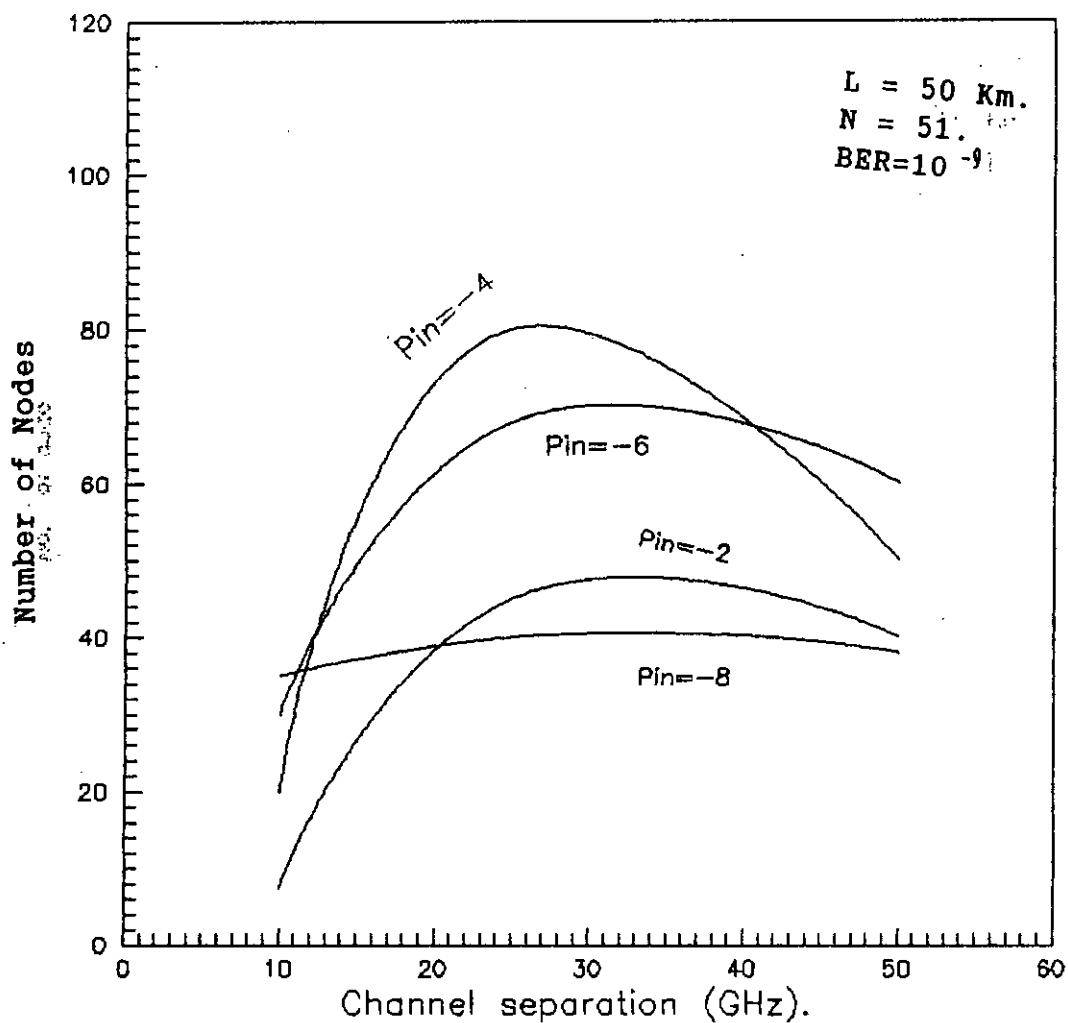


Fig.3.28 Plots of the allowable number of nodes M at $BER=10^{-9}$ as a function of channel separation Δf (GHz) in the presence of FWM effect when the number of WDM channels $N=51$ and fiber span $L=50$ Km for different input power (dBm).

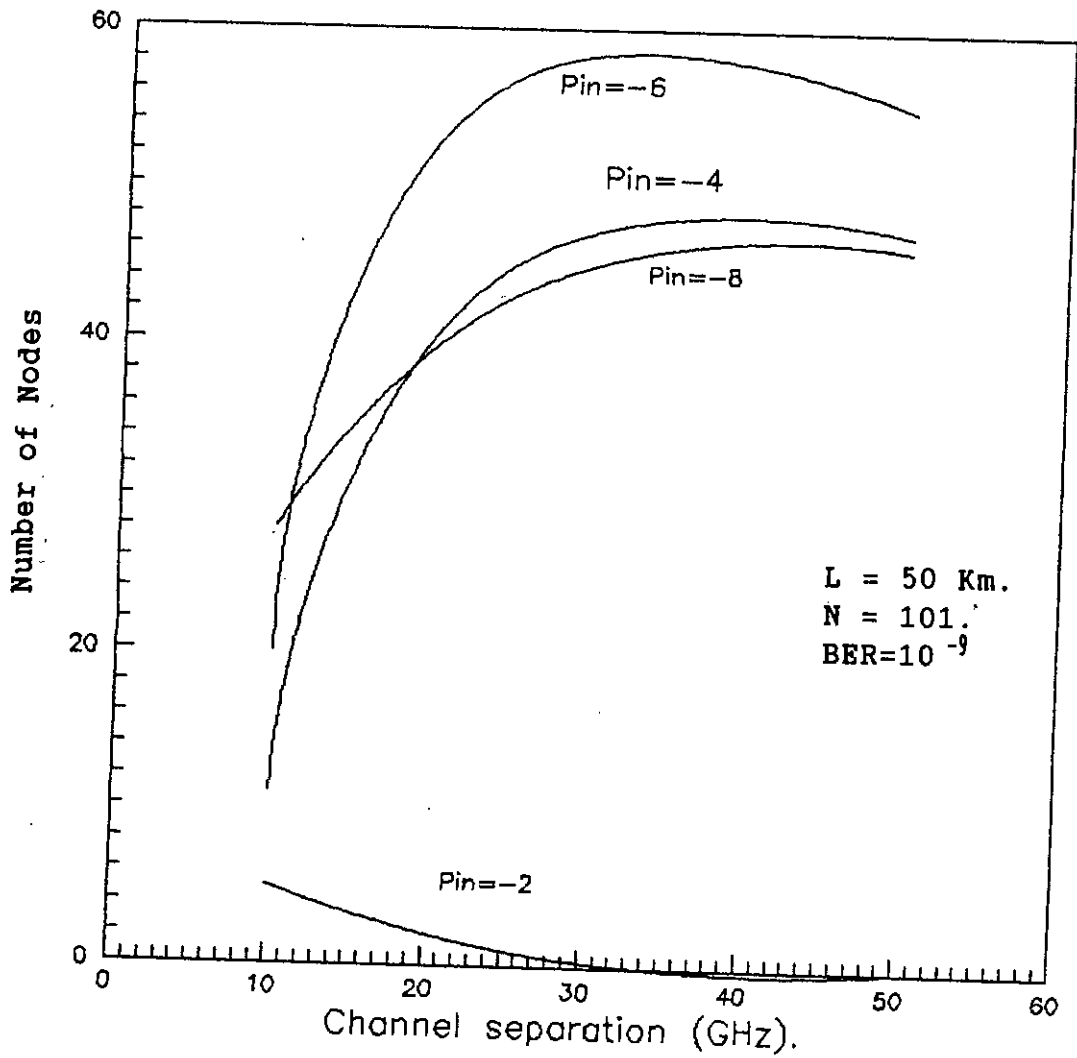


Fig.3.29 Plots of the allowable number of nodes M at $BER=10^{-9}$ as a function of channel separation ΔF (GHz) in the presence of FWM effect when the number of WDM channels $N=101$ and fiber span $L=50$ Km for different input power (dBm).

CHAPTER - 4

CONCLUSIONS AND SUGGESTIONS

4.1 Conclusions:

In this work, a detailed theoretical analysis is carried out to evaluate the impact of fiber nonlinear effects viz. four-wave mixing (FWM) and in low dispersion fiber on the performance of optical multi-wavelength transmission system with in-line optical amplifier's and CPFSK modulation with direct detection MZI based receiver. Performance results are evaluated at a bit rate of 2.5 Gb/s, considering monomode fiber at an wavelength of 1550 nm for several sets of receiver and system parameters.

The computed results indicate that the bit error rate (BER) increases with increasing values of the number of nodes due to accumulation of optical amplifier's spontaneous emission (ASE) noise for one node to another. At a BER of 10^{-9} , the allowable number of nodes are found to be more at higher input power. However, when the fiber span is larger, the allowable number of nodes is less due to increased ASE with increased amplifier gain to meet additional fiber loss due to increased fiber span. The effect of FWM is found to be more pronounced

when the number of channels is increased. For example, for $P_{in} = -4.0$ dBm, the number of allowable nodes at $BER=10^{-9}$ is around 175 for $N=11$, $L=20$ Km whereas it reduces to 145 when N is increased to 101.

The plots of allowable number of nodes M at $BER = 10^{-9}$ show that the number of nodes increases with P_{in} and attains a maximum value of M_{max} corresponding to a maximum input power $P_{in(max)}$. Further increase in P_{in} causes the number of nodes to decrease. The value of M_{max} depends on the number of channels and fiber span, and decreases with increasing value of the number of channels and fiber span due to increased FWM power, and increased ASE and other beat noise components.

Further, it is also observed that the bandwidth of the optical amplifier B_o has a great influence on the maximum achievable number of nodes. At higher optical bandwidth, the influence of FWM and ASE is higher and as a consequence for a given transmitter power P_{in} , the allowable number of channels and/or number of nodes is significantly less. For example, for $B_o = 15$ GHz, channel separation $\Delta F=25$ GHz and $P_{in} = -6$ dBm, the number of nodes at $BER = 10^{-9}$ is around 75 corresponding to $L=50$ Km and $N=11$ whereas it reduces to nearly 28 when B_o is increased to 50 GHz. On the other hand, if the number of nodes

is kept fixed, the number of channels must be decreased if B_0 is increased at a given value of the input power. However, the maximum allowable input power $P_{in(max)}$ is found to be almost independent of B_0 and is significantly less at higher values of N .

It is further noticed that the number of nodes or number of channels can be increased at a given value of P_{in} and fiber span, if the channel separation ΔF is increased. It is observed that the number of nodes at a given value of N increases with ΔF and attains a maximum value corresponding to an optimum value of the channel separation after which it again decreases. The optimum value of channel separation is slightly less at higher values of input power P_{in} . Also, the required optimum channel separation is slightly higher for increased value of N due to increased FWM effect.

4.2 Suggestions for Future Works:

The present research work can be extended to investigate the effect of crosstalk due to optical space switch in the presence of optical amplifier's spontaneous emission (ASE) noise and FWM effect on optically amplified multiwavelength transport network (MWTN). Further analysis can be carried out

to determine the packet error probability at a given node conditioned on a given number of bits in a packet. The analysis can be carried out considering a Shuffle-Net or an optical ring Network. An upper bound on the network performance in terms of maximum achievable data rate and for a given packet error probability can be evaluated.

Future works in this area can also be carried out to include the effect of Raman Scattering, the jitter accumulation due to amplifier's spontaneous emission noise, nonuniform chromatic dispersion along the fiber etc.. A detailed Monte-carlo simulation of the wavelength routed optical network can also be carried out to verify the theoretical results and to determine the optimum system parameters for reliable system performance.

REFERENCES

- [1] Gerd Keiser, "Optical Fiber Communications", McGraw-Hill Book Company, 1983.
- [2] Jr. William, B. Jones, "Introduction to Optical Fiber Communication Systems", Holt, Rinehart and Winston, Inc. New York, 1987.
- [3] T. Okoshi, "Recent advances in coherent optical fiber communication systems", J. Lightwave Tech., vol. LT-5, no. 1, pp. 44-52, 1987.
- [4] T. Kimura, "Coherent optical fiber transmission", J. Lightwave Tech. vol. LT-5, no. 4, pp. 414-428, 1987.
- [5] T. Okoshi, "Heterodyne and Coherent Optical fiber communications : Recent progress", IEEE Transactions on microwave theory and techniques", vol. MTT-30, no. 8, pp. 1138-1148, August 1982.
- [6] K. Emura, S. Yamazaki, M. Yamaguchi, M. Shikada, and K. Minemura, "An optical FSK heterodyne dual filter detection system for taking advantage of DFB LD applications", J. Lightwave Tech., vol. 8, no. 2, pp. 243-250, February 1990.
- [7] U. Timor, and R. A. Linke, "A comparison of sensitivity degradations for optical homodyne versus direct detection on-off keyed signals", J. Lightwave Technology., vol. 6, no. 11, pp. 1782-1788, November 1988.
- [8] Andrew R. Charplyvy, "Limitations on Light wave Communications, Imposed by Optical-Fiber Nonlinearities", IEEE Journal of Lightwave Technology, vol. 8, no. 10, pp. 1548-1557, October, 1990.
- [9] K. H. Kim, H. K. Lee, S. Y. Park, and E. -H. Lee, "Calculation of dispersion and nonlinear effect limited maximum TDM and FDM bit rates of transform-limited pulse in single-mode optical fibers ", J. Lightwave Technology., vol. 13, no. 8, pp. 1597-1605, August 1995.
- [10] A. F. Elrefaie, R. E. Wanger, D. A. Atlas, and D. G. Find,

- " Chromatic dispersion limitations in coherent lightwave systems," J. Lightwave Tech., vol. 6, pp. 704-709, 1988.
- [11] A.Djupsjobacka and O.Sahlen,"Dispersion compensation by time delay", J. Lightwave Tech., vol. 12, no. 10, pp. 1849-1853, October 1994.
- [12] C-Ching Shih, "Analytical theory of four-wave mixing and stimulated brillouin scattering in the saturation regime", IEEE J. Quantum Electron., vol. QE-23, no. 9, pp. 1452-1457, September 1987.
- [13] K.Inoue,"Observation of Cross talk due to Four-wave mixing in a laser amplifier for FDM transmission", Electronics Letters,vol.23, no.24, pp.1293-1295, November 1987.
- [14] M. W. Maeda, W. B. Sessa, W. I. Way, A. Yi-Yan, L. Curtis, and R. I. Laming, "The effect of four-wave mixing in fibers on optical frequency-division multiplexed systems", J. Lightwave Tech., vol. 8, no. 9, pp. 1402-1408, September 1990.
- [15] N. Shibata, K. Nosu, K. Iwashita and Y. Azuma, "Transmission Limitations Due to Fiber nonlinearities in optical FDM systems ", IEEE Journal on selected areas in communications vol. 8, no. 6, pp 1068-1077, August 1990.
- [16] H. Toba, K. Oda and K. Nosu, "Design and performance of FSK-direct detection scheme for optical FDM systems", J. Lightwave Tech., vol. 9, no. 10, pp. 1335-143, October 1991.
- [17] E. Lichtman, "Bit rate-distance product limitations due to fiber nonlinearities in multichannel coherent optical communication systems ", Electron. Letter., vol. 27, no. 9, pp. 757-759, April 1991.
- [18] E. Iannone, F. S. Locati, F. Matera, M. Romagnoli and M. Settembre, "Performance evaluation of single-channel coherent systems in presence of nonlinear effects", Electron. Lett., vol. 28, no. 7, pp. 645-646, March 1992.
- [19] K. Inoue, "Supper position technique for fiber four- wave mixing using optical multi-/demultiplexers and a delay line", J. Lightwave Tech., vol. 11, no. 3, pp. 455-461, March 1993.

- [20] K. Inoue, "Phase-mismatching characteristic of four-wave mixing in fiber lines with multistage optical amplifiers", *Optics Lett.*, vol. 17, no. 11, pp. 801-803, June 1, 1992.
- [21] K. Inoue and H. Toba, "Fiber four-wave mixing in multi-amplifier systems with nonuniform chromatic dispersion", *J. Lightwave Tech.*, vol. 13, no. 1, pp. 88-93, January 1995.
- [22] K. Inoue, H. Toba and K. Oda, "Influence of Fiber Four-Wave mixing on multichannel FSK direct Detection Transmission Systems", *IEEE Journal of Light wave Technology*, vol. 10, no. 3, pp. 350-360, March 1992.
- [23] N. A. Olsson, "Lightwave systems with optical amplifiers", *J. Lightwave Tech.*, vol. 7, no. 7, pp. 1071-1082, July 1989.
- [24] M.E. Bray, J.E. Carroll, "Crosstalk reduction in Semiconductor laser amplifiers", *IEEE Proceedings-J*, vol. 139, no. 2, pp. 93-100, April 1992.
- [25] M. Fujita, Y. Iseki, I. Nomoto and T. Wakoh, "Optical Fiber Amplifier and 1.48 μm High Power Pumping Laser Module", *NEC Research and Development*, vol. 32, no. 1, pp. 69-74, January 1991.
- [26] K. ODA, N. Takato, T. Kominato and H. Toba, "A 16-Channel Frequency Selection Switch for Optical FDM Distribution Systems", *IEEE Journal on Selected areas in Communications*, vol. 8, no. 6, pp. 1132-1140, August 1990.
- [27] K. Inoue, H. Toba, and K. Nosu, "Multichannel amplification utilizing an Er^{3+} -doped fiber amplifier", *J. Lightwave Tech.*, vol. 9, no. 3, pp. 368-373, March 1991.
- [28] A.E. Willner, I.P. Kaminov, M. Kuznetsov, J. Stone and L.W. Stulz, "1.2 Gb/s closely-spaced FDMA-FSK Direct-Detection Star Network", *IEEE Photonics Technology Letters*, vol. 2, no. 3, pp. 223-226, 1991.
- [29] G. R. Hill, "A wavelength routing approach to optical communication networks", *British Telecom. Technology. J.*, vol. 6, pp. 42-31, 1988.

- [30] C. Saxtoft, and P. Chidgey, "Error rate degradation due to switch crosstalk in large modular switched optical networks", IEEE Photonics Tech. Lett., vol. 5, no. 7, pp. 828-831, July 1993.
- [31] N.Takato, T.Kominato, A.Sugita, K.Jinguji, H.Toba and M.Kawachi,"Silica-Based Integrated Optic Mach-Zehnder Multi/Demultiplexer Family with Channel Spacing of 0.01-250 nm",IEEE Journal on Selected areas in Communications, vol. 8, no. 6, pp. 1120-1140, August 1990.
- [32] R. F. Pawula, "On the theory of error rates for narrow-band digital FM", IEE Transaction on Communication., vol. 36, no. 4, pp. 509-512, April 1988.
- [33] M. Schwartz, W. R. Bennett, and S. Stein, "Communication systems and techniques", New York: McGraw-Hill, 1966.
- [34] E. Bedrosian, and S. O. Rice, "Distortion and crosstalk of linearly filtered angle-modulated signals", Proc. IEEE, vol. 56, pp. 2-13, January 1968.
- [35] R. G. Mckay, and J. C. Cartledge, "Performance of coherent optical CPFSK-DD with intersymbol interference, noise correlation, and laser phase noise", J. Lightwave Tech., vol. 11, no. 11, pp. 1845-1853, November 1993.
- [36] I. Garrett and G. Jacobsen, "Theory for optical heterodyne narrow-deviation FSK receivers with delay demodulation", J. Lightwave Tech., vol. 6, no. 9, pp. 1415-1423, September 1988.
- [37] E.Forestieri and G.Prati,"Theoretical analysis of Coherent Optical FSK system with Limiter-Discriminator Detection",IEEE Transactions on Communications ,vol.42, no.2/3/4/,pp.562-573,Feb/March/April,1994.
- [38] C. W. Helstrom, "Computing the generalized Marcum Q-function", IEEE Trans. inform. theory, vol. 38, no. 4, pp. 1422-1428, July 1992.
- [39] R. A. Linke, "High capacity coherent lightwave systems", J. Lightwave Tech. vol. 6, no. 11, pp. 1750-1169, November 1988.

- [40] R. S. Vodhanel, "5 Gbit/s direct optical DPFSK modulation of a 1530-nm DFB laser", IEEE Photon. Tech. Lett., vol. 1, no. 8, pp. 218-210, August 1989.
- [41] R. Gangopadhyay and S. P. Majumder, "Impact of laser phase noise on optical heterodyne single filter FSK system with optical preamplifier", Electron. Lett., vol. 27, no. 21, pp. 1927-1929, October 1991..
- [42] S. P. Majumder, R. Gongopadyay, M. S. Alam, and G. Parti, "Performance of linecoded heterodyne FSK system with nonuniform laser FM response", J. Lightwave Tech., vol. 13, no. 4, pp. 628-638, April 1995.

APPENDIX A

The total FWM power can be calculated as follows [8,14,19-22],

$$P_F(l) = K \cdot P_{in}^3 \exp(-\alpha l) \sum_{p,q,r} D^2 \eta_{pqr}$$

$$K = \frac{1024 \cdot \pi^6 \cdot \chi^2 \cdot L_{eff}}{\eta^4 \cdot \lambda^2 \cdot c^2 \cdot A_{eff}}$$

$$\eta_{pqr} = \left[\frac{\alpha^2}{\alpha^2 + (\Delta\beta)^2} \right] \left[\frac{4 \cdot \exp(-\alpha l) \sin^2(\Delta\beta l/2)}{[1 - \exp(-\alpha l)]^2} \right]$$

$$\Delta\beta = \frac{2\pi D_c \cdot \lambda^2}{c} | (f_p - f_r) | | (f_q - f_r) |$$

$$\equiv \frac{2\pi D_c \cdot \lambda^2}{c} (\Delta F)^2 (p - r) (q - r)$$

(A.1)

Where P_{in} is the power launched into amplifier from transmitter. The symbol ' P_F ' will replace the value of Four-Wave Mixing power P_{pqr} .

f_i ($i = p, q, r$) = optical frequency of the i -th channel.

χ = nonlinear susceptibility of fiber = 6×10^{-14} m³/watt-sec.

A_{eff} = effective core area = $2\pi r^2$, r = modified radius,

$r = W/2$

W = modified diameter = 10.7 μ m

α = attenuation of fiber = nepers/Km.

Chromatic dispersion coefficient,

$D_c = [23 \text{ ps/Km nm}, \lambda = 1300] \text{ DSF}$

$[1 \text{ ps/Km nm}, \lambda = 1550] \text{ DSF}$

$D_c = [1 \text{ ps/Km nm}, \lambda = 1300] \text{ NDF}$

$[17 \text{ ps/Km nm}, \lambda = 1550] \text{ NDF}$

value of $D = 6$ for $p \neq q \neq r$ fully degenerate

$= 3$ for $p = q \neq r$ partially degenerate

$c = \text{velocity of light} = 3 \times 10^8 \text{ m/s.}$

$P_{in} = \text{Input transmitter power.}$

$$L_{eff} = \frac{1 - \exp(-\alpha l)}{\alpha} \quad (\text{A.2})$$

where, $l = \text{fiber length (Km),}$

$L_{eff} = \text{effective fiber length (Km).}$

for $l \gg 1$, $L_{eff} = 1/\alpha$.

$\Delta F = \text{frequency separation between two adjacent channels.}$

$\lambda = \text{wavelength of the signal channel (i.e. the middle channel).}$

If we have M numbers of nodes (section) in the network then the value of η_{pqr} will be replaced by the equation (A.3) as follows,

$$\eta_{pqr}' = \eta_{pqr} \cdot \left[\frac{\text{Sin}^2(M\Delta\beta l/2)}{\text{Sin}^2(\Delta\beta l/2)} \right] \quad (\text{A.3})$$

APPENDIX B

Derivation of different noise components

Generally if loss is large then only one amplifier is not suitable. To compensate the loss, the effect of ASE will be very high. However if we use two amplifiers in a distributed fashion the effect the ASE accumulation will be far less than using a single amplifier of high gain.

Hence we considered in this work two distributed amplifier and cascade of blocks shown in Fig.2.2, we are first interested how many such blocks the signal can pass through and provide at the end the required SNR at a certain BER. The individual block is shown in the chapter 2. The different noise power components are expressed as follows [33,41-42],

$$P_{ASE} = [2\eta_{sp}(G_1-1)h\nu B_o L_s L_f L_{sp} G_2 L_{dm} L_{sw} + 2\eta_{sp} B_o (G_2-1)h\nu L_{dm} L_{sw}] L$$

(B.1)

Where L is the receiver loss. The first and 2nd terms of that equation is the ASE power of the first amplifier G_1 and the 2nd amplifier G_2 respectively. We may write ,

$$G_T = L_m L_s L_f L_{sp} L_{dm} G_1 G_2 L_{sw}$$

(B.2)

Then the total P_{ASE} power will be,

$$\begin{aligned} P_{ASE} &= G_T h\nu B_o \left[2\eta_{sp1} \left(1 - \frac{1}{G_1}\right) \frac{1}{L_m} \right] \cdot L \\ &+ G_T h\nu B_o \left[2\eta_{sp2} \left(1 - \frac{1}{G_2}\right) \frac{1}{L_m G_1 L_s L_f L_{sp}} \right] \cdot L \\ &= G_T h\nu B_o \left[2 \frac{\eta_{sp1}'}{L_m} + 2 \frac{\eta_{sp2}'}{L_m G_1 L_f L_s L_{sp}} \right] \cdot L \\ &= G_T h\nu B_o L \cdot F_o \end{aligned}$$

(B.3)

Where ' F_o ' is the noise figure which replaces $2 \eta_{sp}'$ of a single EDFA as,

$$F_o = 2\eta_{sp1}' \left(\frac{1}{L_m} \right) + 2\eta_{sp2}' \left(\frac{1}{L_m G_1 L_{ps} L_f L_{sp}} \right)$$

(B.4)

Where,

$$\eta_{sp1}' = \eta_{sp1} \left(1 - \frac{1}{G_1} \right)$$

$$\eta_{sp2}' = \eta_{sp2} \left(1 - \frac{1}{G_2} \right)$$

(B.5)

By such arrangement the effective noise accumulation of a cascade amplified system can be kept at a low value.

For receiver loss L dB. The average received signal current and amplifier spontaneous emission current are,

$$I_s = R_d P_{in} G_T L$$

$$I_{ASE} = R_d G_T (h\nu) B_o F_o L$$

(B.6)

The beat noise terms which have their asusual meaning already mentioned in chapter 2 are,

$$N_{sp-sp} = R_d^2 F_o^2 G_T^2 (h\nu)^2 B_o B_e L^2$$

(B.7)

$$N_{s-sp} = 2R_d^2 F_o h\nu G_T^2 P_{in} L^2 B_e$$

$$= 2I_s I_{ASE} \left(\frac{B_e}{B_o} \right)$$

(B.8)

$$N_{c-sp} = 2R_d^2 F_o (h\nu) G_T (2KG_T P_{in} L) B_e$$

(B.9)

Here, the term N_{c-sp} is the crosstalk due to adjacent channels in the same fiber and the channel spacing factor k is,

$$k = \frac{1}{1 + \left(\frac{2\Delta F}{f_{pf}} \right)^2}$$

(B.10)

$$N_{FWM-SP} = 2R_d^2 P_{pqr} F_o h\nu G_T B_e L^2$$

$$= 2I_{FWM} B_e / B_o ;$$

$$N_{S-FWM} = 4R_d^2 (P_{in} G_T L) (P_{FWM} G_T L)$$

$$N_{th} = i_{th}^2 B_e$$

(B.11)

The total noise power is ,

$$\sigma_1^2 = \sigma_o^2 = N_{S-sp} + N_{th} + N_{C-sp}$$

$$+ N_{S-FWM} + N_{FWM-sp} + N_{sp-sp}$$

(B.12)

Here, Δf is the channel spacing and f_{pf} is the MZI/FPI filter bandwidth frequency.

B_o = bandwidth of optical filter (DEMUX is realized by a splitter and tunable optical fiber)

The different loss components have their assumed values as follows,

$$L_m = 4 \text{ dB}$$

$$L_f = 9 \text{ dB}$$

$$L_s = 3 \text{ dB}$$

$$L_{sp} = 6 \text{ dB}$$

$$L_{dm} = 4 \text{ dB}$$

$$L_{sw} = 10 \text{ dB}$$

APPENDIX C

Bangladesh in the era of Optical Communication

In the year of 1989-90 Bangladesh enters into the world of Optical Fiber Technology by installing Optical Fiber as some important Junction Cable in Dhaka City of the network of Bangladesh Telegraphs and Telephone Board (BTTB). The world famous Japanese company NEC installed this Optical Fiber Cable. At the same time Bangladesh Rail Way Board also installed Optical Fiber individually to modernize their communication by digital technique instead of old analog system. The inter Rail Way and its associates are under one network which has no relation with the network of BTTB. However these two networks have Optical Fibers at different points installed at different times by different companies which has shown below. It is not so far that our country will replace all of its old system by Optical Fiber very soon.

Optical Fiber in the network of BTTB

Type of Fiber	: Single mode fiber.
Type of Modulation/Detection:	IM/DD.
Type of Transmitter	: LD (Laser Diode).
Type of Receiver	: APD.
Operating Wavelength	: 1310 nanometer.

Optical Fiber in Dhaka City.

Meanings of the used abbreviations as belows.

CEN: Ramna (Central)
CNT: Cantonment.
SBN: Sher-e-Bangla Nagar.
NLK: Nilkhat.
MPR: Mirpur.
UTR: Uttara.
MOG: Mogbazar.
MHK: Mahakhali.
TNG: Tangi.

1. Year of Installation : 1989 - 90.
 Name of the Company : NEC.

Name of Cable	Length in km.	Number of Fiber.	No. of Spare	Bit rate.
SBN-CEN	7.4	12	6	140 Mb/s
SBN-NLK	4.5	8	4	140 Mb/s
SBN-MPR	6.5	8	4	140 Mb/s
SBN-UTR	18.1	12	8	140 Mb/s
SBN-GUL	6.6	8	4	140 Mb/s
SBN-MOG	3.7	12	6	140 Mb/s
MOG-MHK	4.5	10	2	140 Mb/s

2. Year of Installation : 1994.
 Name of the Company : ALCATEL.

Name of Cable	Length in Km	Bit rate Mb/s.
CEN-NLK	3.7	560
NLK-SBN	4.5	560
SBN-MPR	6.5	560
SBN-GUL	7.0	560
GUL-CNT	3.5	34
GUL-UTR	10.0	140
UTR-TNG	4.0	140
SBN-MOG	3.7	560
MOG-MHK	4.5	560

3. Year of Installation : 1994.
 Name of the Company : Fujitsu.

Ramna to Mogbazar 3 Kilometer fiber using 140 Mb/s.

Optical Fiber in Chittagong City.

Meanings of the used abbreviations as follows:

NDK: Nandan Kanan.
AGB: Agrabad.
EPZ: Export processing zone.
SAG: Sagarika.
MUR: Muradpur.
BJB: Baizid Bustami.
KAG: Kalur Ghat.

4. Year of Installation : 1994.
Name of the Company : ALCATEL.

Name of Cable	Length in Km.	Bit Rate Mb/s.
NDK-AGB	4.8	140
AGB-EPZ	6.5	140
AGB-SAG	4.0	140
NDK-MUR	4.0	140
MUR-BJB	4.5	140
MUR-KAG	6.0	140

Optical Fiber in Khulna City.

Meanings of the used abbreviations as follows:

KUL: Khulna.
KLS: Khalispur.
DPR: Daulutpur.
SHI: Shiramani.

5. Year of Installation : 1994.
 Name of the Company : ALCATEL.

Name of Cable	Length (Km)	Bit rate (Mb/s)
KUL-KLS	3	140
KLS-DPR	10.5	34
KLS-SHI	5.5	34

Optical Fiber in Rajshahi City.

6. Year of Installation : 1995.
 Name of the Company : ALCATEL.

a). Rajshahi main exchange to Salban exchange about 4 kilometer using 34 Mb/s.

b) Rajshahi main exchange to Talimari exchange about 5.5 kilometer using 34 Mb/s.

Optical Fiber in Jessore.

7. Year of Installation : 1989.
 Name of the Company : Fujitsu.

There is one junction from Jessore main exchange to Rajarhat carrier station about 5 km fiber using 34 Mb/s.

Optical Fiber in Bangladesh Rail Way Network.

8. Year of Installation : 1989.
 Name of the Company : Fujitsu.
 Total length of Fiber : 1450 Km.
 Maximum repeater distance : 68 Km.
 Minimum repeater distance : 08 Km.
 Type of Fiber : Single mode fiber.
 Type of Modulation/Detection: IM/DD.
 Type of Transmitter : LD (Laser Diode).
 Type of Receiver : APD.
 Operating wavelength : 1310 nanometer.

All rail way stations are interconnected by optical fiber except Sayedpur to Chilahati route. The east and west zone are interconnected by microwavelink. Here it should be mentioned that there is no spare fiber in the Rail way network and also this vast network has no link with the network of BTTB. The highest officials of BTTB and Bangladesh Rail Way Board are now on discussion to find out the means of how this two network can be interconnected and used.

